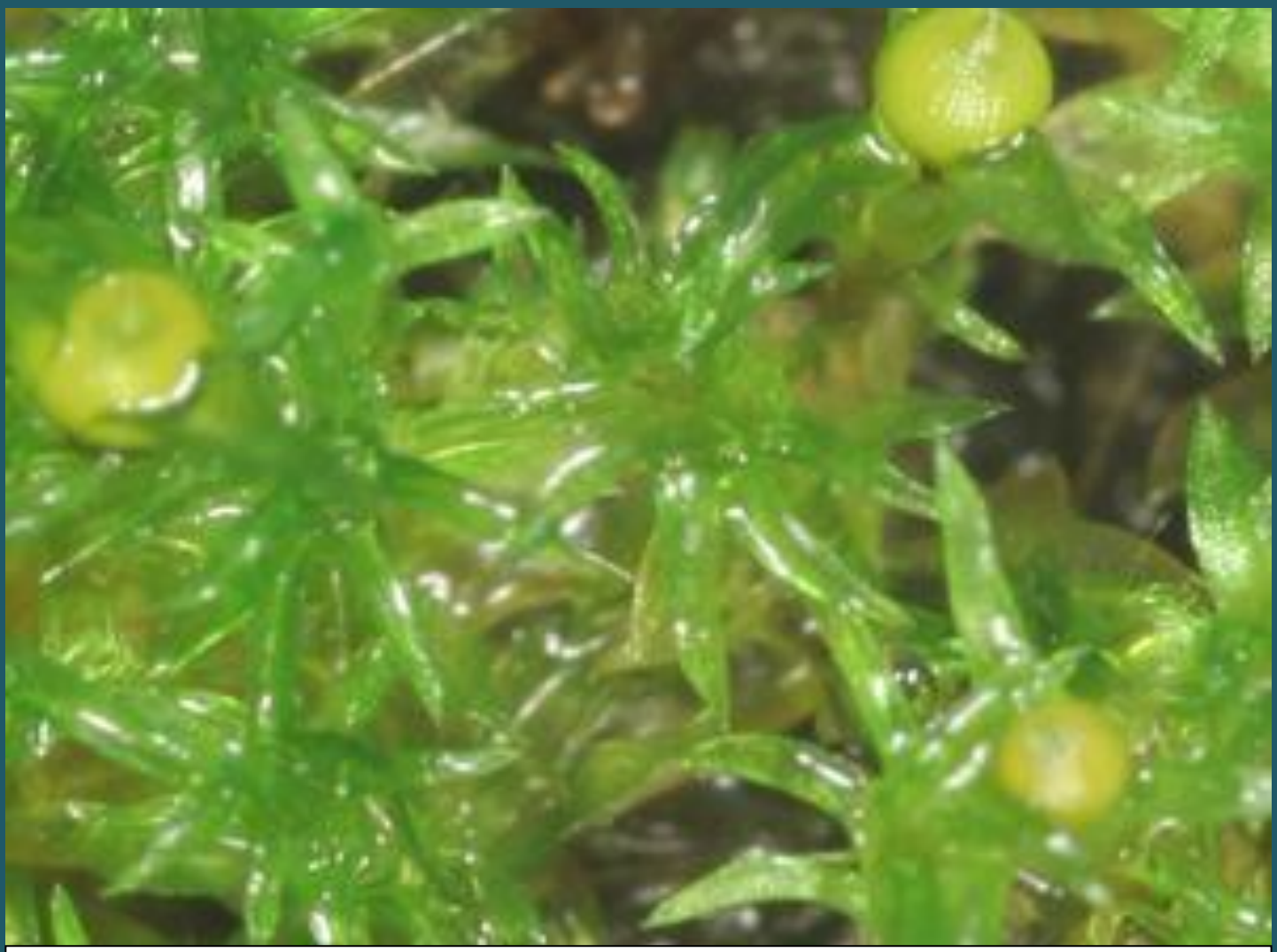

STUDY OF MOSS VACUOLES

AND FUNCTIONAL CHARACTERIZATION OF THE PUTATIVE VACUOLAR RECEPTORS, THE RMR PROTEINS

UNIVERSITÉ DE NEUCHÂTEL

PhD thesis presented by Sanaa Ayachi
PhD director Prof. Jean-Marc Neuhaus
Dr. Didier Schaefer

" INSTITUTE OF BIOLOGY - DEPARTMENT OF CELLULAR AND MOLECULAR BIOLOGY"Rue Emile - Argand 11, 2009 Neuchâtel "

UNIVERSITÉ DE NEUCHÂTEL

Faculté des sciences
Secrétariat-décanat de Faculté
Rue Emile-Argand 11
2000 Neuchâtel - Suisse
Tél: + 41 (0)32 718 2100
E-mail: secretariat.sciences@unine.ch

IMPRIMATUR POUR THESE DE DOCTORAT

La Faculté des sciences de l'Université de Neuchâtel autorise l'impression de la présente thèse soutenue par

Madame Sanaa AYACHI

Titre: Study of moss vacuoles and functional characterization of the putative vacuolar receptors, The RMR proteins

sur le rapport des membres du jury:

- Prof. Jean-Marc Neuhaus, Université de Neuchâtel, directeur de thèse
- Prof. Felix Kessler, Université de Neuchâtel
- Prof. ass. Niko Geldner, Université de Lausanne
- Dr Andrija Finka, Université de Lausanne
- Dr Didier Schaefer, Université de Neuchâtel

Neuchâtel, le 14 mars 2013

Le Doyen, Prof. P. Kropf

Pour Toi et par Toi

A ma mère et à mon père

Thanks

Firstly I want to thank my supervisor **Prof. Jean-Marc Neuhaus** for giving me the opportunity to follow this PhD project.

I want to thank sincerely **Dr. Didier Schaefer,** my mentor for teaching me the moss system.

I want to thank all the members of the Laboratory of Molecular and Cell Biology for their support and the scientific discussions and support; Sonia Negro, Livia Autauri, Dirk Balmer, Sophie Marc-Martin, Dr. Nadia Feddermann, Dr. Guillaume Gouzerh and Noémie Fahr.

I thank particularly my colleagues **Dr. Egidio Stigliano** and **Dr. Alessandro Occhialini** for being my PhD mate and for the unforgettable moment with them.

I thank Prof. Niko Geldner for the nice suggestions and the interesting discussion we had during my mid-thesis defense.

Table of Contents

Abbreviations

ABA: Abscisic Acid

ADP: Adenosine Diphosphate

AP: Adaptin Protein

ARF: ADP Ribosylation Factor

ATP: Adenosine Triphosphate

ATPase: Adenosine Triphosphate Hydrolase

Bip: Binding immunoglobulin protein

BFA: Brefeldine A

BP-80: Binding Protein of 80 kDa

CCV: Clathrin-Coated Vesicle

COPI: Coat Protein I

COPII: Coat Protein II

Ct-VSD: C-terminal Vacuolar SortingDeterminant

DIP: Dark-Induced Protein

DNA: Deoxyribonucleic Acid

DV: Dense Vesicle

ERAD: Endoplasmic Reticulum Associated Degradation

ERES: Endoplasmic Reticulum Exportin Site

ESCRT: Endosomal Sorting Complex Required for Transport

GDP: Guanosine Diphosphate

GEF: GTP Exchange Factor

GFP: Green Fluorescent Protein

Hsp: Heat Shock Protein

Ko: Knock-out

LV: Lytic Vacuole

MS: Mass Spectrometry

MVB: Multivesicular Body

PA domain: Protein Associated domain

PAC: Precursor Accumulating Vesicle

PM: Plasma Membrane

PSV: Protein Storage Vacuole

psVSD: Protein Structure dependent Vacuolar Sorting Determinant

PVC: Prevacuolar Compartment

Rab: Ras-related in Brain

RING: Really Interesting New Gene

RFP: Red Fluorescent Protein

RMR: Receptor-like Membrane Ring-H2

RNF13: RING Finger Protein 13

SNAP: Soluble NSF Attachment protein RNA: Ribonucleic Acid

SNARE: Soluble N-ethylmaleimide-sensitive Protein Attachment Protein Receptor

SP: Signal Peptide

SRP: Signal Recognition Particle

ssVSD: Sequence-specific Vacuolar Sorting Determinant

TIP: Tonoplast Intrinsic Protein

UPR: Unfolded Protein Response

VAMP: Vesicle Associated Membrane Protein

VSD: Vacuolar Sorting Determinant

VSR: Vacuolar Sorting Receptor

YFP: Yellow Fluorescent Protein

Abstract

The vacuolar system of plants is a key element of plant growth and development, it fulfils many other functions. Plant cell can have more than two different vacuolar sorting systems: the lytic and the (seed) protein storage or vegetative storage vacuoles. Soluble vacuolar proteins are sorted through the secretory pathway to these vacuoles by three different routes, depending on different types of Vacuolar Sorting Determinants (VSD) and involving several types of receptors and vesicles. The AtRMR proteins has been identified in cellular structures associated with the seed storage vacuole pathway (Jiang et al. 2000). Based on its localisation and homology to a known vacuolar receptor, it has been hypothesised to be a receptor protein for the C-terminal type of VSD (ct-VSD) involved in sorting to the storage vacuole. The genome of *Physcomitrella patens* contains five genes coding for RMR proteins.

My work hypothesis is that the vacuolar system of higher plants has evolved from simple ancestors, which might have been preserved in lower plants. This evolution is reflected in the gene families involved in vacuole biogenesis. In a first part, we established the moss *P. patens* as a model system for the study of the secretory pathways. In a second part, we performed a comparative study of the plant-specific aspects of the vacuolar system. And finally in a third part, we tried to establish the functional role of PpRMR genes by the analysis of the complete RMR deletion mutants. Several strategies were considered to investigate a putative disorder due to RMRs loss of function. So far, no phenotype was detected in the mutants. Nevertheless the absence of the RMR family gene seems not to be necessary for moss development.

Chapter I: Introduction

Part 1: The plant secretory system

1. The endomembrane system

The endomembrane system (secretory pathway) of plant cells has been studied by analogy with those of animals and yeasts, which have been well characterized. In plants, the secretory pathway comprises the endoplasmic reticulum (ER) as site of protein and lipid synthesis, the Golgi apparatus (GA) as maturation and sorting compartment for proteins and lipids, the *Trans*-Golgi-Network (TGN), the prevacuolar compartment (PVC), the vacuoles, and several types of vesicles involved in transport between these compartments and to the cell surface. In a review based mainly on observations of plant cells, Morre and Mollenhauer (Morre et al. 1974) defined the endomembrane system as the functional integration of ER, Golgi complex, secretory vesicles, plasma membrane, and hydrolytic compartments (fig. 1).

Most secretory proteins are transported by vesicles from the ER to the GA where they are matured and sorted. If they contain the necessary sorting information, they will be retained or transported to the correct target compartment (Paris et al. 1996). In the absence of such specific information, they will be packaged into vesicles that will then fuse with the plasma membrane and release their content to the apoplast (Denecke et al. 1990b).

On their way to secretion or to vacuoles, proteins have to pass several organelles such as the *trans*-Golgi network, early or late endosomes or prevacuoles. One final compartment of the plant secretory system is the vacuole (Marty 1999)**.** The vacuole plays a major role in storage and recycling of various compounds (Taiz 1992); it contains the various hydrolases which degrade and recycle proteins, lipids and carbohydrates (Otegui et al. 2005). Depending on the tissue type, a single cell can harbor two vacuoles with distinct functions: the lytic vacuole (LV) and the protein storage vacuole (PSV) (Epimashko et al. 2004; Neuhaus and Rogers 1998; Paris et al. 1996; Surpin and Raikhel 2004).

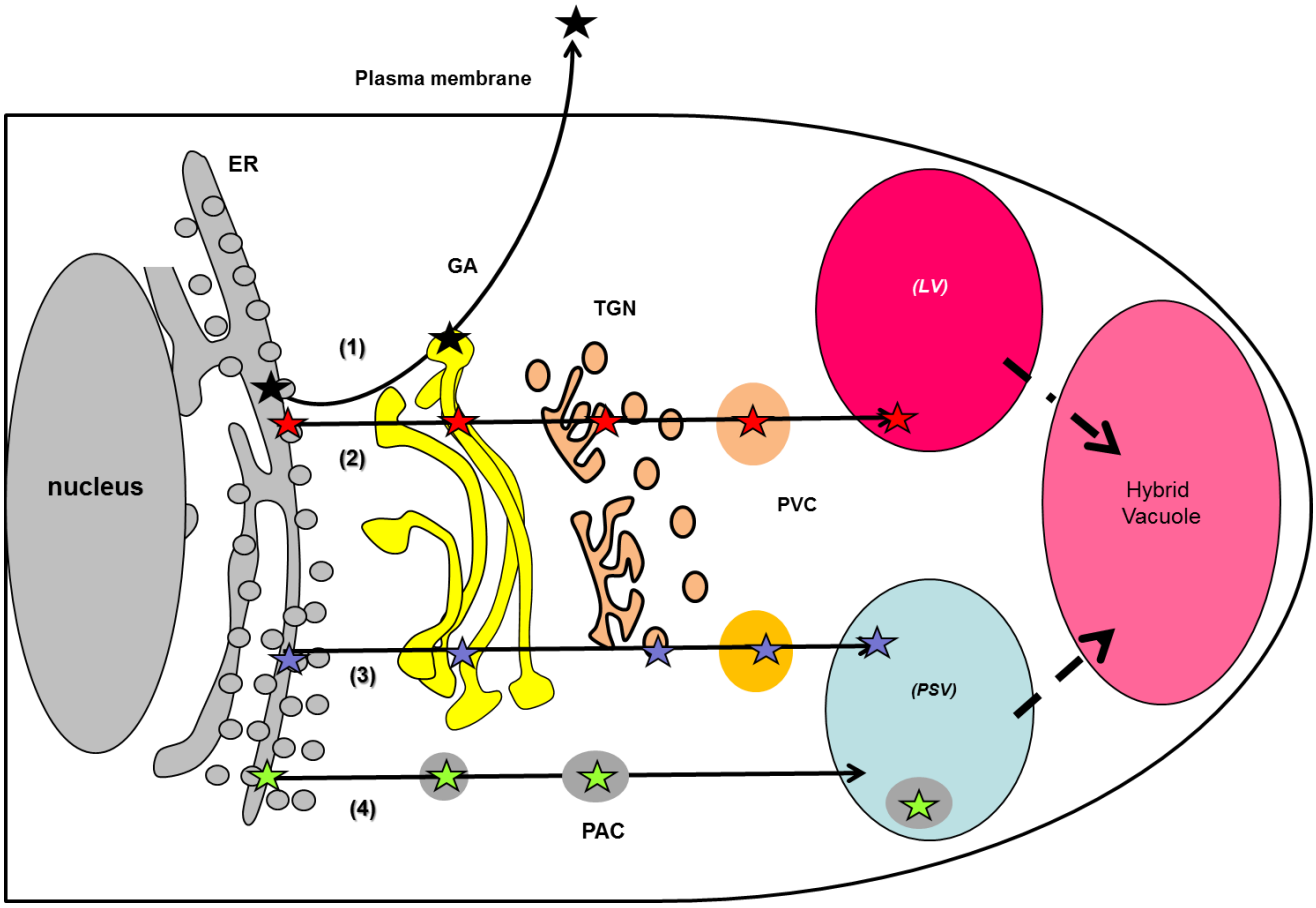

Figure 1: Model of vacuolar protein sorting in plants

Soluble proteins with a specific sorting signal reach the vacuole via the secretory pathway: ER (Endoplasmic Reticulum), GA (Golgi Apparatus), TGN (Trans-Golgi-Network), PVC (Prevacuolar Compartment) and lytic vacuoles (LV) or protein storage vacuole (PSV). This model is based on different studies and was described in Vitale's review (Vitale and Raikhel 1999). However this model was recently challenged.

(1) Soluble protein precursors are synthesized in the ER. The proteins lacking a specific vacuolar sorting signal (black stars) are secreted out of the cell at the plasma membrane.

(2) Proteins with ssVSD (red stars) interact with a receptor (VSR) in the membrane of the TGN. These ligand-receptor complexes are recruited into clathrin-coated vesicles (CCVs). The CCVs release their contents into the prevacuolar compartment (PVC). In PVC (or MVB), the cargo dissociates from the receptor. Vacuolar proteins then reach the central vacuole while the cargo receptor is recycled back to the GA for another cycle of transport.

(3) Proteins with ct-VSD (blue stars) aggregate at the rim of the *cis*-cisternae and at the TGN. They are probably packed in the precursors of dense vesicles (DVs). DVs either fuse directly to PSVs or form a PVC for PSV.

(4) Storage proteins in pumpkins seeds (green stars) are transported by Precursor-Accumulating (PAC) vesicles which develop from the ER and fuse directly to the PSVs, bypassing the GA.

2. The ER is the starting point of the secretory system

The ER can be subdivided into three domains with distinct function; the nuclear membrane, the smooth ER (SER) and the rough ER (RER). The nuclear membrane is a specialised part of the ER which harbours the nuclear pore complexes. The SER is the site of lipid biosynthesis, xenobiotic detoxification and calcium regulation (Vertel et al. 1992). The RER appears rough in the electron microscope because ribosomes are associated to its cytosolic face. It is the entry point into the endomembrane system for newly synthesized proteins (Vitale and Denecke 1999). Proteins addressed to the endomembrane system possess N-terminal signal peptide (SP) or have analogous transmembrane domains at other places within the protein. The newly synthesized SP emerges from the ribosome and is recognized by a signal recognition particle (SRP). The ribosome stops translating until the SRP-ribosome complex can attach to a receptor at the ER surface. The nascent polypeptide can then enter the RER cotranslationally through a protein pore, the translocon (Hamman et al. 1998). The translocation is a passive process which does not require additional energy, since the pressure provided by translation is enough for translocation (Vitale and Denecke 1999). Once it reaches the ER lumen, the signal peptide (SP) is cleaved by a signal peptidase and yield the maturing protein.

2.1. The role of the ER

ER-localised proteins undergo post-traductional modifications and acquire their mature conformation with the help of chaperone proteins resident in the ER (endoplasmins, calnexin, calreticulin, BiP, protein disulfide isomerases (PDI)) (Bednarek and Raikhel 1992). The best characterized ER chaperone is BiP which belongs to the Hsp 70 family (70 kDa proteins) of ATPases involved in the catalysis of protein folding and assembly (Hartl 1996). PDI which catalyses the formation and rearrangement of disulphide bonds plays also an important role in protein folding and maturation (Vitale and Denecke 1999).

The ER is also an important site for protein modification, in particular for N-glycosylation on specific asparagines (Asn) present in the consensus sequence Asn–X–Ser/Thr (X is any amino-acid except Pro). The main role of N-glycosylation in plant cells is to assure correct protein folding and to increase the protein solubility. N-glycosylation is catalyzed by the multisubunit enzyme oligosaccharyl transferase which is associated on the

luminal side with the translocon pore. The modification usually occurs cotranslationally but post-translational glycosylation does also occur (Vitale and Denecke 1999).

The ER can become a storage compartment in seeds. Cereal storage proteins accumulate in the ER lumen forming electron-dense structures called protein bodies (PB) (Herman and Larkins 1999). PB can be permanently stored in the ER or transferred to PSV by a specific pathway (Vitale and Ceriotti 2004). The mechanism leading to the retention of storage proteins in the ER and subsequent formation of protein bodies is still unclear. The lack of an export signal and actions of molecular chaperones such as BiP might be involved in aggregations of storage proteins in the ER. An interaction between storage proteins and the membrane bilayer has also been demonstrated (Kogan et al. 2004; Vitale and Denecke 1999).

2.2. Quality control

The ER has important check points for correct protein folding and assembly with a process called ER quality control (Hurtley and Helenius 1989). Misfolded proteins affected by physical or chemical stresses are recognized by molecular chaperones such as BiP and retained in the ER lumen. The chaperones help the proteins to refold to their native structure, recovering their normal cell functions (Hiller et al. 1996). If binding time to the chaperone is abnormally long, the malfolded proteins are degraded in a process called ER-associated degradation (ERAD) (Vitale and Boston 2008). Two ER-resident lectins (calnexin and calreticulin) are also involved in protein quality control. They recognize misfolded glycoproteins and cooperate with glucosylation and deglucosylation enzymes (Helenius et al. 1997).

2.3. ER retention signals

Soluble proteins with a C-terminal H/KDEL sequence are retained in the lumen of the ER (Pelham 1998). KDEL proteins which accidentally escaped from the ER to the GA are retrieved by membrane receptors such as ERD2 at a *cis*-Golgi cisterna and sent back to the ER by retrograde transport (Lewis and Pelham 1992).

2.4. Traffic between ER and Golgi

2.4.1. COPII vesicles

In eukaryotic cells, the ER and Golgi are connected via two types of vesicles, the COPII vesicles for the anterograde traffic from ER to Golgi and the COPI (Coatomer) vesicles for retrograde traffic from the Golgi to the ER (Barlowe et al. 1994). The anterograde traffic starts at specific ER domains called ERES (ER exporting site) (Bassham and Blatt 2008). The anterograde transport has been studied by analogy to mammalian cells and yeast, and homologues of COPII coat proteins have been identified in the *A.thaliana* genome (Movafeghi et al. 1999). The process of COPII vesicle formation requires a specific GTPase, a Sar1p family protein, which recruits the adaptor complex Sec23/Sec24 and cargo membrane proteins. Recruitment of Sec13/Sec31 completes the coat assembly (Movafeghi et al. 1999). Sar1p is recruited by the guanine nucleotide exchange factor (GEF) Sec12p at the membrane of ER. Once activated, Sar1p can recruit all coat proteins (Hanton et al. 2005). When Sar1p hydrolyses its bound GTP and then dissociates from the membrane, it causes the disassembly of the coat and thus allows vesicle fusion with the membrane of *cis*-Golgi. Proteins of the COPII coat are recycled back to ER for another cycle of vesicle formation (Hanton et al. 2005).

2.4.2. Endoplasmic reticulum export site (ERES) and signals

The anterograde ER export occurs from a specific domain named ERES where the different factors needed for COPII vesicle formation are assembled (Hawes et al. 2008). The recruitment of cargo proteins at ERES is poorly understood in plant cells. The process may be similar to mammalian cells where protein cargoes are recruited to ERES, incorporated in COPII vesicles and then transported to Golgi (Aridor et al. 2001). A study has shown an increase of the ERES site number when cargo is over-expressed (Hanton et al. 2007). In mammals and yeast, studies showed that (Sec16) a protein associated to ER exit sites was involved in ER protein export (Connerly et al. 2005). However, a protein with similar function has yet to be identified in plant.

2.4.3. COPI vesicles

COPI vesicle formation starts when the ARF1 GTPase interacts with the GA protein p23 (Gommel et al. 2001). Then, an ARF-GEF exchanges GTP for GDP, leading to a conformational change of ARF1 which allows its membrane binding (Helms and Rothman 1992). Activated ARF1 recruits the COPI coatomer from the cytosol causing vesicle budding (Rothman and Orci 1996). The COPI coatomer consists of the F adaptor subcomplex (four subunits: β-, γ-, δ-, ζ-COP) and of the B cage subcomplex (three subunits: α-, β' and ε-COP) (Waters et al. 1991). ARF1 inactivation by an ARF-GAP after vesicle budding from the membrane causes coat disassembly and allows fusion with the ER membrane. ARF1 activation can be inhibited by the lactone antibiotic Brefeldin A (BFA). This prevents COPI coat formation, blocking the retrograde transport from cis-Golgi to ER and then indirectly blocking also anterograde transport. This drug is widely used to study protein transport by blocking the ER/Golgi transport (Helms and Rothman 1992; Ritzenthaler et al. 2002; Robinson et al. 2008).

3. The Golgi Apparatus

3.1. Roles of the Golgi Apparatus

After leaving their production site (ER), most of secretory proteins are transported to the Golgi apparatus (GA). It is composed of stacked cisternae. In plant cells, the GA is dispersed throughout the cytosol, and the stacks move around whereas in mammalian cells the stacks are localized near the nucleus. The stacks are interconnected by tubular elements (Andreeva et al. 1998; Mellman and Simons 1992). A Golgi stack can be composed of four to eight cisternae organized in three different regions with distinct functions: *cis*-Golgi, *medial*-Golgi and *trans*-Golgi. The *cis*-Golgi constitutes the entrance of the apparatus while, from the *trans*-Golgi, vesicles transport secretory proteins to their final destination (Hawes et al. 2008; Matheson et al. 2006). The Golgi apparatus is an important traffic point between different organelles, such as ER, TGN and endosomes. This compartment is also a major site of post-translational modifications of N-glycans and O-glycosylation of glycoproteins and proteoglycan. The N-glycans modification starts already in the ER and is continued sequentially by numerous GA glycosidases and glycosyltransferases. Glycoproteins are

transported across the stack (Zhang and Flint 1992), each cisterna containing specific modification enzymes to form a multistage processing unit. This functional differentiation between *cis*-, *medial* and *trans*-Golgi was demonstrated by localizing different glycan-modifying enzymes in different cisternae of the stack (Glick 2000). The Golgi apparatus is also involved in the biosynthesis of many polysaccharides such as hemicellulose and acidic pectic polysaccharides which are very important components of the cell wall matrix (Bolwell 1988). The GA is also a biosynthesis site for lipids such as sphingolipids ubiquinone and plastoquinone, as described in spinach (Swiezewska et al. 1993).

3.2. Transport through the Golgi apparatus

Cargo from the ER passes sequentially through *cis*-, *medial*-, and *trans*-cisternae before arriving at the TGN. Transport through the Golgi cisternae is a matter of controversy (Pelham and Rothman 2000). Three models have been suggested to explain the vectorial transport of secretory proteins through the GA.

The first model ("old model") postulated that the GA is a static organelle, proteins transit from *cis*-cisternae to *trans*-cisternae and are matured on their way, and anterograde protein traffic between cisternae is assured by COPI vesicles (Donaldson and Williams 2009; Rothman 1994).

Cisternal maturation was proposed as an alternative model to explain scale transport in algae (Becker and Melkonian 1996) and was studied in yeast (Glick and Malhotra 1998). In this model, the cisternae are transient structures formed by fusion of ER derived vesicles with retrograde vesicles at the GA's *cis* side. In this model, cargo proteins remain in the cisternae during maturation from *cis*- to *trans*-Golgi, while the GA enzymes modifying the cargo are relocated back to precursor cisternae by COPI vesicles. The *trans* cisternae are destroyed by the formation of transport vesicles for other compartments and of retrograde vesicles recycling trans-Golgi enzymes to younger cisternae. Alternatively, the *trans* cisternae may detach from GA stack and become a TGN. This mechanism was visualized in budding yeast, which does not have Golgi stacks but rather isolated single cisternae (Donaldson and Williams 2009; Losev et al. 2006; Matsuura-Tokita et al. 2006).

The third model proposed is a modification of the cisternal maturation model which was supported by recent evidences, especially in plants (e.g. see (Donohoe et al. 2007; Otegui et al. 2006). It is called the "rapid-partitioning model" (Patterson et al. 2008) because GA cisternae are partitioned into subdomains where enzymes perform modifications. Cargoes are

able to move rapidly between the cisternae via vesicles and tubular connections to undergo specific modifications (Donaldson and Williams 2009). Consequently, cargoes are able to move in a bidirectional manner by specific vesicular or tubular traffic depending on the modification location (Patterson et al. 2008). All these models are not exclusive; they may vary between different organisms and different steps of development.

4. Direct traffic from ER to vacuoles

In plant cells, a pathway from ER to protein storage vacuoles (PSV) bypassing the GA was demonstrated by electron microscopy on maturing pumpkin cotyledons. The storage protein proglobulin is sorted via precursor accumulating (PAC) vesicles (Hara-Nishimura et al. 1998), with sizes ranging from 200 to 400 nm, and containing unglycosylated precursors of storage proteins. Once in the vacuolar lumen, these precursors undergo a maturation process. PAC vesicles fuse with PSV either by autophagy or by direct membrane fusion. The autophagy uptake of PAC vesicles was observed in maturing pea seeds and in mungbean seedlings (Robinson et al. 1995). However, another study supported the fusion theory, showing small G-proteins involved in membrane fusion between PACs and PSV on the surface of PACs (Shimada et al. 1994). Most recently, a similar direct pathway was also suggested for certain membrane proteins (Rivera-Serrano et al. 2012).

5. The Trans-Golgi-Network

5.1. The TGN

The TGN is the site of cargo sorting and the organelle where proteins are targeted to their final destination (Gu et al. 2004). Its size differs, and it is mainly located near the *trans*-side of the Golgi (Traub and Kornfeld 1997). The plant TGN is physically and functionally distinct from the *trans*-Golgi (Uemura et al. 2004). In tobacco epidermal cells, a fluorescent marker for TGN does not co-localize with a Golgi marker (Foresti et al. 2008). In animal cells, upon BFA treatment, the TGN aggregates with endosomes to form a TGN-endosomal hybrid compartment, while the GA fuses with the ER (Samaj et al. 2004). Therefore the TGN is part of the endocytic network and consequently a more appropriate name would be post-Golgi network (Uemura et al. 2004). At the TGN, cargoes are packed into coated vesicles and sorted

according to their sorting signals, proteins without information are transported to the plasma membrane through a "constitutive pathway" (Denecke et al. 1990a). The TGN has a very important role in the traffic to several post-Golgi compartments such as endosomes/pre-vacuoles, lytic (LV) and protein storage (PSV) vacuoles and plasma membrane (Jürgens 2004). Cargoes are transported from TGN to the endosomal compartment by clathrin-coated vesicles (CCVs).

5.2. Clathrin coated vesicles (CCVs)

CCVs are mainly found at the PM and at TGN/endosomes and are involved in traffic of protein cargo between these organelles. Clathrin is a trimer consisting of three heavy and three light chains associated to form a three-legged structure called a triskelion (Fotin et al. 2004). The clathrin coat is formed by the assembly of single units of clathrin which interact to form a characteristic cage surrounding the vesicles. The Clathrin forms the outer layer of the coat whereas the internal layer is formed by others proteins, adaptor proteins such as adaptins (AP), linked to the membrane by small G-proteins from the ARF family, and/or phosphoinositides (Bassham and Blatt 2008). Four different types of AP complexes have been identified in eukaryotic cells, probably involved in different traffic pathways (Boehm et al. 2001; Dacks and Doolittle 2001; Dacks et al. 2008).

6. The endosomes

Endosomes are important branching points for newly synthesized proteins derived from the ER, as well as for proteins coming from the plasma membrane (Lam et al. 2007). In animal cells the endosomal system is divided in early endosomes (EE), late endosomes (LE) and recycling endosomes which are morphologically and functionally distinct domains. The TGN is physically and functionally distinct from these endosomes (Raposo et al. 2007). Each of these compartments is characterized by specific marker proteins, such as the Rab GTPases (Huotari and Helenius 2011). For example, RAB4 and RAB5 are found in early endosomes, whereas RAB7 or mannose 6-phosphate receptors are localized in late endosomes, and RAB11 was used as a marker in recycling endosomes.

In plant cells, endosome functions are similar to those in animal cells, however they are organized differently. A fluorescent tracer FM4-64 was used to distinguish these compartments. This dye is actively endocytosed into the cell, and during it passage through

the cell, a succession of different compartments are visualized (Samaj et al. 2005). In these experiments, the TGN was labeled early whereas the PVC was labeled later and finally the tonoplast (Dettmer et al. 2006). By analogy with animal cells, it was thus proposed that the plant TGN corresponds to the animal early endosomes and PVC (or MVB) to the late endosomes (Foresti and Denecke 2008) (fig. 2). Recent studies suggest that a TGN was indeed receiving endocytosed material from the plasma membrane, acting similarly to the animal recycling endosome (Lam et al. 2007). In animal cells, the Rab11 GTPase localizes to the recycling endosome which is distinct from both TGN and EE (Iversen et al. 2001). In contrast, in plant cells, the Rab11 homologue was found in the TGN, suggesting that this compartment could, also be the recycling endosome in plants (Foresti and Denecke 2008).

The endosomes containing luminal vesicles are called LE or multivesicular bodies (MVB). Structurally, the MVBs are membrane-bound compartments, containing small internal vesicular structures which are released into the vacuole. It was also shown that MVBs represents the prevacuolar compartment (PVC) in seeds and vegetative tissues where they carry storage proteins and proteases to the PSV (Otegui et al. 2006; Tse et al. 2004; Wang et al. 2007).

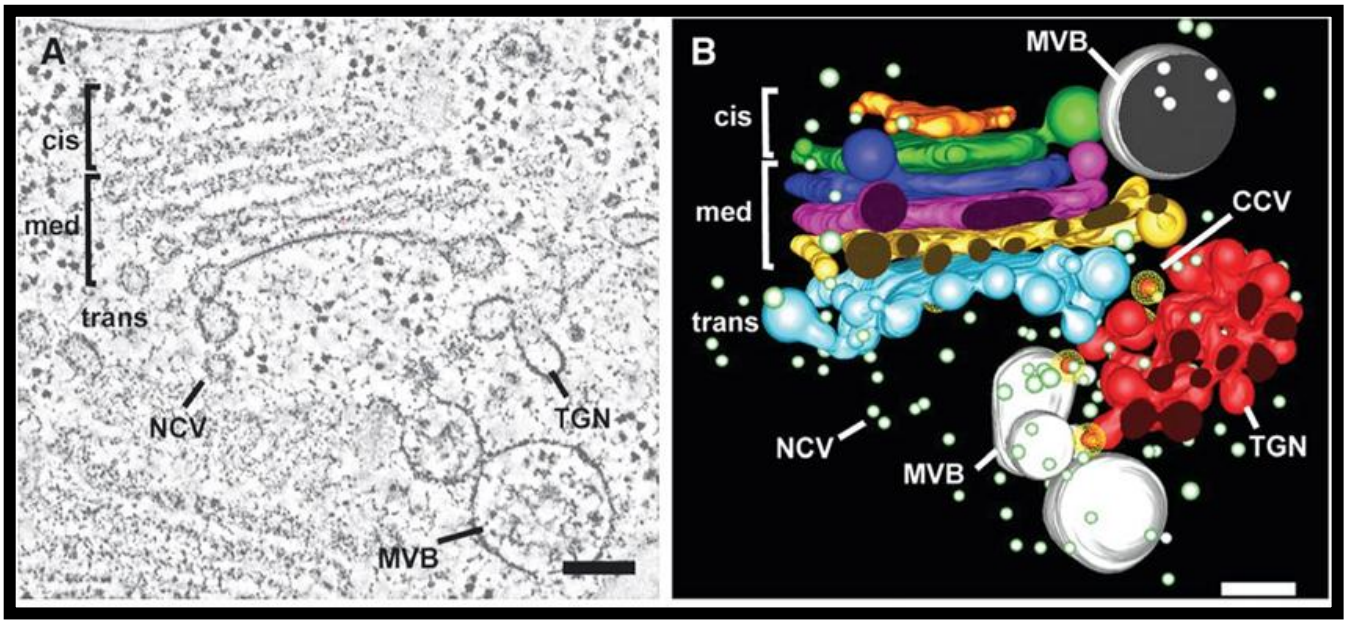

Figure 2: Electron tomographic reconstruction of a Golgi stack and associated structures of developing Arabidopsis seed.

(A) Transmission electron microscopy (TEM) image of a prepared tomographic slice (4.3 µm thick) through a region of the Golgi complex. (**B**) Three dimensional reconstitutions of the same region as in A.

Compartments are colour-coded: *cis*-Golgi (orange and green), *medial*-Golgi (blue, purple, yellow), *trans*-Golgi (blue) and the trans-Golgi-network (TGN) (red).

A CCV, non-coated vesicle (NCV) and multivesicular bodies (MVB) are also labelled. Scale bars: 100 nm.

Figure reprinted from Otegui et al. (Otegui et al. 2006).

7. Vesicle trafficking

In all eukaryotic cells, transport between the different compartments of the secretory system is provided by vesicular trafficking. Vesicles are small compartments enclosed by a lipid bilayer which bud from a donor compartment and fuse with an acceptor compartment. Vesicle formation, recognition of and fusion with the acceptor organelles are not passive events but require several factors (Bassham et al. 2008; Bassham and Blatt 2008; Jürgens 2004; Sanderfoot et al. 1999).

.

7.1. Coat proteins and G-proteins: vesicle formation

Specific cargoes located in the lumen of the donor organelles are first recognized, by receptors. Coat proteins are involved in the membrane deformation and scission from the donor compartment to produce the vesicle. There are different types of coat proteins related to vesicle formation at specific organelles: COPII, COPI, CCV, retromer. COPII vesicles are involved in anterograde ER-Golgi transport, while COPI (Coatomer) vesicles are required for retrograde GA-ER transport (Barlowe et al. 1994). Specific small GTPases (G-proteins) initiate the budding process, the incorporation of the cargoes into the evaginated membrane and the scission of the vesicle from the donor organelle. In plant cells, there are several such G-proteins. ARFs are required for COPI and CCV formation, while SAR1 is involved in COPII vesicle formation (Bassham and Blatt 2008; Jürgens 2004; Sanderfoot et al. 1999). Coat formation implies the coordinated recruitment of activated G-proteins, specific phosphatidylinositides, membrane protein cargoes as well as receptors for soluble luminal cargoes and a layer of adaptor proteins. Finally an external coat layer is recruited (Sec13/Sec31 for COPII, the B subcomplex for COPI and the clathrin triskelion for CCV), which contributes to the membrane deformation required for vesicle formation.

7.2. Machines of membrane fusion

Vesicle formation is followed by several events: coat disassembly, trafficking to the target organelle, attachment to it by tethering and docking factors and fusion (Bassham and Blatt 2008; Jürgens 2004; Sanderfoot et al. 1999). Once detached from the donor membrane in the cytosol, the vesicles move through the cytosol by association with cytoskeletal motors or other docking factors. Through the action of docking , tethering factors and members of the SNARE family, the vesicles identify their target compartment and then fuse with it to deliver their cargoes (fig. 3). Rabs are large family of small GTPases involved in the recruitment of motor proteins and of tethering and docking factors (Bassham and Blatt 2008; Jürgens 2004; Sanderfoot et al. 1999). Two groups of SNAREs have been classified: v-SNAREs, t-SNAREs. The v-SNAREs are found in vesicles originating from the donor compartment. The vesicles harbor v-SNAREs and a Rab-GTP. The second type of SNAREs: t-SNAREs, are localized in the membrane of the target compartment (Bassham and Blatt 2008; Jürgens 2004; Sanderfoot et al. 1999). The target organelle contains a t-SNARE complex associated with a Sec1 which maintains the t-SNARE in an inactive form. Sec1 proteins (6 family members in *A.thaliana*) control the formation of this bundle (Hanson and Stevens 2000; Sanderfoot 2007) (fig. 3).

When the vesicle and the target organelle interact, interaction with the Rab-GTP removes the Sec1 protein and exposes the t-SNARE, which becomes active. The t-SNAREs are then able to interact with the v-SNAREs : this is the “docking process” (Chen et al. 1999). Formation of the form-helix bundle of v- and t-SNAREs pulls the two membranes together, causing their fusion. Membrane fusion follows. Subsequently, NSF catalyzes the disassembly of v-/t-SNARE complex upon hydrolysis of ATP, and the released v-SNARE is recycled back to the donor compartment, while the t-SNAREs stay associated with a Sec 1 protein and are ready for another cycle of vesicle fusion (fig. 3) (Hay et al. 1997; Rothman and Söllner 1997). α-SNAP specifically binds to the v-/t-SNARE complex, recruits the NSF factor to the SNARE complex. This ATPase dissociates the v/t-SNARE complex to allow the recycling of v-SNAREs to their starting compartment (Malhotra and Rothman 1988; Sato et al. 1997).

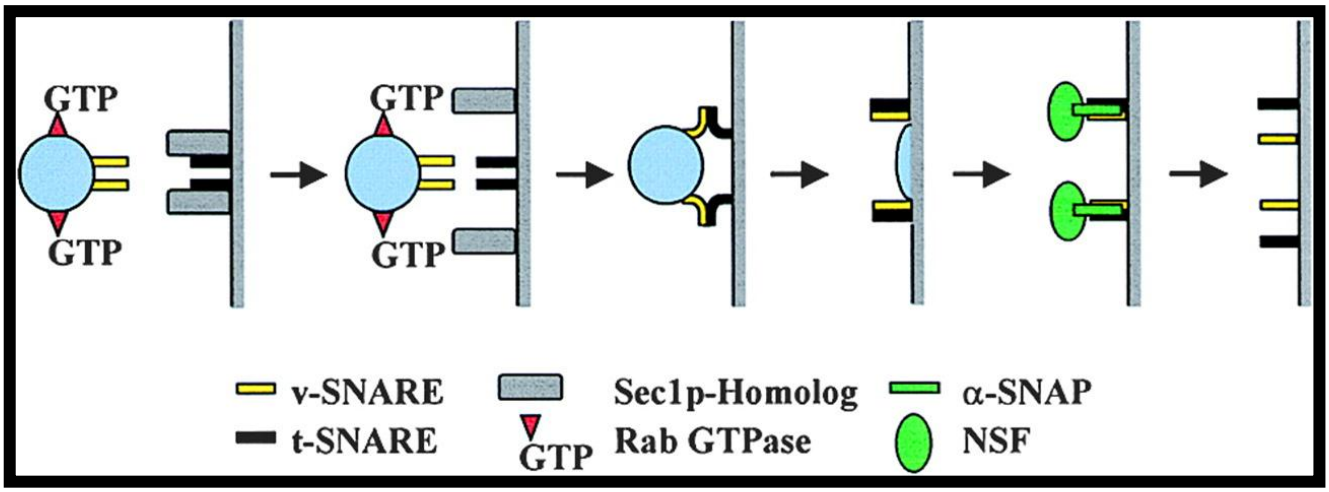

Figure 3: The SNARE mechanism of vesicle fusion

Vesicle fusion is mediated by SNARE proteins, a Rab GTPase, a Sec1p-Homolog, α-SNAP and NSF. The v-SNARE and a Rab-type GTPase associated with the vesicular membrane recognize the t-SNARE and a Sec1p homolog on the surface of the target membrane. Sec1p maintained the t-SNARE in an inactive form. After recognition (docking), the Rab-GTP displaces the Sec1p homologs and exposes the t-SNARE which becomes active to interact with the v-SNARE and mediates vesicle fusion. α-SNAP and NSF work in collaboration to disassociate the v-SNARE/t-SNARE bundle to prepare for another fusion event. Figure copied from (Sanderfoot, Kovaleva et al. 1999).

8. Endocytosis process

The endocytosis machinery of eukaryotes involved in the internalization of protein cargoes to endosomes/prevacuoles is well conserved in plants. Internalization of cargo proteins is mediated by specific membrane receptors. The cargo/receptor complex is packaged into vesicles and then delivered to EE which have been identified as TGN in plants (Russinova et al. 2004). Another endocytotic pathway involving lipid rafts has been proposed: cargo proteins are internalized into cells at plasma membrane micro-domains (Borner et al. 2005; Murphy et al. 2005; Samaj et al. 2005). Mono-ubiquitination is an endocytic signal for many membrane receptors and in some cases it plays a role in sorting into internal vesicles of MVB (Mukhopadhyay and Riezman 2007). ESCRT complexes (endosomal sorting complexes required for transport) are involved in the internalization of ubiquitylated proteins. The cargo proteins can be transported from the TGN to MVBs (identified as late endosomes). The complexes named ESCRT-I, -II and III (endosomal sorting complexes required for transport) collaborate step by step to achieve transport of proteins. The role of ESCRT-0 is to cluster ubiquitylated cargoes, ESCR-I and ESCRT-II form membrane invaginations and ESCRT-III causes vesicle scission (Bassereau 2010). ESCRT complexes are well characterized in animal and yeast and are likely to have a conserved role in all eukaryotic cells including plants (Bassham and Blatt 2008). Figure 4 (Contento and Bassham 2012) indicates the components of the plants endocytic pathways and the sorting pathways.

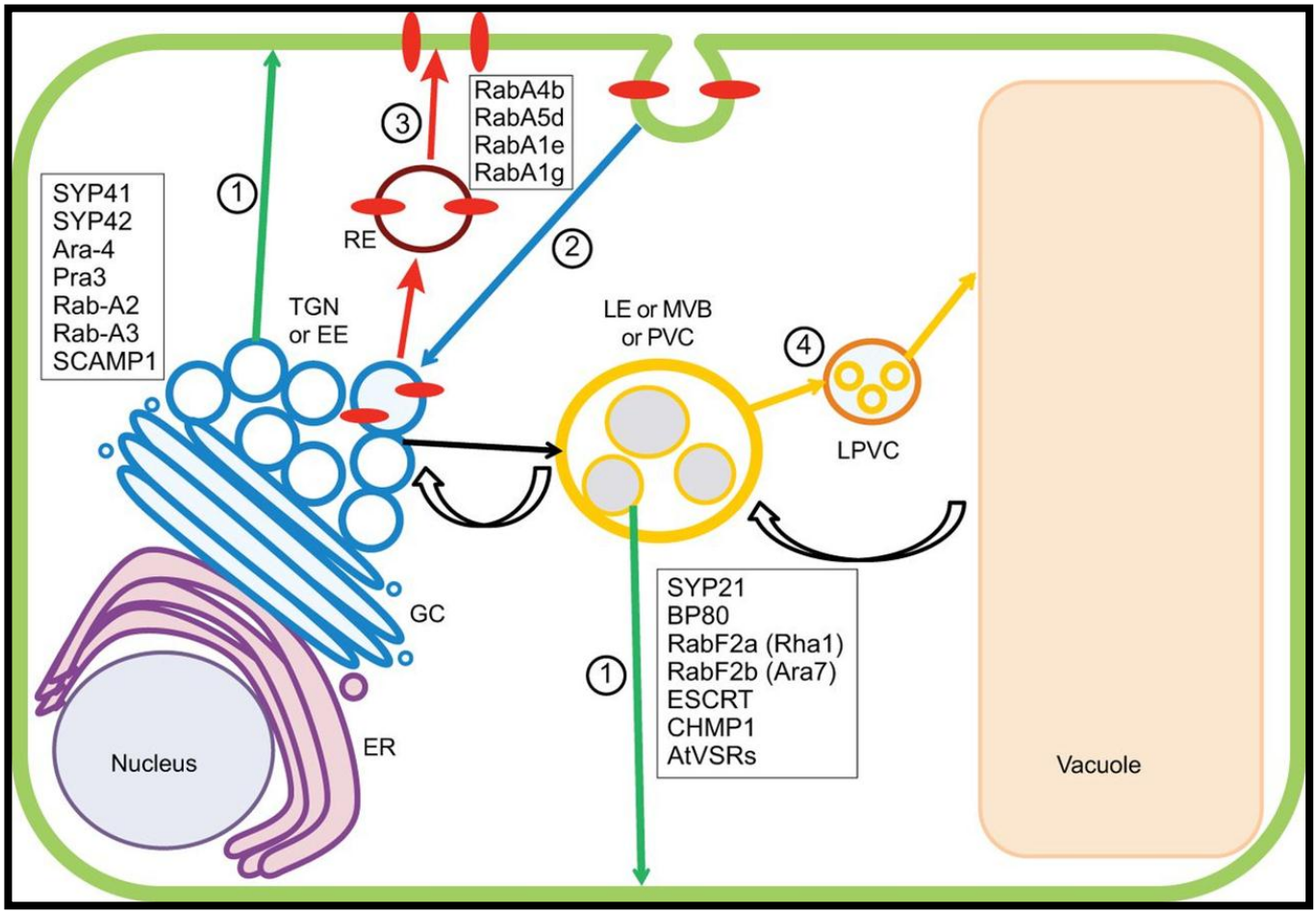

Figure 4: The sorting and endocytic pathway in plants.

The endomembrane is constituted of the nucleus, endoplasmic reticulum (ER), Golgi complex (GC), trans-Golgi network (TGN) or early endosome (EE), late endosome (LE) or multivesicular body (MVB) or prevacuolar compartment (PVC), late prevacuolar compartment (LPVC), vacuole (VAC) surrounded by the tonoplast, recycling endosome (RE), plasma membrane (PM). The TGN or EE is the start point of four principals sorting and endocytotic pathways.

-Pathway 1 (green arrows) indicates a sorting route to the PM that passes through the TGN and the MVB.

-Pathway 2 (blue arrow) is the endocytotic process from plasma membrane to the TGN.

-Pathway 3 (red arrow) represents a recycling pathway, by which PM proteins (red ovals) returned to the PM.

-Pathway 4 (orange arrow) shows the sorting route to the VAC. Transport from the TGN to MVBs is indicated by a black arrow and the retrograde transport from the VAC to the MVB is showed by curved black arrows.

Proteins associated with the different organelles are listed in the figure: TGN (Bassham et al., 2000; Chow et al., 2008; Lam et al., 2007; Sanderfoot et al., 2001; Ueda et al., 1996), with the RE (Geldner et al., 2009; Preuss et al., 2006;Rutherford and Moore, 2002), with MVBs (Bottanelli et al., 2012; Jiang and Rogers, 1998; Lee et al., 2004; Li et al., 2002; Paris et al., 1997;Sanderfoot et al., 1998;Spitzer et al., 2009).

Figure copied from (Contento and Bassham 2012)

9. Vacuoles

Vacuoles are the endpoint of the secretory system for soluble vacuolar proteins. Plant vacuoles vary in size, function and content in the different tissues and cell types. Most plant cells possess a large central vacuole, which can occupy more than 90% of the total cell volume. Plant cells can also contain distinct vacuole types at particular stages of development (Marty 1999). Vacuoles are highly dynamic compartments surrounded by the tonoplast. Vacuoles assume fundamental physical and chemical functions indispensable for cell viability such as mechanical support by turgor, which is also involved in cell growth. Moreover vacuoles participate in homeostasis of ions and water, degradation, storage of many plant compounds such as ions, pigments, secondary metabolites, enzymes involved in defense (Frigerio 2008; Marty 1999). After pathogen infection, vacuoles may respond by eliminating the pathogen through autophagy. If the cell is not able to recover a normal physiological function, it activates a specific program of cell death which leads to mobilization of hydrolytic enzymes in the cytosol to permeabilize the tonoplast (Gietl and Schmid 2001; Greenwood et al. 2005; Hara-Nishimura et al. 2005). Vacuoles are also involved in programmed cell death (PCD), which is an active process of selective elimination of certain cells upon biotic or abiotic stresses. Two mechanisms of PCD involving vacuoles in plants have been described : (i) disruption of the tonoplast causing the release of vacuolar contents in the cytoplasm, efficient against intracellular pathogens, (ii) and fusion of the tonoplast with the plasmalemma, releasing vacuolar contents in the cell wall, efficient against extracellular pathogens (Hara-Nishimura and Hatsugai 2011).

.

Part 2: Vacuole biogenesis

1. Vacuole types

Regarding all the diverse functions the vacuole assumes, the theory of multiple vacuole types was proposed. The presence of LV and PSV was demonstrated by different studies. However, recently this model has been challenged by a series of studies. Existence of distinct vacuole types was provided by using pH-sensitive dyes, such as Neutral Red (Di Sansebastiano, Paris et al. 1998). Upon staining, acidic and neutral compartments were detected within a single cell. For instance, the mesophyll cells of *Mesembryanthemum crystallinum*, presented two different vacuoles, an acidic and a neutral vacuole. The acidic vacuole had a maximal volume at the end of the night and shrunk during the day, as malic acid was retrieved (Epimashko et al. 2004).

At the molecular level, two soluble vacuolar GFP markers have been described : the GFP-Chi and the Aleu-GFP possessing different vacuolar sorting determinants (VSD) from tobacco chitinase A or barley aleurain. They were localized in PSV and in LV respectively (Di Sansebastiano et al. 1998; Di Sansebastiano et al. 2001). During cell senescence, small acidic vacuoles named senescence-associated vacuoles (SAV) appeared in soybean mesophyll and guard cells. SAVs were characterized by the presence of senescence-specific cysteine protease SAG12 (Otegui et al. 2005).

The presence of distinct vacuoles was also demonstrated using fluorescent reporters of tonoplastic aquaporins, TIPs (Tonoplast Intrinsic Proteins). TIPs were used to characterize *A.thaliana* vacuoles which contain 10 TIP isoforms: 3 γ-TIPs, 3 δ-TIPs, 1 α-TIPs, 1 β-TIPs, 1 ε-TIPs, 1 ζ-TIPs (Johanson et al. 2001). Based on tissue expression analysis, the ε-TIP and δ-TIP are preferentially expressed in roots, and in floral organs. γ-TIP3 and ζ-TIP are expressed in flowers, whereas α-TIP and β-TIP were expressed during seed maturation, and δ-TIP1, δ-TIP2, γ-TIP1 and γ-TIP2 are expressed during early stages of seed development (Frigerio et al. 2008). δ-TIP3 is also called DIP (Dark-Induced Protein). It has been found in root tip cells and developing seeds (Culianez-Macia and Martin 1993). In barley and pea root tip cells, two different vacuoles were characterized: PSV was characterized by the presence of α-TIP and the storage protein barley lectin; and the LV was characterized by the presence of γ-TIP and aleurain (Paris et al. 1996). Immunolocalisation experiments showed that α-, δ- and γ-TIPs did not colocalise in some plant cells (Jauh et al. 1999). In barley aleurone protoplasts, treated with ABA (Absissic Acid) or gibberellic acid, a second kind of vacuole was generated

containing α-TIP which was physically separated from the PSV (Swanson et al. 1998). In 1999, Jauh *et al.* showed that α-, δ- and γ-TIP did not colocalise in some plant cells, therefore some vacuoles were identified with two different TIPs.

1.1. The lytic vacuole

The LV is an acidic compartment that contains enzymes analogous to the lysosomal enzymes of animal cells. This vacuole is important to maintain turgor pressure for the storage of metabolites, and to sequester xenobiotic compounds (Taiz 1992). The barley cysteine protease aleurain was used as soluble reporter for this vacuole (Di Sansebastiano et al. 1998; Flückiger 1999; Paris and Rogers 1996). Several studies supported that the LV tonoplast contains the aquaporin **γ**-TIP (Barrieu et al. 1998; Höfte and Chrispeels 1992; Jiang et al. 2000; Marty-Mazars et al. 1995; Paris and Rogers 1996). However, Hunter *et al.,* in 2007 failed to detect γ-TIP in LV of meristem and stele cells of pea root tips or in cells of developing Arabidopsis embryos.

1.2. The protein storage vacuole

Seed cells can have up to three different vacuoles with different functions in one single cell: a LV, a vegetative storage vacuole (neutral) and a seed PSV (Di Sansebastiano et al. 1998; Di Sansebastiano et al. 2001; Hoh et al. 1995; Paris and Rogers 1996).

The vegetative storage vacuole was found in specialized vegetative cells in response to wounding or to developmental switches (Jauh et al. 1998). δ-TIP was identified as its tonoplast marker (Jauh et al. 1998; Neuhaus and Rogers 1998; Park et al. 2004).

The PSV was found in cells from storage tissue of seeds and fruits. It major function was the storage of proteins such as 7S lectin, 2S albumin and 11S globulins (Herman and Larkins 1999; Muntz 1998; Okita and Rogers 1996). PSV can be labeled with α- and δ- TIPs antibodies (Jiang et al. 2000; Paris et al. 1996; Swanson et al. 1998). PSV can contain subcompartments, globoids and large crystalloids. Globoids contain for example aleurain, while the crystalloids are composed of crystalline 11S globulin. The matrix compartment contains a mixture of 7S lectins and 2S albumins. DIP was discovered to be associated with the crystalloid membranes (Jiang et al. 2000).

1.3. Evidence supporting unique vacuole

In root tips, only one vacuole containing storage proteins was characterized by both α-TIP and γ-TIP (Olbrich et al. 2007b). Data supporting the presence of several vacuoles in the same cell is rather an exception, limited to some particular stages of development, or in some tissue types (Frigerio et al. 2008). For instance, it has been shown that when soybean plants were subjected to changed physiological conditions, the γ-TIP marker diminished while the δ-TIP marker became present in the tonoplast indicating the conversion of a lytic vacuole to a vegetative storage vacuole (Murphy et al. 2005). In a study, the different fluorescent TIPs (α-, γ and δ-TIP) detected the same vacuoles in *A.thaliana*. Indeed, even the developing embryos which contain only a PSV, all three markers localized in its tonoplast. The expression profile of the TIP markers was established: γ-TIP and δ-TIP were limited to vegetative tissue except for root tips, while α-TIP was specifically expressed during seed maturation (Hunter et al. 2007).

2. Vacuolar sorting determinants

Plant vacuolar proteins are synthesized as precursors with propeptides, which are proteolytically removed upon targeting to the vacuole. These propeptides may also contain the VSD (Matsuoka and Nakamura 1999; Neuhaus and Rogers 1998). Three different types of VSD have been described: sequence-specific (ssVSD), C-terminal (ct-VSD) and condensation dependent (conVSD) (Neuhaus and Rogers 1998).

2.1. The ssVSD

Proteins carrying an ssVSD are addressed to LV (Holwerda et al. 1992; Koide et al. 1999; Matsuoka and Nakamura 1991). The barley aleurain and sweet potato sporamin have both been identified with an N-terminal propeptide that contains an NPIR motif. A sporamin mutant lacking the propeptide was secreted supporting the role of the propeptide in vacuolar targeting. The isoleucine (Ile) amino acid played a central role, however it can be replaced only with a leucine (Leu) (Kirsch et al. 1996; Matsuoka and Nakamura 1999; Matsuoka and Neuhaus 1999). Other proteins have been identified with a ssVSDs with no NPIR motif, but an essential Ile or Leu could be identified. The ssVSD can be localized in N-terminal, C-terminal (castor bean 2S albumin, (Brown et al. 2003), or in an internal parts of vacuolar proteins (Frigerio et al. 2001).

2.2. The c-terminal VSD

A C-terminal propeptide was found to be necessary for vacuolar targeting of several proteins. Ct-VSDs were identified at the C-terminal end of these propeptides of several vacuolar proteins: barley lectin (Bednarek et al. 1990), tobacco chitinase A (Neuhaus et al. 1991a), phaseolin (Frigerio et al. 1998). A consensus sequence could not be identified, but these sequences seem to be enriched in hydrophobic amino-acids (Matsuoka and Neuhaus 1999). Complete deletion of ct-VSD leads to protein secretion but many single point mutations or partial deletions of tobacco chitinase or barley lectin ct-VSDs had no effect on protein sorting (Dombrowski et al. 1993; Neuhaus et al. 1994). However, terminal glycines or terminal N-glycosylation caused secretion of the proteins. Therefore, no critical motif is important in ct-VSD for the correct targeting of the protein, but its three-dimensional structure might be involved in binding to a vacuolar receptor (Nielsen et al. 1996).

2.3. The psVSD

The third class of vacuolar sorting determinant is the condentation-dependant (conVSD) (Neuhaus and Rogers 1998). It has been described for the phytohemagglutinin of common bean and for legumin-like proteins. The conVSD signal was localized in different regions of the polypeptides or in the PSI (Protein-Specific Insert) domain of phytepsin (Kervinen et al. 1999; Tormakangas et al. 2001) supporting an important role for 3D structures (Tague et al. 1990; Vitale and Raikhel 1999). Therefore, the aggregation process was proposed as a possible mechanism for vacuolar sorting of these proteins (Vitale and Chrispeels 1992).

3. Vacuolar sorting receptors

3.1. The VSRs

A vacuolar receptor involved in trafficking of ssVSD proteins was identified from pea CCVs and was called BP-80 (Binding Protein of 80kD) (Kirsch et al. 1994; Paris et al. 1997). This receptor was able to bind barley aleurain and sporamin ssVSDs and the C-terminal propeptide of Brazil nut 2S albumin in a pH-dependent manner (Kirsch et al. 1994; Kirsch et al. 1996). In *A.thaliana,* there are seven homologues of BP80 the AtVSR multigene family (Ahmed et al. 2000; Neuhaus and Paris 2005).

3.1.1. Structure of VSR

VSR proteins are class I membrane proteins. They are constituted of a large N-terminal luminal domain, a transmembrane domain (TM) and a cytosolic tail domain. The luminal domain contains a PA (Protease-Associated) domain, followed by a large VSR-specific domain and three Cys-rich EGF (Epidermal Growth Factor) repeats (fig. 5).

3.1.2. Localisation of VSR

Antibodies produced against pea BP-80 detected VSRs in the PVC in pea and tobacco cells (Li et al. 2002). Different homologs of BP80 were identified such as PV72 found in pumpkin PAC (Shimada et al. 1997) and AtELP was identified in *A.thaliana* (Da Silva Conceiçao et al. 1997; Paris et al. 1997; Sanderfoot et al. 1998). Another study localized AtVSRs mainly in PVC and to a minor extent in TGN (Miao et al. 2006).

3.1.3. Function of VSR

Several studies supported the involvement of VSRs in protein sorting to LV. BP80 is able to bind *in vitro* barley aleurain ss-VSD and prosporamin from sweet potato (Kirsch et al. 1994). However the receptor does not bind to the ct-VSD of barley lectin (Kirsch et al. 1996). A chimeric reporter protein was constructed using a mutated form of proaleurain (lacking ss-VSD) connected via its C-terminus to the BP-80 TM domain and cytoplasmic tail. When expressed in tobacco cells, the construct was correctly addressed to the PVC, where the proaleurain moiety was processed to mature form (Jiang and Rogers 1998).

It has been proposed that VSRs are involved also in storage proteins targeting to PSV. The AtVsr1 null mutant leads to secretion of some seed storage proteins. However, the effect on storage protein transport is partial (Shimada et al. 2003a). This has been interpreted as evidence for VSRs as salvage receptors for stray storage protein that escaped from their classic route (Craddock et al. 2008; Hinz et al. 2007). More recently, Zouhar et al., (2010) observed a mistargeting of storage proteins in several simple VSR mutants, VSR1, VSR3 and VSR4, indicating that VSR could also be receptors for specific storage cargoes in seeds and in vegetative tissues (Zouhar et al. 2010).

The short cytosolic tail of VSRs contains a tyrosine motif (YMPL) which interacts with the muA component of adaptor protein type 1 complex (AP-1), that is involved in the formation of CCVs (Happel et al. 2004). Mutations of this domain resulted in accumulation of VSR2 in the vacuole in *Nicotiana tabacum*, indicating that recycling of VSR is impaired (Foresti et al. 2010; Saint-Jean et al. 2010). The mutations also showed that VSRs use two pathways to target vacuolar proteins: the major route leading directly to the lytic vacuole, and a minor route retrieving missorted ligands from the apoplast, a pathway requiring dipeptide Ile-Met motif in the cytosolic tail (Saint-Jean et al. 2010).

3.2 The RMRs

A second family of putative receptors was identified by their homology to the PA domain of the VSR proteins. They were named Receptor-Membrane-RingH_2 or RMR (Cao et al. 2000; Jiang et al. 2000). The genome of Arabidopsis harbours six homologs (AtRMR1 to AtRMR6) (Park et al. 2005).

3.2.1. Structure of RMRs

These proteins are composed of an N-terminal luminal domain restricted to the PA domain, but lacking EGF-repeats, a transmembrane domain, and a cytosolic tail with a RING-H_2 (Really Interesting New Gene, with two His) domain, and most have also a C-terminal serine-rich region (lacking in AtRMRs 1, 5, 6) (Jiang et al. 2000; Park et al. 2005) (fig. 5). The luminal PA domain shared with VSR proteins is known in other protein families to participate in ligand binding (Cao et al. 2000; Mahon and Bateman 2000). It constitutes a protein-protein interaction domain in addition to mediating substrate recognition for peptidases. The Ring-H_2 domain found in RMRs is of the C3H2C3 type. This type of domain

is likely to be associated with an E3 ligase activity (Joazeiro and Weissman 2000; Tranque et al. 1996).

3.2.2. Localisation of RMR

Only few studies were performed on RMR localization. In Arabidopsis and tomato seeds, antibodies against RMR detected the same organelles as antibodies against DIP. DIP is associated with the crystalloid precursors of PSV during seeds development. The DIP-positive organelle was proposed by Jiang as PVC for PSV which fuse to it to deliver internal proteins (Jiang, Phillips et al. 2000).

Studies performed by Park *et al*., (2005) focused on the localization (by immunohistochemistry) and the biological function of AtRMR1 in leaf protoplasts. They found that endogenous AtRMR1 and AtRMR1-HA colocalized with DIP but not with AtPEP12p (a marker of the PVC). The colocalization of AtRMR1-HA and phaseolin in leaf protoplasts was supported by the specific *in vitro* binding of the luminal part of AtRMR1 to the phaseolin ct-VSD. Their results suggested that AtRMR1 functions as cargo receptor by interacting with the ct-VSD of phaseolin, which is transported to the PSV through the DIP/AtRMR1-positive organelle (Park et al. 2005).

AtRMR2 binds strongly to the chitinase ct-VSD but only if presented with a free C-terminus and only weakly to the proaleurain ssVSD. Immunogold labeling with AtRMR2 specific antibodies revealed a similar distribution to cruciferin in the GA stacks, and in DVs. RMR may associate with protein aggregates carrying ct-VSD during transit from the GA to the vacuole by DVs (Park et al. 2007). This pathway would be distinct from the CCVs pathway for ssVSD targeting through the VSR. This model is consistent with the results provided by Hinz *et al*., (2007) who localized *At*RMR2 in the early stack of GA and in DVs (Hinz et al. 2007).

Additionnally, it has been recently demonstrated that OsRMR1 proteins localized in GA, TGN, PSV and in an organelle identified as PVC for PSV called (PVCs) in both rice cultured cells and in developing rice seeds. This localization seems to be conserved since OsRMR1 proteins were also found in Golgi, TGN, and PVCs in BY-2 and Arabidopsis cultured cells (Shen et al. 2011; Wang et al. 2011).

3.2.3 Function of RMRs

RMR proteins were found in strategic places: in the crystalloid membrane in PSV Arabidopsis seeds (Jiang et al. 2000) and in *cis*-Golgi stacks and DVs (Hinz, Colanesi et al. 2007). This localization is consistent with the studies of Castelli and Vitale (2005), which showed that the aggregation of the storage protein phaseolin depended on the presence of the ct-VSD and was an early event in the *cis*-Golgi stacks. RMRs have been detected in the PSV crystalloids whereas neither the lytic nor the storage protein tonoplast contained VSRs (due to recycling) (Jiang et al. 2000). Therefore, RMRs have characteristics of protein receptors which traffic through the Golgi complex and PVC to PSV.

It has been shown that *At*RMR2 (protein JR702) and its ligands were not dissociated at low pH (Park et al. 2007). This observation suggested that RMRs either use a different mechanism to release their ligands, or are not recycled from an acidic PVC and thus accompany their cargos into the PSV. Two hypotheses were proposed: individual storage proteins could bind to RMR proteins and act as nuclei for further condensation of storage proteins. Alternatively, storage protein could form microaggregates which would expose on their surface free ct-VSDs accessible for RMRs-cargo interaction. Therefore, RMRs could function as storage protein receptor or assemble factors without being recycled. (Hinz et al. 2007).

However the role as a receptor was recently questioned since simple KO mutants of each AtRMRs did not show any missorting of storage proteins. A system to screen Arabidopsis mtv mutants (for ‘modified transport to the vacuole’) which are affected in the trafficking of the marker VAC2 was used in simple KO RMR mutants (Sanmartin et al. 2007). VAC2 is a fusion protein constituted of the ligand CLAVATA3 fused to the barley lectin ct-VSD (Rojo et al. 2002). If VAC2 is correctly transported to the vacuole, where it is inactive, plants develop normal meristems. If VAC2 is not targeted to the vacuole it will be secreted causing premature termination of shoot apical meristems and flower meristems, allowing identification of the mtv mutants. Simple KO AtRMR mutants had a normal meristem development, indicating that VAC2 was correctly addressed to the vacuole. There was also no accumulation of precursor forms of 12S globulins and 2S albumins, indicating that their transport was not affected either. Double AtRMR KO mutants of AtRMR1&2 and AtRMR3&4 also did not show any seed storage protein phenotype (Zouhar et al. 2010).

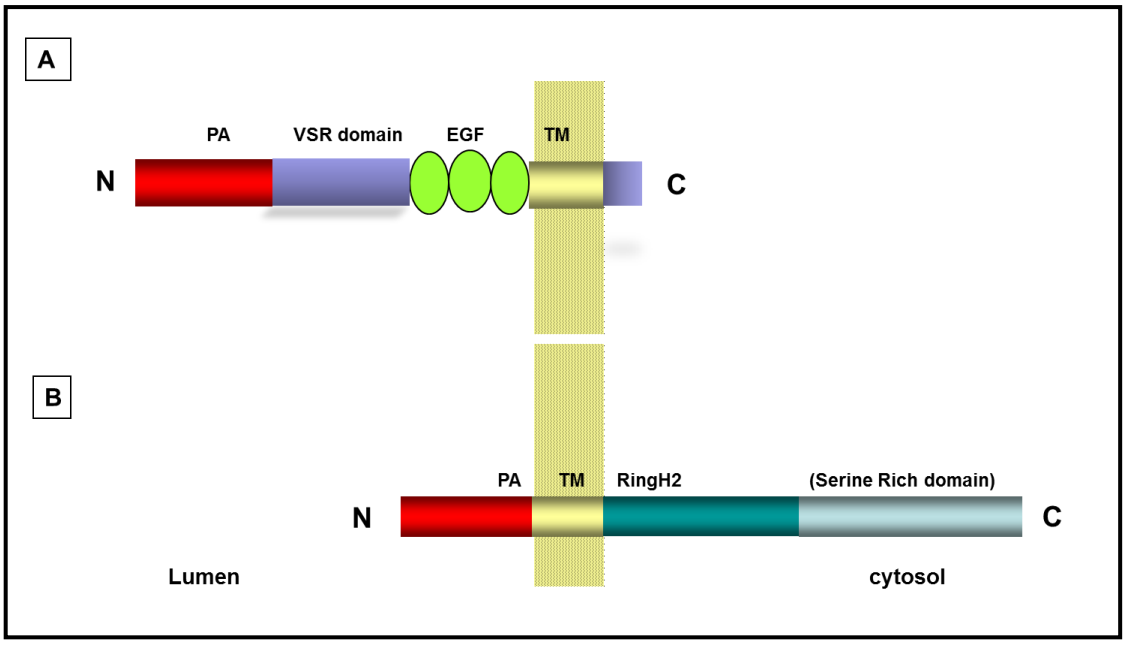

Figure 5: Structure of plant vacuolar receptors

- **(A)** ***VSRs*** have a Protease –Associated domain (PA red), a VSR-specific domain (purple), three Cys-Rich EGF Repeat (Epidermal Growth Factor) (green), and a single trans-membrane domain (TM), the cytosolic domain of AtVSRs is restricted to a small Tail (purple).

- **(B)** ***RMRs*** have a Protease-Associated Domain (PA) (in red), a single TM. At the cytosolic part includes a Ring-H_2 Domain (blue) and for most RMRs a Ser-Rich Domain (grey).

4. Vacuolar sorting pathways

For vegetative cells, Neuhaus and Paris (2005) proposed two main pathways which could be identified in vegetative cells (fig. 6) (Neuhaus and Paris 2005). The route of proteins to the LV starts after recognition of their ssVSD ligands in the Golgi by the VSR receptors. The complex ligand-VSR complex is then transported by CCVs to the PVC (fig. 6B). Once in the PVC, the acidic pH causes ligand release and enables receptors recycling. Finally, the PVC fuses with the acidic vacuole (Jiang et al. 2000). In the other pathway, ct-VSD proteins are thought to be recognized by RMRs and sent to a storage vacuole. Mechanisms involved in the RMR pathways are unknown and their implication remains to be clarified (Neuhaus and Rogers 1998; Park et al. 2004) (fig. 6A). Recently, a new study supported the existence of particular PVC for PSV. In rice cultured cells and developing seeds, OsRMR1 was found in GA, TGN, PSV and a distinct organelle proposed to be a storage PVC (sPVC) (Shen et al. 2011). The effect of wortmannin (a specific inhibitor of mammalian phosphatidylinositol 3-kinases) was also indicative of these two different protein sorting pathways to the vacuole. In tobacco cells, treatment with 33 µM wortmannin caused the inhibition of the ct-VSD proteins transport to vacuoles, while the ss-VSD protein targeting were not affected (Matsuoka et al. 1995).

Since some vacuoles appeared labeled with both TIP isoforms (∂- and ɣ-TIP) (Jauh et al. 1999), it has been proposed that the LV and the PSV can fused to form a hybrid vacuole. It have been shown that the ct-VSD of barley lectin and ss-VSD of sporamin were both addressed to the same vacuole in transgenic tobacco plants (Schroeder et al. 1993). The hybrid vacuole model allows a possible switch of the vacuole from storage to lytic functions (Murphy et al. 2005). In Arabidopsis seedlings, two pathways for TIP targeting to the tonoplast were proposed: one pathway (taken by TIP1;1) which is Brefeldin A (BFA) and therefore Golgi-dependent sensitive and another pathway (route taken by TIP3;1 and TIP2;1) which is Golgi-independent and BFA insensitive, but sensitive to C834 a newly discovered drug (Rivera-Serrano et al. 2012).

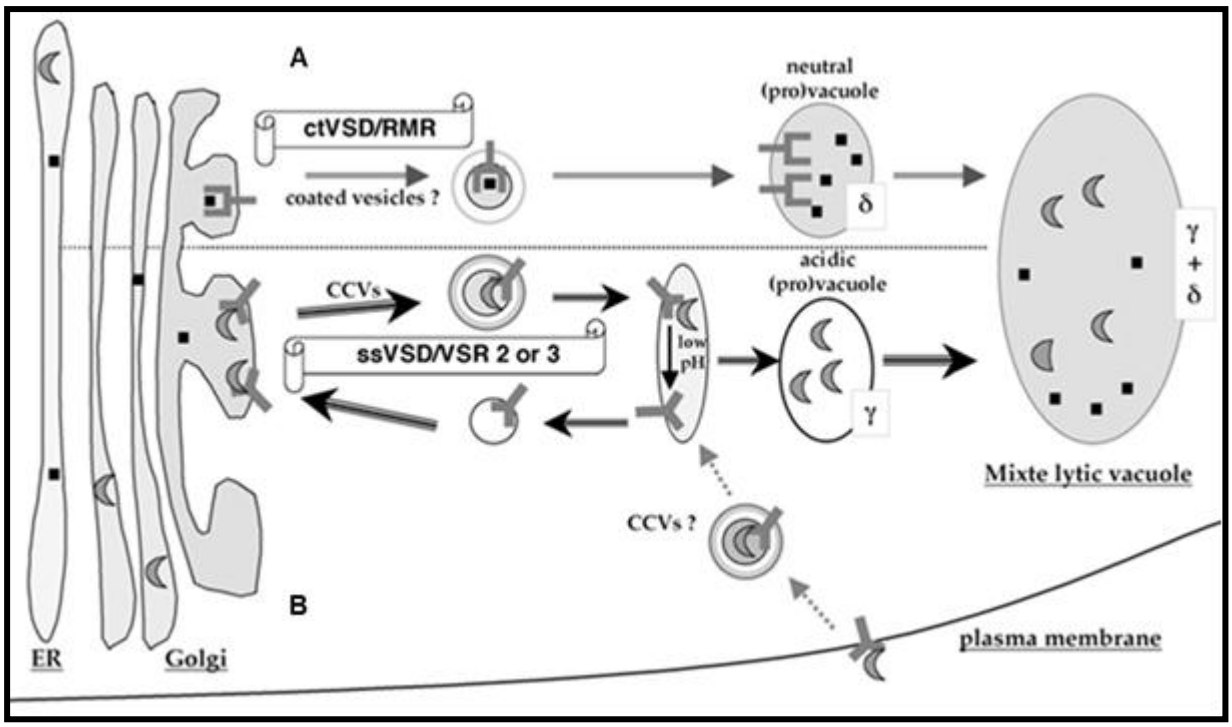

Figure 6: Model of vacuolar sorting pathways in vegetative cells.

(A) In the biogenesis of neutral vacuoles, RMR receptors bind the ctVSD of proteins in the Golgi, and then the complex is transported to the neutral prevacuole. These neutral prevacuoles have a tonoplast with δ-TIP isoforms. They then may fuse with a preexisting large hybrid vacuole.

(B) In the biogenesis of lytic vacuoles, VSRs (subfamily VSR2 or VSR3) bind the ssVSD of proteins in the Golgi, the complex is then transported by CCVs to the acidic prevacuolar compartments. The acidic pH causes ligand release and the receptors are recycled to the Golgi. These acidic prevacuoles have a tonoplast with γ -TIP. They then fuse with a preexisting large acidic or hybrid vacuole. Figure copied from (Neuhaus and Paris 2005)

5. *De novo* vacuole biogenesis

De novo vacuole biogenesis is still not characterized, however, it has been postulated that vacuoles can be generated from small pre-existing vacuoles during cell development (Zouhar and Rojo 2009). For instance globoids, with characteristics of LV, could correspond to preexisting LVs that are incorporated inside of PSV (Frigerio et al. 2008; Jiang et al. 2001).

Autophagy could be an important mechanism of vacuolar enlargement. In meristematic daughter cells, the LV was formed from small vacuoles which enlarged by autophagy (Inoue and Moriyasu 2006). A KO mutant of *VCL1* gene blocked the LV formation and showed an accumulation of autophagosomes during embryogenesis. Homologues of the *VCL1* gene in yeast and mammals are involved in autophagosomes fusion with the vacuole (Zouhar and Rojo 2009).

The PVC origin of the PSV was supported by a study in seeds which showed that the *vamp727/syp22* double mutant presented a fragmented PSV and partial secretion of storage proteins in seeds (Ebine et al. 2008). VAMP727 and SYP22 are known to be involved in SNARE complex formation which plays a role in the fusion between PVC and PSV (Ueda et al. 2004; Uemura et al. 2004).

Part 3: *P. patens* as model system

1. P.patens a simple system

1.1 The life cycle of *P.patens*

One of the advantages of moss is its relatively simple developmental pattern and the dominance of the haploid gametophyte in the life cycle (Cove et al. 1997). Studies have mostly been performed on species like *Funaria hygrometrica, Ceratodon purpureus,* and *Physcomitrella patens*. The main advantage who lead scientist to choose *P.patens* for genetic approaches was the possibility to perform *in vitro* crosses. *P.patens* is monoecious meaning that both sexual organs can be present on the same plant. This advantage, among many others, allows to grow it in very simple laboratory conditions to complete its life cycle (Cove et al. 1997). Like other land plants, *P.patens* shows an alternation between a haploid phase and a diploid phase. However, in contrast to ferns and seed plants, in mosses the haploid phase is the dominant. The haploid phase produces gametes through the generation of the gametophyte and the diploid phase produces haploid spores by meiosis through the generation of the sporophyte (fig. 7).

The gametophyte stage starts from a spore's germination which produces the protonema. This comprises network of filamentous cells displaying one-dimensional apical growth. The protonema extends by division and produces side branches. Most side branches develop into filaments, but some develop into the leafy shoots called gametophores. Once mature, gametophores give rise to sexual organs at their apex. The male gametes, or antherozoids, are produced in antheridia, whereas female gametes or egg cells are produced in archegonia. Self-fertilization is usual since both organs differentiate on the same shoot. The antherozoid reaches the archegonia, through water flux, and fuse with the egg cell to form a diploid embryo, the sporophyte. The sporophyte stage starts at fertilization and the zygote develops into a sporophyte, constituted of a diploid spore capsule which can contain up to 5000 haploid spores (fig. 7). Finally, spores germinate to produce the protonema of the gametophyte stage. *P. patens* develops in early summer in temperate zones. It grows along lakes and rivers on soil that has been exposed by falling water levels. Reproductive organ development is induced by short day. Fertilization needs temperatures below 18^{o}C (Engel *et al.*, 1968). As a result, sporophytes are produced in the late summer, and spores during winter. Several accessions are recognized, and the Gransden wild-type strain is widely used is by the hole community.

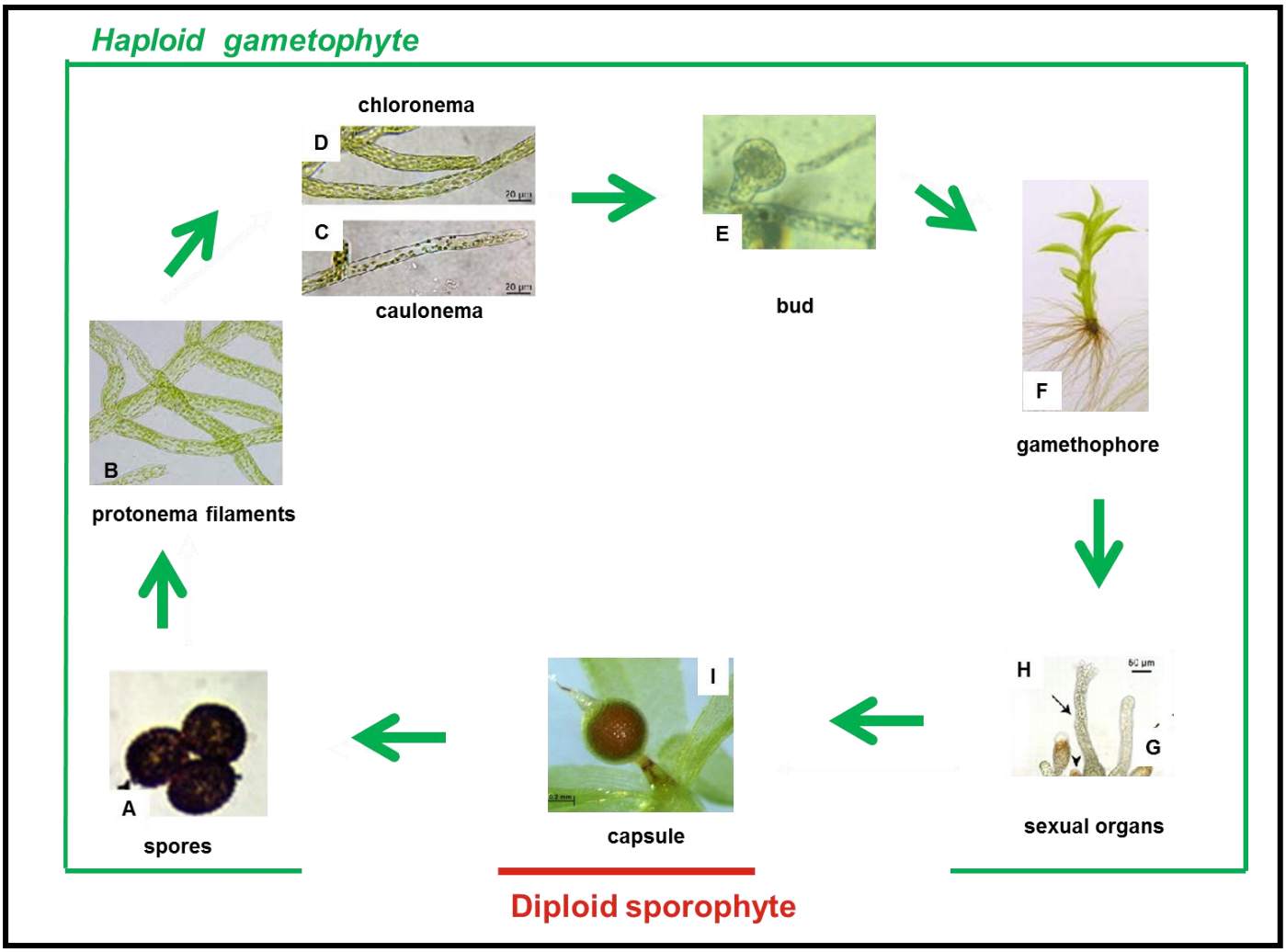

Figure 7: The life cycle of *Physcomitrella patens*

The *P.patens* life cycle is characterized by an alternation of two generations; the haploid gametophyte that produces gametes (yellow line) and the diploid sporophyte (red line). **(A)** Spores, **(B)** Protonema filaments composed of two types of cells; the caulonema **(C)** and the chloronema (**D).** Some side branches from caulonema cells can differentiate into buds **(E)** which give rise to gametophores **(F)** a meristematic structures bearing leaf-like structures, rhizoids and the sexual organs. When water is available flagellate sperm cells can swim from the antheridia **(G)** to an archegonium (**H**) and fertilize the egg within. The resulting diploid zygote **(I)** originates a sporophyte composed of a foot, seta and capsule, spores **(A)** are produced by meiosis of spore mother cells.

1.2. Tissue types

The development of moss is relatively simple, and it generates only a few tissues and cell types which can be observed directly by microscopy. The filamentous cells display apical growth, whereas gametophore stages display three-dimensional meristematic growth. A single stem cell resides at the apex of each filament and leaf. The simplicity of filamentous cells allows it to be monitored. The gametophores structure display developmental processes analogous to these of flowering plant.

1.2.1. The protonema

The first cell type produced by spores is the chloronema. Each chloronema cell contains about 150-250 chloroplasts, and cell plates between cells are perpendicular to the cell axis. Chloronema apical cells extend at a rate of 2-5μm.h^{-1} and divide every 12h (Reski 1998). After 5 days, some chloronema apical cells divide to give rise to the second protonema cell type: the caulonema. This second cell type contains fewer chloroplasts and its cell plate forms an oblique angle to the cell axis. These cells grow faster since their apical cells extend at a rate of 25 to 40μm h^{-1} and they divide every 6-8 h (Reski 1998).

1.2.2. Gametophores

Gametophores develop from buds, where the divisions form oblique cell plates to the axis of the cell. Cell divides following a characteristic pattern to form leaflets (Harrison et al. 2009). Gametophores are composed of a stem bearing a phyllids. Mosses are thus referred as non-vascular plants. Specialized conducting cells within moss gametophore 'stems' that transport water or nutrients may be homologous to the provascular cells in vascular plant (Ligrone et al. 2000). Provascular cells involve the auxin-signaling pathway and specific transcription factors (Rolland-Lagan 2008), which are both conserved in moss (Rensing et al. 2008). The gametophore is anchored by rhizoids cells which are functionally equivalent to root hairs. The same shoot can bear both sexual organs: the antheridia and archegonia, which produce the antherozoids, and eggs respectively. After fertilization, the zygote develops into the sporophyte, which is composed of a spore capsule.

1.3. Evolutionary position

The green lineage, also called the Chlorobiontes clade comprises; green algae (Chlorophyceae), and all land plant (Embryophytes) (Karol et al. 2001) (fig. 8). These organisms are characterized by chloroplasts, and they store amidon provided by photosynthesis. Plastids come from an early endosymbiosis of a unicellular eukaryote and cyanobacteria (Karol et al. 2001). Phylogenetic studies showed that Embryophytes have a monophyletic origin from an ancestor close to algae (Charophyceae). The first plants to colonize land by the early Silurian (430 million years ago) were Bryophytes, non-vascular including liverworts, hornworts and mosses. Recent phylogenetic investigations showed that moss is representative of the first land plant that colonized successfully into terrestrial niches (Renzaglia et al. 2007). Mosses diverged from seed plants more than 430 million years ago (Rensing et al. 2008; Theissen and Saedler 2001). However, gene families encoding most of the basic developmental `tool kit' identified in flowering plants are conserved in the genome of the moss *P.patens* (Rensing et al. 2008). Therefore, *P.patens* stands in an important phylogenetic position for providing information on the evolutionary development of seeds plant.

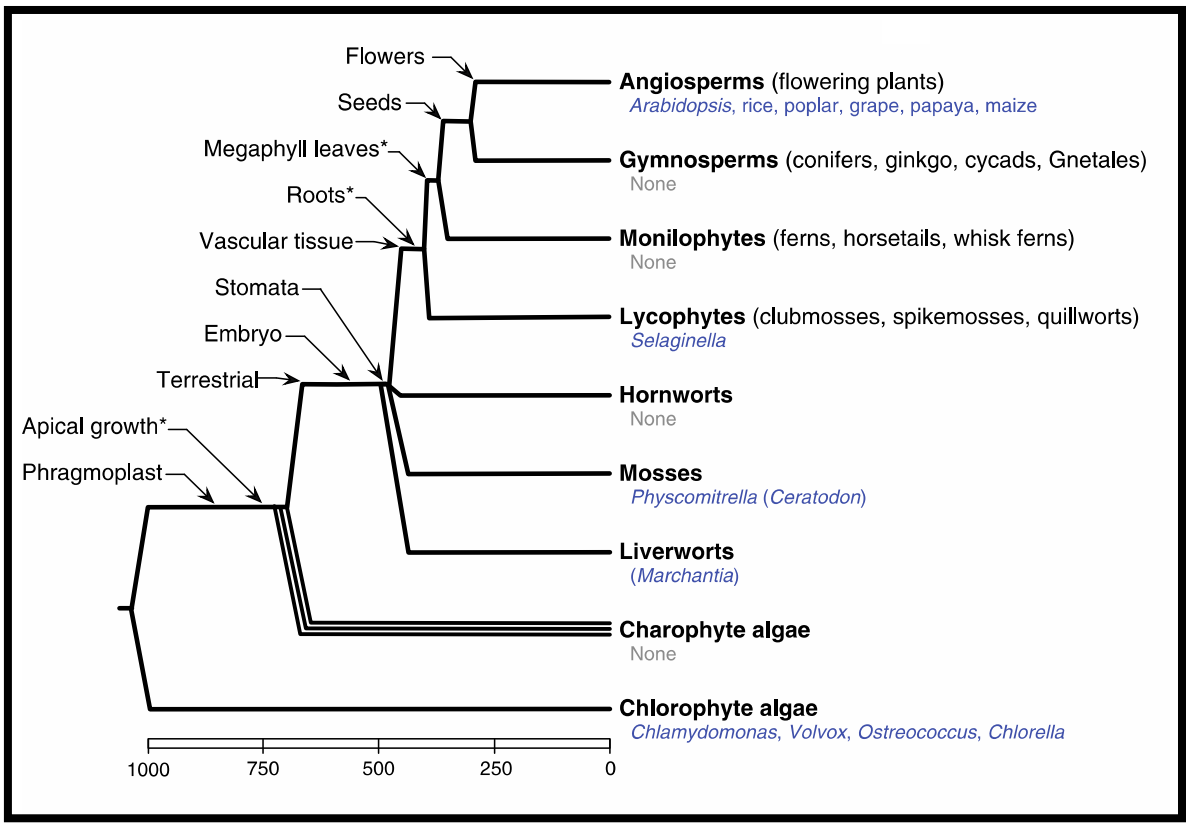

Figure 8: Phylogenetic tree of green plants

The phylogenetic tree indicates the position of mosses in the green plant lineage. The timeline at the bottom indicates the approximate time (millions of years before present) at which lineages diverged. Important morphological innovations are indicated with asterisks (*). Plants, with a complete sequenced and annotated genome, are indicated in blue color, those which are in progress are within parentheses. Figure copied from (Brown *et al.*, 2007).

1.4. Efficient gene targeting

1.4.1. Moss genome

Moss species show a surprisingly small range of genome sizes compared with angiosperms (Voglmayr 2000). The haploid genome size of *P. patens* has been estimated to 511 Mb. Its chromosomes estimated is n = 27. Over 300,000 ESTs from *P. patens* are publicly available, organized into over 36,000 putative transcripts and annotated (Lang et al. 2005).

1.4.2. Gene targeting

Bryophytes and especially mosses, have already been used as model systems to investigate the cellular and molecular mechanisms of plant biological process (Cove et al. 1997). Homologous recombination in *P.patens* was discovered by Schaefer (Schaefer and Zryd 1997). This very useful mechanism, along with the haploid gametophyte established *P.patens* as a model genetic system to study gene function. Moreover, the complete genome sequencing in 2007 was the ultimate tool allowing to choose gene sequences for further studies.

Gene Targeting (GT) allows the generation of specific mutations in a genome. In moss, GT is mediated by homologous recombination where the integration of foreign DNA sequences occurs via the DNA repair mechanism. Homologous recombination (HR) occurs efficiently in bacteria, yeast, and several filamentous fungi, and it contributed to many functional studies of their genomes. So far, *P.patens* is the only plant allowing specific targeting of its genome. The intended mutation can be a deletion, an insertion of a DNA sequence or any point mutation within the gene.

1.4.3. Efficiency

The GT efficiency *P.patens* ranges from 25 to 90% (ratio of targeted to random integration events), whereas this ratio hardly reaches 0.1% in plant and animal cells (Schaefer and Zryd 1997). It places *P.patens* in a unique position among model systems in multicellular eukaryotes (Schaefer and Zryd 1997).

1.4.4. Working strategy

In order to achieve GT in moss, the transforming DNA must carry a sequence homologue ranging from 600 to 1000 bp homologous to the target locus (Schaefer 2001). The transforming DNA must also carry a selectable marker. Depending on the desired effect on the genome, targeting vectors can be designed in two main ways: insertion and replacement vectors (Schaefer et al. 1991).

(i) An insertion vector carries a single homologous targeting sequence next to a selectable marker. It integrates into the moss locus by a single HR event, resulting HR in the recombination of the homologous sequence and an insertion of the selectable marker. This strategy is not suitable for gene deletion, since it generate an insertion of the transformant DNA.

(ii) Replacement vector carries two homologous targeting sequences flanking a selectable marker. The homologous sequences should flank the beginning (5'targeting sequence) and the end (3'targeting sequence) of the genomic DNA to replace (fig. 3A). The replacement vector integrates the genome by two HR events (at the 5' and 3' targeting sequences) resulting in gene conversion at the targeted genomic locus. This strategy is used to delete an entire coding sequence, to introduce a tag i.e. a fluorescent protein sequence or to generate a point mutation. The replacement vector can however also be insert by a single HR resulting in insertion rather replacement. PCR genotyping demonstrating both 5'and 3' HR events is required to discriminate between insertion and replacement (fig. 9).

HR often associated causes the integration of one or several tandem repeats of the transforming vector. Elimination of the resistance marker and of these repeats is performed by of the site-specific Cre-recombinase. Two LoxP sites have been previously introduced into the transforming vector flanking the resistance marker. Cre-mediated recombination after transformation eliminates direct repeats of the targeting sequences and the resistance marker leaving a single LoxP site (fig. 9B-C) at the deletion position.

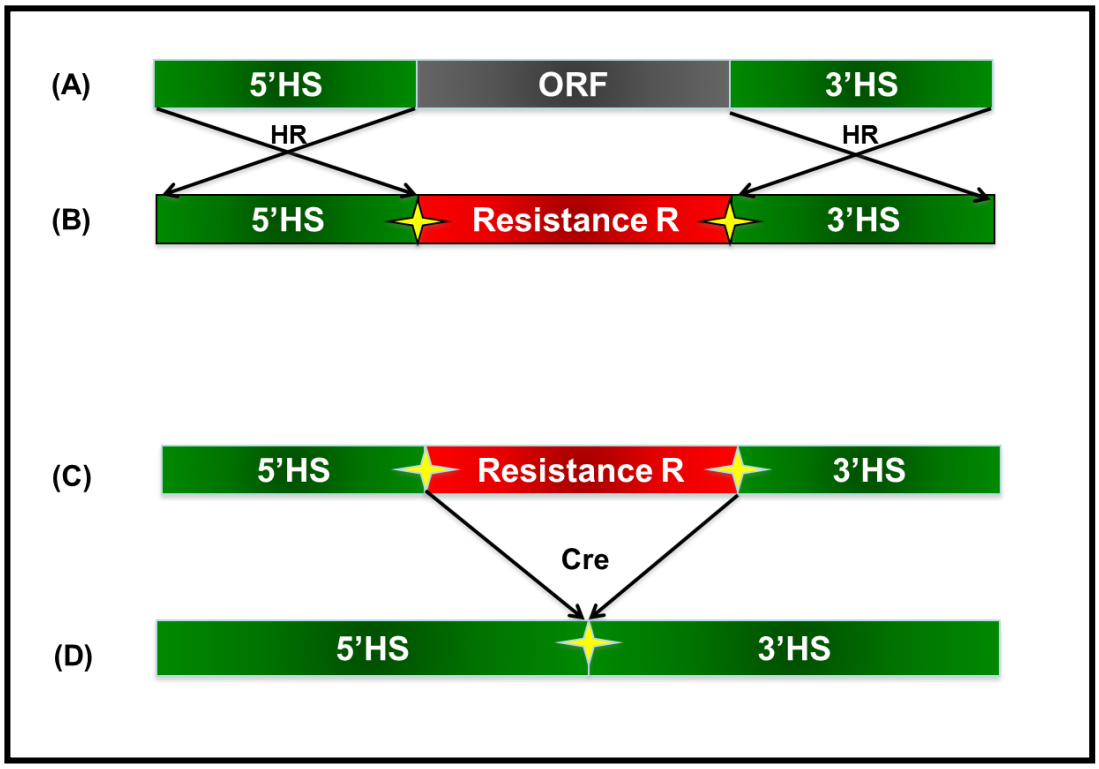

Figure 9: ORF deletion using a replacement vector in *P.patens*

(A) The Wild-Type genomic locus is constituted by the Open Reading Frame (ORF blue box) and the 5'and 3' extremity of the locus (green).

(B) The replacement vector carries the selection cassette (R) (red box), between two homologous sequences upstream and downstream of the gene locus (green box). Gene Conversion occurs by two homologous recombination events (HR) (at 3' and 5' extremity of targeted gene).

(C) Replacement of the ORF by one or several tandem repeats of the replacement cassette.

(D) Transient expression of the site-specific Cre-recombinase eliminates the resistance marker leaving a single LoxP site (yellow stars). It generates a complete deletion of the resistance cassette.

2. The moss vacuole

Root hairs, pollen tubes, and moss protonema undergo polarized cell growth where expansion occurs only at the tip of the elongating cells. Therefore the moss *P.patens is* particularly suitable as plant model system to investigate this specific type of polarized "tip growth". Comparison of seed plants and moss vacuoles presents similarity, which are detailed below.

2.1. Vacuole forms

In moss, so far, the only study performed on vacuole morphology revealed one single vacuole type in subapical protonema cells. Transgenic moss expressing a fusion construct of GFP and an Arabidopsis tonoplast t-SNARE, encoded by *AtVAMP3/SYP22,* were used for investigations into vacuolar structures. Investigation of the three-dimensional structure of vacuoles revealed that the vacuoles had diverse shapes and were continuously changing their structure. Three main vacuolar structures were categorized: tubular vacuoles, TVSs (Transvacuolar Strand), bubbles (Oda et al. 2009b) (fig. 10).

(i) Tubular vacuoles (fig. 10 B) have already been identified by electron microscopy in *Euphorbia characias* meristematic cells and in pea root tip cells (Marty 1978; Paris et al. 1996). More recently, 3-D reconstructions of shoot apical meristem cells of Arabidopsis, demonstrated that similar tubular vacuoles were interconnected with globular vacuoles (Segui-Simarro and Staehelin 2006). The role of TVMs (tubular vacuolar membranes) is still not defined. In *Vicia faba* guard cells, tubular vacuoles became transformed into spherical vacuoles during stomata opening, and in *A. thaliana* pollen tubes these tubular vacuoles expanded to form larger vacuoles (Hicks et al. 2004). Moreover, in tobacco BY-2 miniprotoplasts, tubular vacuoles appeared during vacuole expansion (Okubo-Kurihara et al. 2009). These results suggested that TVMs are not only involved in the storage of excess VMs but could be the destination of membranes retrieved from cell plates, during their maturation and used for vacuolar enlargement (Kutsuna et al. 2003) (fig. 10 B).

(ii) TVSs (fig. 10 C) are cytoplasmic tunnels through vacuoles that serve as routes for transport of organelle such as GA bodies, mitochondria, endosomes and amyloplasts (Nebenführ et al. 1999; Ovecka et al. 2005; Saito et al. 2005; Van Gestel et al. 2003). TVSs could be observed in various tissues and seem to have many roles. They were suggested to be

involved in gravisensing via regulation of amyloplast movement in endodermal cells, in determining the cell division sites, in nuclear positioning (Goodbody et al. 1991; Panteris et al. 2004; Saito et al. 2005). In tobacco BY-2 cells, TVSs appeared very dynamic since they underwent rapid changes by displacement, branching, and fusion (Hoffmann and Nebenfuhr 2004) (fig. 10C).

(iii) Spherical structures were described as ‘‘bubbles’’ (Saito et al. 2002). Their existence has been demonstrated using different tonoplast markers; GFP-AtVAMP3, AtTIP1;1-GFP, GFP-∂TIP, BobTIP26-1-GFP phosphate transporter homolog-GFP, and YFP-2xFYVE, a phosphatidylinositol 3-phosphate probe (Boursiac et al. 2005; Escobar et al. 2003; Reisen et al. 2005; Sheahan et al. 2007; Uemura et al. 2002; Vermeer et al. 2006). They are located within the vacuoles, and are formed from a double membrane sandwiching a thin layer of cytoplasm (Reisen et al. 2005; Saito et al. 2002; Uemura et al. 2002). In rapidly expanding cells, bubbles were numerous, but disappeared in older expanded cells. It has been suggested that they serve as VM reservoirs for rapid vacuole expansion (Saito et al. 2002). Bubbles seemed to be connected with sheet-like VM invaginations and TVSs, suggesting that these structures have similar functions (Kutsuna and Hasezawa 2005; Reisen et al. 2005; Saito et al. 2002; Uemura et al. 2002) (fig. 10D).

TVSs, bubbles and sheet-like membranes were localized in the inner side of the vacuole, while, tubular structures on the outer side of the vacuole. They were observed to be associated with microtubules. In chloronema subapical cells, compared to apical cells, the vacuole has a simpler structure without inner sheets and outer tubules (Oda et al. 2009b).

2.2. Vacuole dynamics

Dynamic tubular vacuoles have been observed in root hair cells and pollen tubes of seed plants (Hepler et al. 2001; Hicks et al. 2004), and also in moss chloronema and rhizoid cells. In *P.patens*, these vacuolar tubules underwent rearrangements by separation and fusion with other vacuolar regions between chloroplasts. This interesting feature of the vacuole in moss may be a feature of rapidly tip-growing cells. Through its flexibility, the vacuole would facilitate mobility of and cooperation with organelles (Oda et al. 2009b) (fig. 10).

2.3. Vacuole cooperation with other organelles

In moss, vacuoles developed along the apical region in chloronema cells. Vacuoles interacted with plasma membrane via small protrusions which may facilitate membrane traffic between vacuoles and the plasma membrane. Such interaction might play a role in anchoring the vacuole for inheritance by the next apical daughter cell. Another type of interaction was also observed: the tubular structures from vacuole appeared when chloroplast movement was induced. This might indicate cooperation between chloroplasts and the vacuolar membrane (Oda et al. 2009a; Oda et al. 2009b) (fig. 10 C).

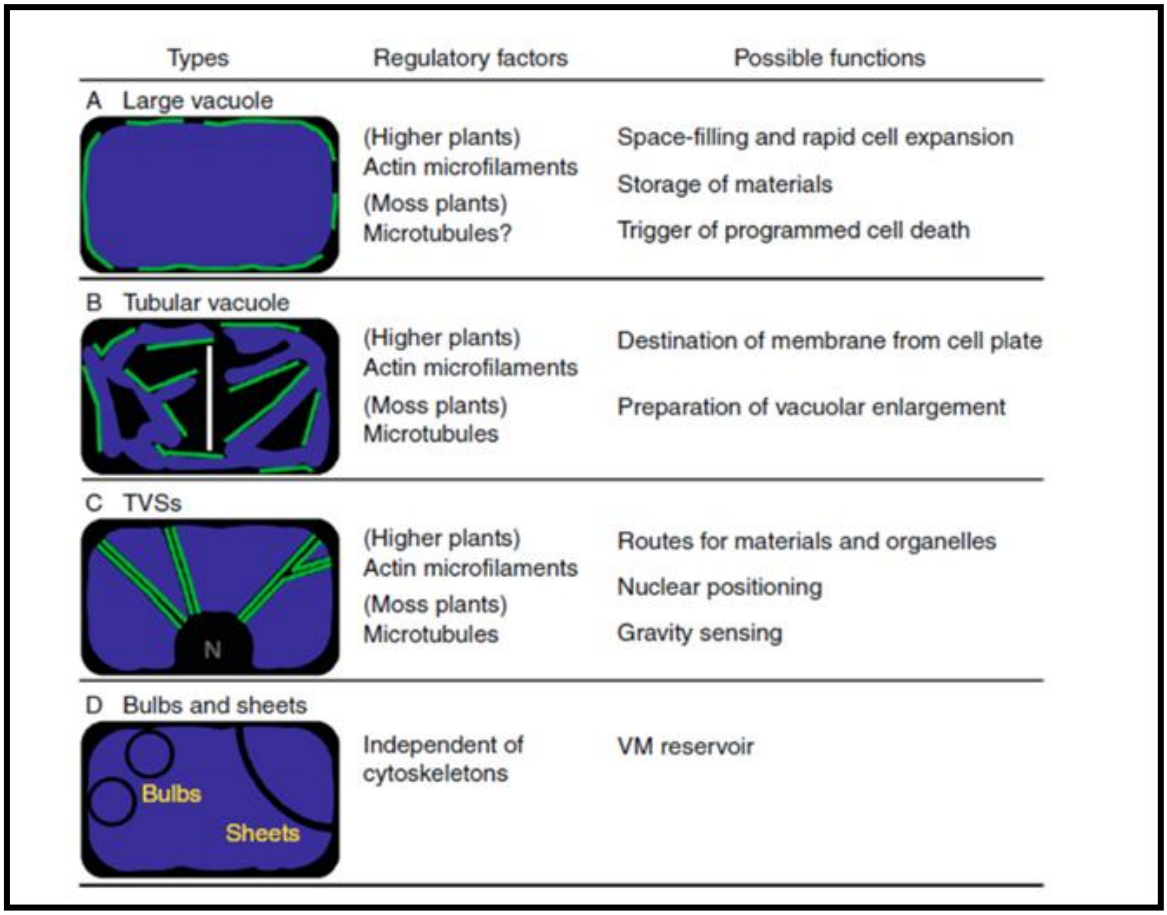

Figure 10: Vacuolar structures in plant cells

Vacuole (purple), cytoskeleton (green), cytosol (dark)

(A) Large central vacuole as observed in most cell types

(B) Tubular vacuoles are mostly found in meristematic cells. The white line represents a developing cell plate. The green lines represent the vacuolar membrane.

(C) TVSs. They form routes for materials. N represents the nucleus.

(D) Bulbs and sheets.

Tubular vacuoles and TVSs are also present in tip-growing cells, such as root hairs, pollen tubes, protonema cells, and rhizoid cells. Bulbs and sheets are observed in various cells.

Figure copied from (Oda et al. 2009a)

3. Moss organelles

3.1. Organelle distribution

Caulonema cells have a specific organelle organization consistent with their function in nutrient uptake and their energy requirement for faster growth and division compared to chloronema cells. They have an enhanced trafficking and secretion activity, and accordingly they contain 1.2 to 2.7 times more Golgi dictyosomes to ensure protein and lipid sorting. The density of mitochondria was the same in caulonema and chloronema. However chloronema contains up to 3.7 times more chloroplasts than caulonemata, which is consistent with a high photosynthetic activity. In both chloronema and caulonema cells, organelles were distributed in a gradient starting from the tip of the apical cell to the base of the sub-apical cell. Organelles accumulate at the apical cell tip, where cell division occurs, to facilitate inheritance of organelles to daughter cells (Furt et al. 2012).

A compartmentalization occurs only in caulonema cells: chloroplasts and peroxisomes are totally excluded from a 9-15 μm region at the extreme apex, the mitochondria from a 2-3 μm and the Golgi from 1-2 μm region at the tip. Like pollen tubes and root hairs from flowering plants, *P.patens* and other mosses accumulate vesicles at the extreme apex of the cell in this organelle-free zone (Furt et al. 2012).

3.2. Organelles dynamics

Dynamics of moss organelles in caulonema cells was monitored using fluorescent markers (Furt et al. 2012). The highest speed was observed for mitochondria (~75 nm/s), and chloroplasts were the slowest organelles (~30 nm/s). However, chloroplasts moved slowly in a given direction while mitochondria moved mainly around the same position, therefore chloroplast were transported over longer distances (Furt et al. 2012).

In flowering plants, plant cell polarization and growth are regulated by the actin cytoskeleton (Hepler et al. 2001). In particular the organization of the vacuolar membrane system by the actin microfilaments was shown in *Nicotiana alata* pollen tubes, where F-actin disorganization preceded the breakdown of the vacuolar membrane (Roldan et al. 2012). On the contrary in *Physcomitrella*, the organellar transport seems to be based on microtubules as

in animals. The distribution of vacuoles, plastids, ER, and mitochondria was affected by the microtubule inhibitor Oryzalin (Oda et al. 2009b; Pressel et al. 2008). This suggests a functional divergence of cytoskeletal functions in land plant evolution.

Experimental aims

So far, the plant secretory system has been studied in different model species such as *A. thaliana, O. sativa,* or *N. tabacum*, and several features of vacuolar sorting were determined in these model systems. Nevertheless, some mechanisms are still not well understood such as the RMR function in the secretory system. Several studies performed on Arabidopsis, and rice described the RMRs' localization and interactions (Cao et al. 2000; Hinz et al. 2007; Park et al. 2005; Shen et al. 2011). However their implication as vacuolar receptor for storage proteins remains to be clearly demonstrated. Simple RMR KO mutant were generated in *A.thaliana* and they did not show any phenotype or default in storage protein sorting, possibly due to redundancy among the six RMR (Zouhar et al. 2010).

Therefore we decided to take advantage of *P.patens* haploid genome and of its highly efficient GT facilities to study the RMR family genes. The aim of this PhD project was to realize in moss, an experiment that is not possible in flowering plants: a complete deletion mutant of all RMR genes. The challenge was to developed moss as a model system complementary to the other models for the study of the secretory system. For this purpose, two main strategies were used: (i) investigation of the secretory system and in particularly characterization of vacuoles in moss and, (ii) generation of deletion mutants of the whole RMR family and their characterization.

Chapter 2: The secretory system in moss

I. INTRODUCTION

The secretory system comprises morphologically and functionally distinct organelles, including the endoplasmic reticulum (ER), the Golgi apparatus, the trans-Golgi network, endosomes, vacuoles and the plasma membrane. These elements work together to achieve the correct protein secretion (Matheson et al. 2006). Vacuoles are one end point of the membrane trafficking and play different roles in metabolism, homeostasis and storage in plant cells. Their regulation of osmotic pressure is indispensable for plant morphogenesis. Recently, a reconstructed three-dimensional structures revealed the complexity of vacuoles in tobacco BY-2 cells (Yoneda et al. 2007). For instance, spherical and sheet-like membranes were reported within the vacuolar lumen of Arabidopsis epidermal cells (Saito et al. 2002). Dynamic changes of vacuolar structures have been observed during cell cycle progression in tobacco BY-2 cells (Kutsuna and Hasezawa 2002; Kutsuna et al. 2003). The model for vacuolar transport arises from a large number of biochemical and microscopic observations in different plant species and tissues. In particular different isoforms of tonoplast intrinsic proteins (TIPs) have been localized initially to the tonoplast of separate vacuolar compartments in a variety of species and cell types. They were therefore used as specific markers for different vacuolar types, with α -TIP labeling PSVs and γ-TIP labeling LVs (Jauh et al. 1999). However, evidence for this separate vacuole type model may not be as clean-cut as initially postulated. Recent studies localized all TIPs (α, γ, δ) in the same tonoplast of cotyledons and of young or mature leaves (Hunter et al. 2007). Previous models of vacuolar differentiation in the most popular model plant, Arabidopsis need thus revision.

The moss system is used here as a new model complementary to *Arabidopsis thaliana* to study the secretory system. By taking advantage of it highly efficient gene targeting (Schaefer and Zryd 1997), reporter genes fused to fluorescent protein DNA sequence can be inserted into the moss genome at preselected sites. Heterologous reporter are addressed and recombined into non-coding loci. Moreover, moss is very suitable for microscopic observation particularly of the filamentous tissue the protonema; which comprises only two cell types, caulonema and chloronema, in single cell files. This tissue contains an apical meristematic cell that repeatedly divides in short time lapses (Cove et al. 1997). This allowed the monitoring of the sequential events of cell division and elongation (Kammerer and Cove 1996). Finally, by using in *P.patens* heterologous reporters already characterized in flowering

plants (Baldwin et al. 2001b; Hunter et al. 2007; Peremyslov et al. 2004; Uemura et al. 2004), a comparative study of the evolution of the endomembrane system can be performed. The use of reporter genes from flowering plants in *P.patens* (which diverged 450 million years ago) leads us to discuss the divergence and the evolution of the studied organelles. Heterologous reporters were also used instead of homologous reporters for more pragmatic reasons: 1) To identify reporters with conserved localization, 2) when homologous gene candidates were not expressed at a sufficient level.

In this study we have developed efficient heterologous fluorescent reporters for visualization of several organelles in *P.patens.* Our study also revealed an unusual localization of TIP.

II. Results

1. Visualization of the ER

Transgenic lines expressing the ER marker P6 fused to a YFP were produced. P6 is a 6-kDa non-structural protein required for cell-to-cell movement of the beet yellow closterovirus. It possesses an N-terminal, single-span transmembrane domain and a C-terminal hydrophilic domain facing the cytosol. It accumulates in the rough ER (Peremyslov et al. 2004). The construct was driven by the heat-inducible soybean promoter Gmhsp 17.3B (Saidi et al. 2005) and was addressed to a non-coding locus (*Pp*-108 genomic loci) (Schaefer and Zryd 1997) in *P. patens*. The construct was first transiently expressed in protoplasts. 48h after transfection, fluorescence was observed in a reticulated pattern typical of ER (fig. 1A, B). YFP signals were sometimes observed in nuclei and in dots, which could be due to over-expression. To probe the subcellular localization in differentiated cells, transgenic lines expressing Hsp-P6-YFP were generated. Four Hsp-P6-YFP strains were obtained that carried one or multiples tandem repeats of the reporter. Confocal microscopic images revealed the familiar pattern of ER membrane labelling in chloronema, caulonema and leaf cells. Assuming that expression level is related to the copy number of the inserted reporter, two different lines were used one with a low expression level (fig. 1C to F) and an overexpressor line (see supplementary fig. 1). In chloronema (fig. 1A), caulonema (fig. 1B), and in leaf (fig. 1C, D), the construct was located in reticulated structures and in the nuclear membrane which are typical ER pattern. Clones which overexpressed the construct (see supplementary fig. 1) showed dots in addition to the typical reticulated structure. These dots were also observed during transient expression of the reporter and might be artefacts due to the overexpression of the fluorescent construct. Therefore, P6-YFP is correctly addressed in moss cells during transient expression and in heat-inducible lines showing a pattern of a well-developed ER very similar to the ER pattern observed in other plant systems like *A.thaliana* or *N.bentamiana*.

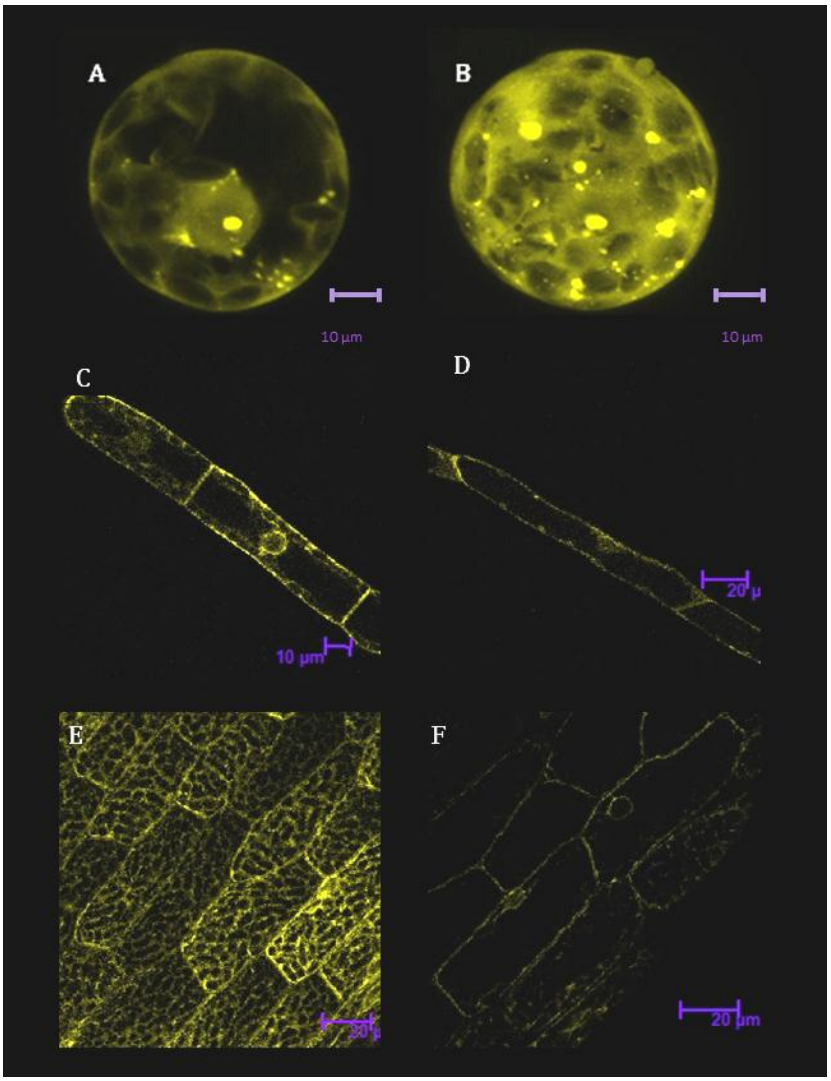

Figure 1: Subcellular localization of the ER marker.

Confocal microscopic images of P6-YFP expression in moss cells.

(A, B) Transient expression, **(C-F)** Heat-induced expression in a transgenic line.

(A) Section of a transfected protoplast through the nucleus, **(B)** Complete z-stack, **(C)** Section of apical chloronema cell through the nucleus, **(D)** Section of subapical caulonema cell, **(E)** Complete Z-stack of leaf cells, **(F)** Section of leaf cells.

2. Visualization of Golgi in moss cells

Among many roles, the Golgi of plant cells is the place where secreted proteins are segregated in order to be delivered to their final destination (Hinz et al. 2007). To investigate the Golgi pattern in moss cells, the *A. thaliana* gene encoding a Golgi-localized Nucleotide Sugar Transporter (GONST1) was chosen. It moves GDP-mannose across Golgi membranes (Baldwin et al. 2001b). The fusion protein consisted of Gonst1 fused to YFP at its C-terminus exposing the fluorescent protein to the cytosol. The construct was driven by the heat-inducible soybean Gmhsp 17.3B promoter (Saidi et al. 2005) and was addressed to a non-coding locus (*Pp*-108 genomic loci) in *P. patens.* The Gonst1-YFP fusion protein was targeted to the Golgi apparatus, displaying a typical punctate pattern of fluorescence in chloronema and caulonema cells (fig. 2A to D). In order to characterise this pattern a Gonst1-YFP line was treated with the Brefeldin A (BFA) a lactone antibiotics which causes the fusion of the Golgi cisternae with the ER forming hybrid compartments. BFA was demonstrated to inhibits COPI vesicle formation at the Golgi apparatus blocking the ER/Golgi traffic (Langhans et al. 2007). After BFA treatment, the Golgi marker was redistributed as expected into bigger dots and ring-like structures which might correspond to the hybrid Golgi-ER structures (fig. 2E to H). This confirms that the fluorescent reporter was localized in the endogenous moss Golgi. Therefore AtGonst1-YFP is suitable as a Golgi reporter in moss studies.

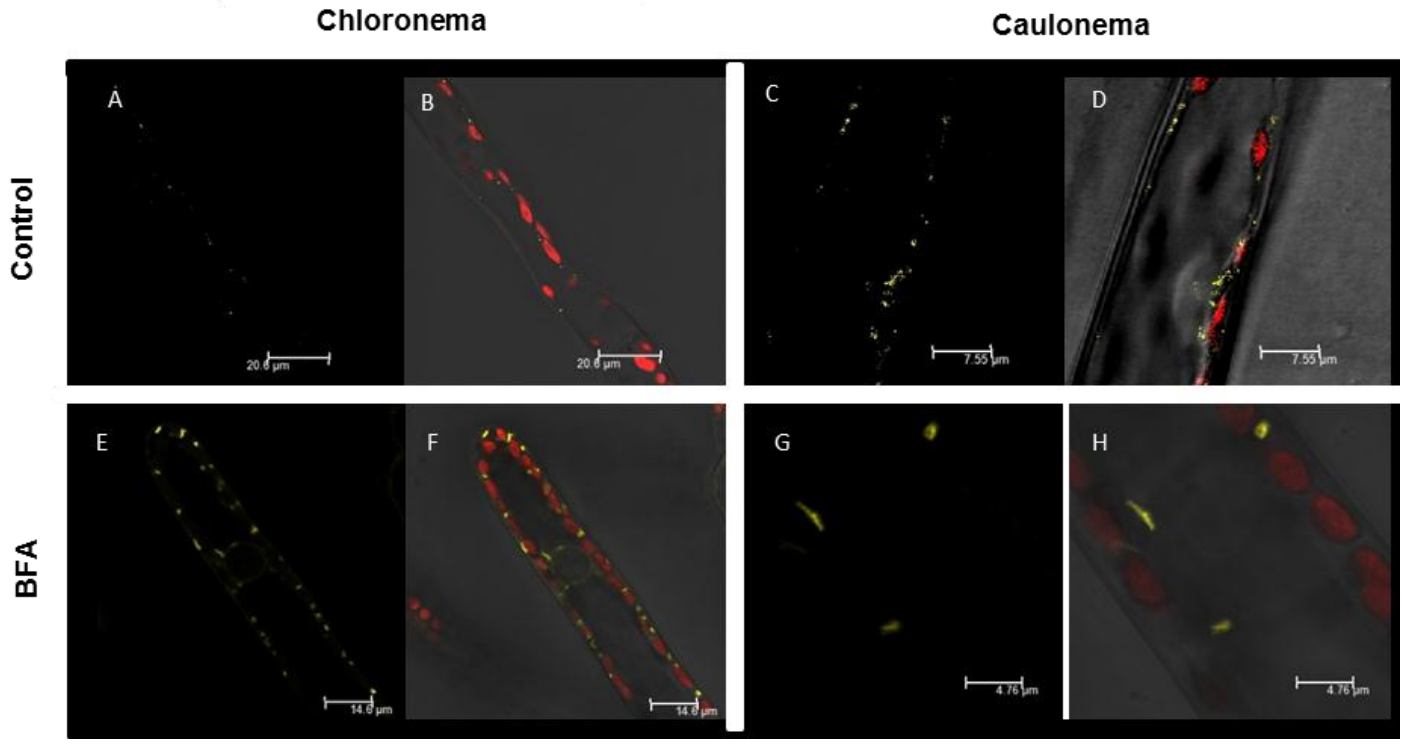

Figure 2: Subcellular localization of the Golgi marker

Heat-induced expression of AtGonst1-YFP in transgenic moss**.**

(A, B) Chloronema cells, **(C, D)** caulonema cells. Chloroplasts fluoresce in red color. **(A-D)** control treatment, **(E-H)** BFA treatment (10µg/ml during 10min).

(E, F) Structures labeled with AtGonst1-YFP upon BFA treatment, in chloronema cells **(G, H)** Magnified image of the apical cell treated with BFA that causes the AtGonst1-YFP to form bigger and ring-like structures.

3. Visualization of *trans*-Golgi-network in moss cells

The TGN is a reticular compartment at the *trans*-face of the Golgi stacks. SYP61 (a Syntaxin Protein) (Uemura et al. 2004) was used as a TGN reporter in *A.thaliana*. Syntaxins are members of the larger family of tSNAREs required on the target membrane for selection and fusion of vesicles (Bassham and Blatt 2008; Jürgens 2004; Sanderfoot et al. 1999). In moss, Syp61 was expressed under the control of a double 35S promoter, and fused to the yellow fluorescent protein Venus at its N-terminus. Constitutive expression of the construct in wild type moss showed a punctate pattern in chloronema (fig. 3 A, B), and in leaf cells (fig. 3 C, D). Two different strains were analysed, and it appeared that the reporter could also localize in ER membrane in addition to the dots. This is consistent with the observed pattern in flowering plant (Uemura et al. 2004). Time sequential observations revealed a rapid movement of these dots (fig. 3E), indicating that the TGN are very dynamic structures which constantly move around the cell.

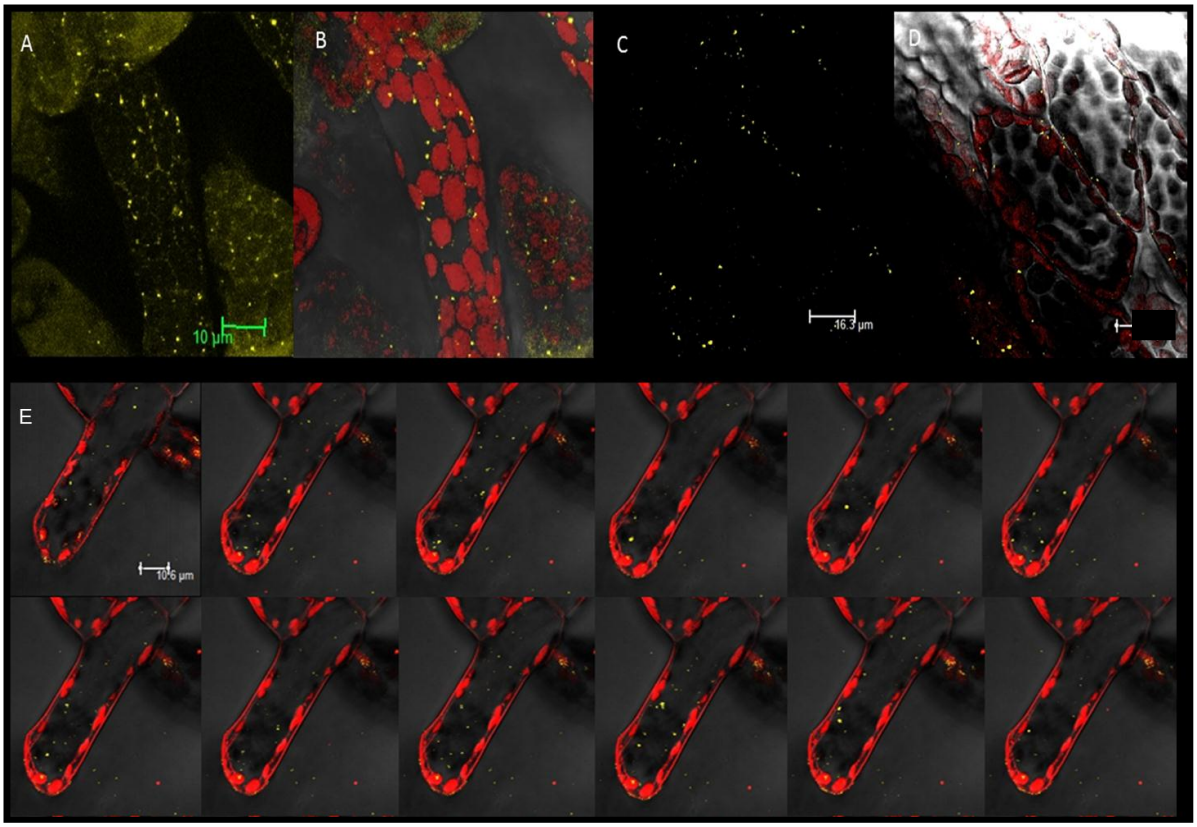

Figure 3: Subcellular localization of the TGN reporter

(A, B) Constitutive expression of a chloronema cell expressing Venus-Syp61 (yellow), Chloroplasts fluoresce in red. **(C, D)** Section images of leaf cells. **(E)** Time-sequential images (3 seconds) of apical chloronema cell showing dots movements between the different focal of the cell.

4. AtTIP localization in moss cells

AtTIP labels 2 types of structures in moss

In order to obtain tonoplast labelling in moss, we generated transgenic lines stably expressing γ-TIP-YFP and δ-TIP-YFP under 35S promoter. The lines were analysed under the confocal microscope. The different lines basically displayed the same pattern (fig. 4). As shown in a general view images, γ-TIP-YFP and δ-TIP-YFP proteins produced very strong fluorescence inside the cells (fig. 4A to H). Many bright structures with diameters between 1 and 10µm were detected in all cells types. These structures are likely to be 'bubbles', in which the yellow fluorescent markers are concentrated, resulting in saturating levels of signal (fig. 4 A-B). Closer examination revealed that the reporters localized in different kind of structures (fig. 4I to T). Single section images showed that fluorescent structures could be: linear structures (fig. 4I-J), tubular structures (fig. 4K-L), or round and empty like bubbles (fig. 4M-N). In older tissue, additional complex structures appeared labelled by γ-TIP-YFP or δ-TIP-YFP (fig. 4O to T). These complex structures seem to result from an accumulation and a merging of the simple structures described above; linear, tubular, and bubble structures. There was no correlation between these structures and the observed cell types neither in caulonema (fig. 4O-R), nor in chloronema cells (fig. 4S-T) or leaf cells (fig. 4C-D).

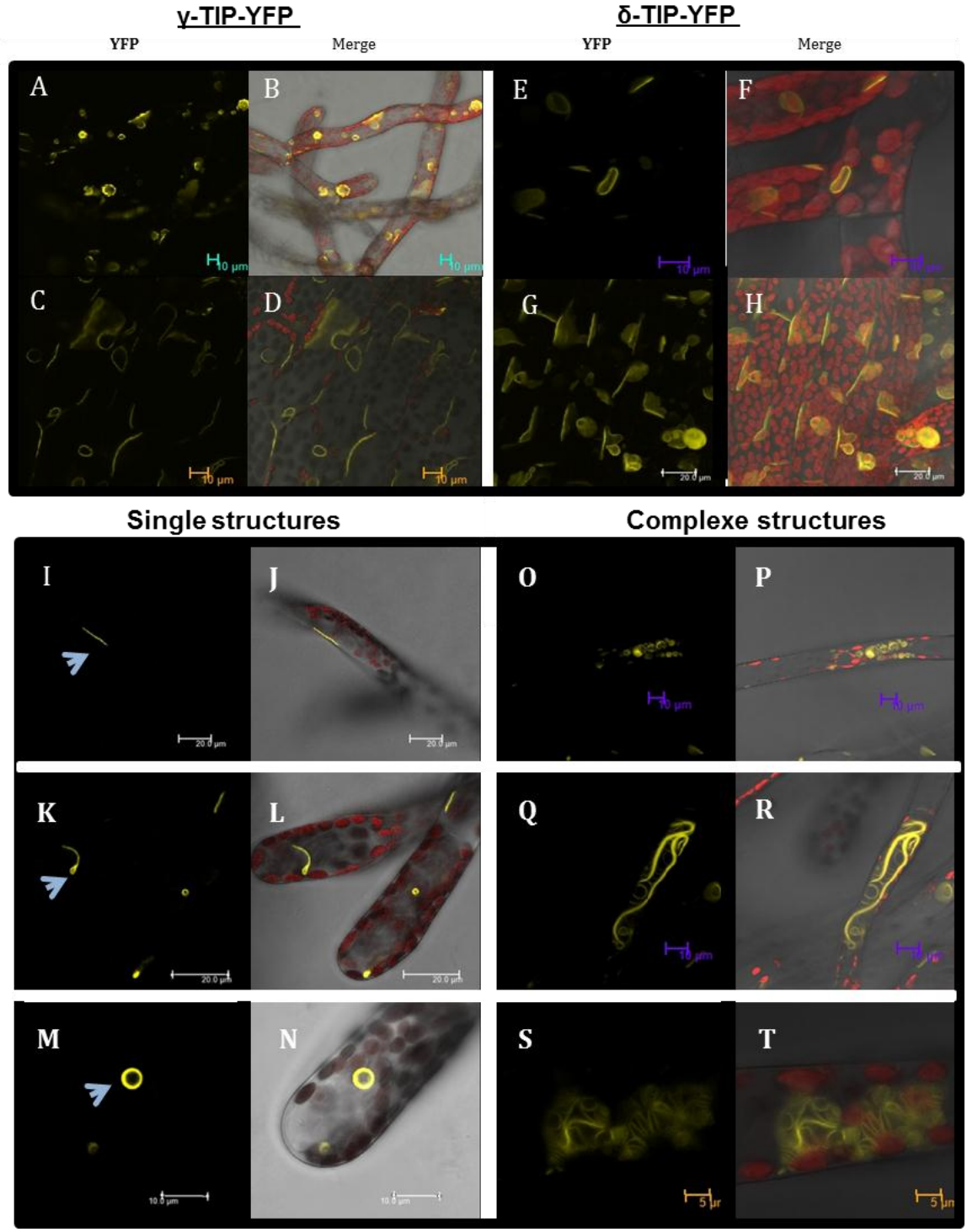

Figure 4: Structures labelled by heterologous reporters

Transgenic lines expressing γ-TIP-YFP or δ-TIP-YFP (under 35S promoter) were analysed by confocal microscopy under YFP channel **(left columns)**. Images **(right columns)** represented merge of the bright field, the chloroplastic and the YFP channel.

(A, B) Protonema cells, **(E, F)** Section images of subapical chloronema, **(C, D, G, H)** Section images of leaf cells, **(I, to N)** Zoom images of the AtTIP-YFP signals; in linear **(I-J),** tubular **(K-L),** round structures **(M-N)**

(O to T) In older tissue (20 days old protonema culture), there were complex structures.

AtTIP labels independent structures from the moss tonoplast

Additional experiments were performed to determine if the AtTIPs localized inside the moss vacuole, in its tonoplast or in independent structures. After FM4-64 staining, the merged images (fig. 5C) revealed no superposition of AtTIP-YFP and FM4-64 staining. While the AtTIP constructs labelled membrane structures, they seemed independent from the tonoplast. Consequently, AtTIP sequences were not addressed to the moss tonoplast. Do AtTIP-YFPs localize within the vacuole? Neutral Red staining was used on the transgenic lines to stain the vacuoles (fig. 6A to D). The AtTIP structures localized completely outside of vacuoles (fig. 6). Additionally an experiment of protoplast evacuolation of the δ-TIP-YFP transgenic line was performed. Observation of the evacuolated vacuoles showed that AtTIP structures were not found in the vacuole or linked to the tonoplast but were released freely in the medium (see supplementary fig. 2).

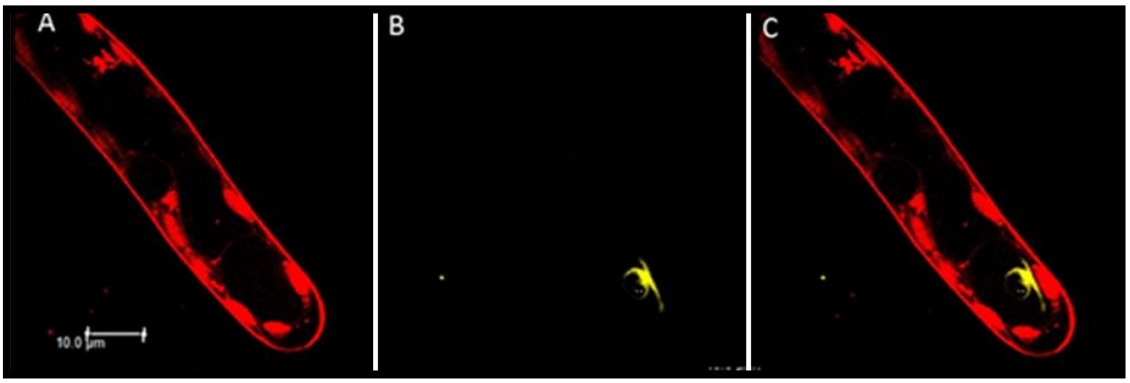

Figure 5: Localization of γ-TIP-YFP compared to vacuoles.

Transgenic line stably expressing γ-TIP-YFP and stained with FM4-64**,** and analysed by confocal microscopy: (**A)** Red channel, **(B)** YFP channel, **(C)** Merge image showing no superposition of signals.

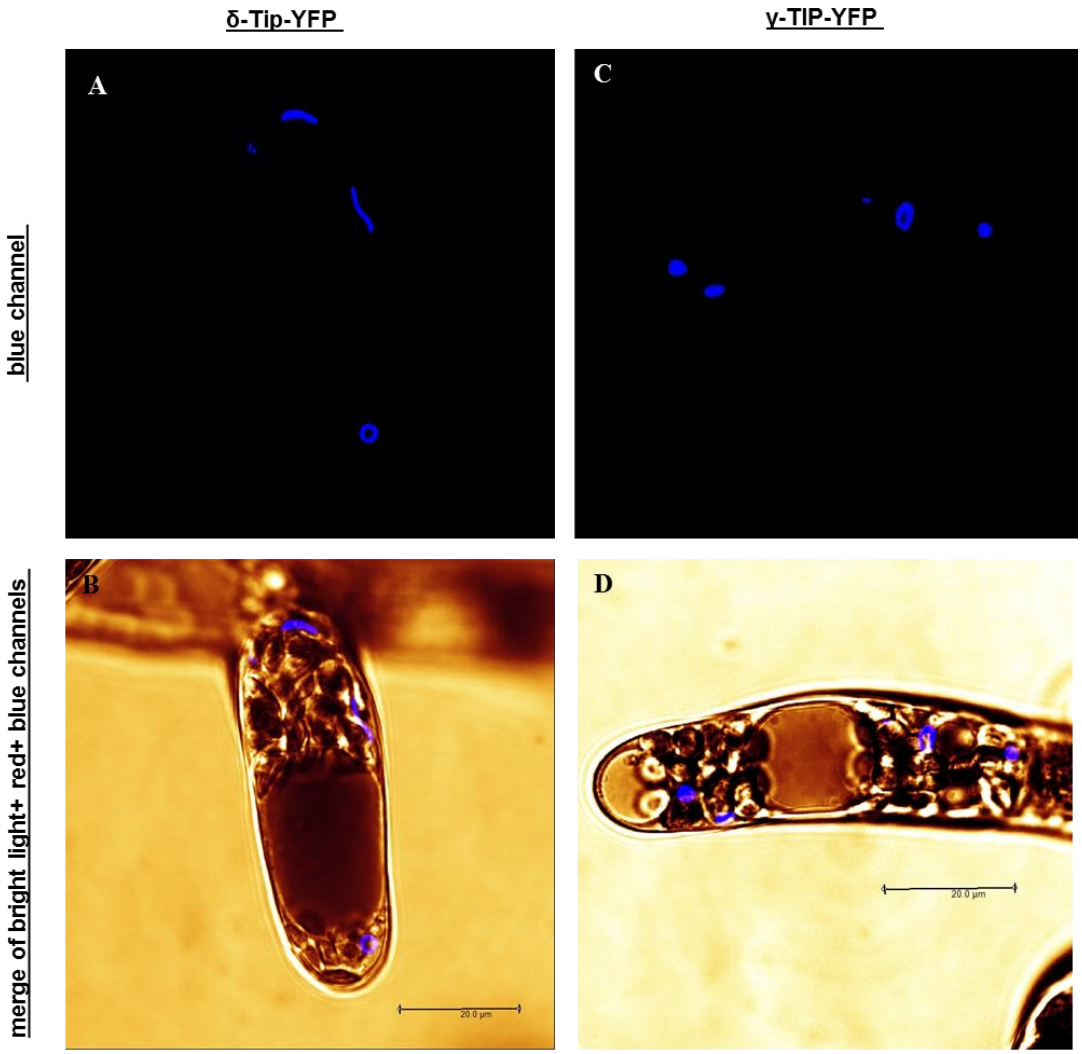

Figure 6: Localization of γ-TIP-YFP and δ-TIP-YFP structures separate from vacuoles

Transgenic lines expressing stably **(A, B)** the δ-TIP-YFP and **(C, D)** the γ-TIP-YFP stained with NR.

(A, C) Images were taken in YFP channel the yellow label is represented in blue colour**.**

(B, D) Merge Images of different channels; the bright field, the chloroplast (brown colour) and the YFP channel (blue colour). The large vacuole is stained by the NR (dark-red area). The blue signals of γ-TIP-YFP and δ-TIP-YFP are located out of the vacuole.

5. The moss vacuole structure and mobility

To visualize moss vacuolar membranes *in vivo,* Oda *et al*., used an Arabidopsis tonoplast t-SNARE, encoded by AtVAMP3/SYP22a fused to a GFP and generated transgenic lines expressing the tonoplast reporter in moss cells (Oda et al. 2009b). This tonoplast marker had already been used successfully to visualize vacuolar membranes in flowering plant cells (Uemura et al. 2002). In this study, we used one of this moss lines to investigate the vacuole. Different vacuolar structures were observed; the large central vacuole, tubular vacuoles on the vacuole outer side, the transvacuolar strands on the vacuole inner side (fig. 7).

Large vacuoles appeared to occupy most of cell volume (fig. 7A). Tubular structures were observed on the outer side of the vacuole. They extended from the vacuole to the cytoplasm and between chloroplasts (fig. 7A-B white arrow). Many inner vacuolar membranes which penetrated into the large vacuole were also detected, in the cell-apex (fig. 7C to F blue arrows). The transvacuolar strands (TVSs), which are cytoplasmic strands, spread towards the apex (fig. 7E-F), or from the basal region of the cells (fig. 7C-D). Both outer tubular structures and inner transvacuolar strands were mostly observed either in the apical or the basal region of the cell.

An additional marker was used to visualize vacuole membranes; the styryl dye FM4-64. This dye is widely used as an endocytotic marker; after tissue staining the FM4-64 is first incorporated into the plasma membrane and then transferred to the vacuolar membrane via endosomes (Bolte et al. 2004). Protonema cells were stained with FM4-64 and for the first hour after staining, it localized mainly to the plasma membrane and endosomes. After 3 h it moved to the vacuolar membrane and stained the tonoplast and all compartments involved in the trafficking between the plasma membrane and the tonoplast. Observation of protonema cells three hours after FM4-64 incorporation revealed bubble structures inside the vacuole (fig. 7J), labeled at the same time as the tonoplast. Time-sequential observations were performed (fig. 7H-I-J). Inner transvacuolar strands underwent dynamic and repeated wave movements inside the large vacuole in the cell-apex (fig. 7H-I). Likewise, bubble membrane observed in the basal region of a chloronema cells, showed a dynamic cycle of splitting and fusion with other regions of tonoplast (fig. 7J).

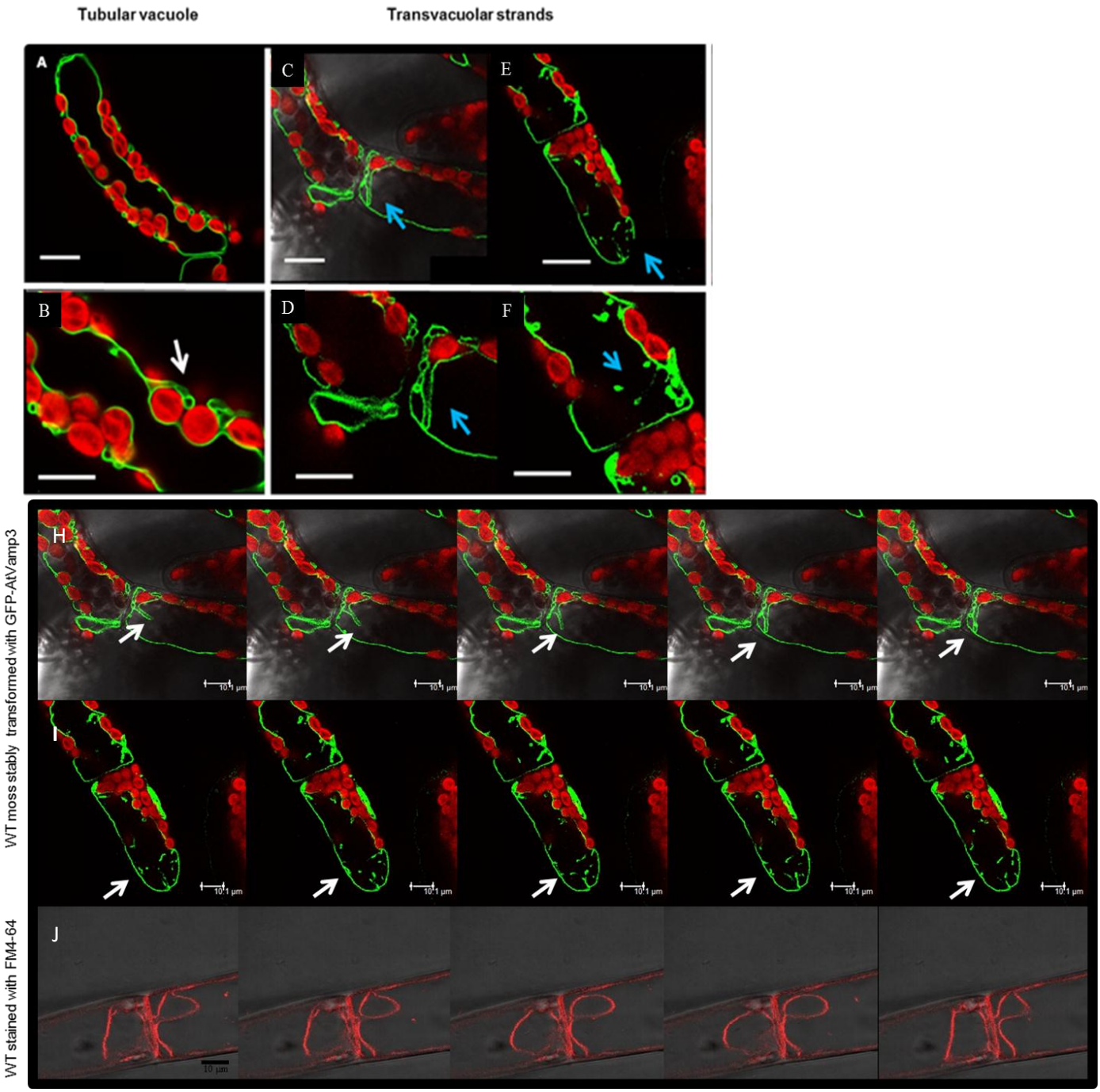

Figure 7: Dynamic of the vacuole visualized with the tonoplast reporter GFP-AtVAMP3

Confocal microscopic images of the transgenic line expressing stably GFP-AtVAMP3 (green signal) in chloronema apical cell

(A) Large vacuole, (**B)** Zoom showing tubular structure on the outer side of the vacuole (white arrows). **(C-D)** TVSs (blue arrows) at basal region of cell. **(E-F)** TSVs in the inner side of the vacuole spread towards the apex of apical cell (blue arrows).

(H-I-J) Time sequential (3seconds) images **(H)** A single TVS (white arrow) **(I)** Many TVSs (white arrow) movements. **(J)** The intravacuolar protrusion (white arrow) observed in chloronema cells basal region (by FM4-64 staining) showing cycles of splitting and fusing processes with tonoplast and plasma membrane.

6. Interactions of vacuoles with other organelles

Time sequential observations underlined the mobility of the vacuolar tubules which underwent rearrangements with other vacuolar regions. Close contact with the plasma membrane and chloroplasts were also observed (fig. 8). Contact between tonoplast and plasma membrane (fig. 8A to C), or tonoplast and chloroplasts were observed (fig. 8D-E). Such contact would facilitate the interaction between the tonoplast and the plasma membrane. The folding of tonoplast around chloroplasts suggests either a functional interaction with chloroplasts or vacuole rearrangement to modulate or facilitate the organelle‘s motility.

.

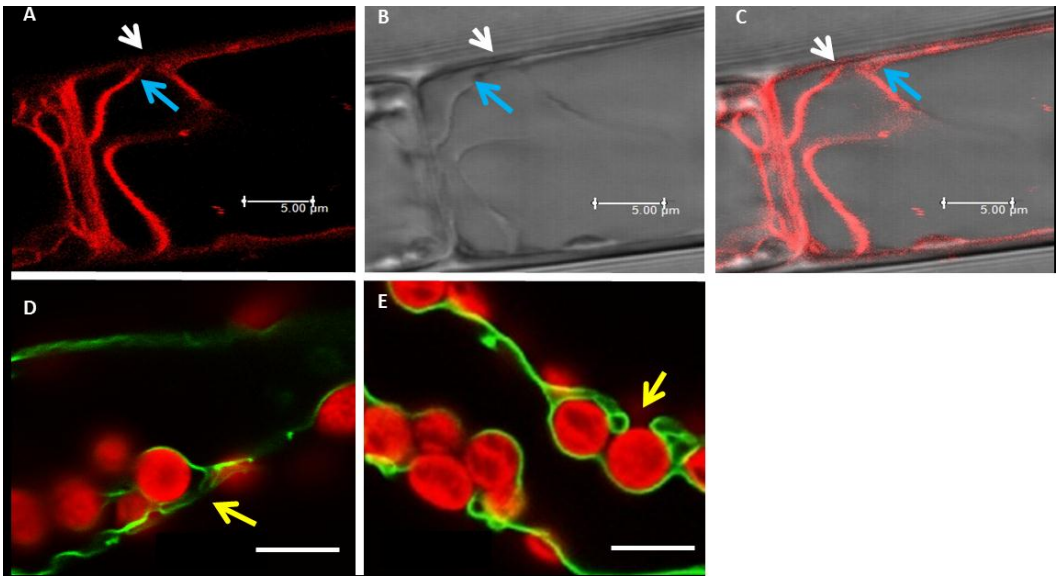

Figure 8: Interaction of the tonoplast with the plasma membrane and chloroplasts.

Confocal microscopic images of chloronema cells stained with FM4-64 (first line) or expressing tonoplast reporter (bottom line).

(A) Red channel, **(B)** bright field channel **(C)** merge image of red channel and bright field. The tonoplast (blue arrows) and the plasma membrane (white arrows) (3 hours after FM4-64 incorporation without wash out).

(D-E) Tubular vacuolar membranes (green signals) surrounding a chloroplast (red signals) Scale bar =5µm.

III. Discussion

1. Qualitative study of the organelles of the secretory system

The study of the moss secretory system opens important questions such as: how conserved is it between bryophytes and seed plants? What are the sorting and targeting mechanisms? To answer these questions we developed tools to visualize the organization of the secretory system in different cell types of *P.patens*. Transgenic lines expressing P6-YFP (ER), AtGonst1-YFP (Golgi) or Venus-Syp61 (TGN) showed a similar pattern as previously described in other plant models (fig. 1-2-3) (Baldwin et al. 2001a; Fukuda et al. 2000; Peremyslov et al. 2004). These heterologous protein reporters were correctly recognized and addressed to their target compartments in the moss secretory system. Moreover, the pattern of the fluorescent reporters revealed that the organization of ER, Golgi and TGN organelles was similar to seed plants. Using the same strategy to study the moss vacuole, AtTIP-YFPs were expressed in wild type moss. Analysis of transgenic plants showed a mislocalization of the reporters, which did not label the moss tonoplast, indicating a major difference in TIP localization in Angiosperms. In contrast, another tonoplast reporter the GFP-AtVAMP3, which had already been characterized in moss, correctly labeled the tonoplast (Oda et al. 2009b).

2. Vacuole organization

In a transgenic moss plant expressing GFP-AtVAMP3 the vacuoles had diverse shapes and they were continuously changing their structures. In a recent review, Oda et al., (2009) categorized these vacuolar structures into two types: tubular vacuolar membranes (TVM), tubular vacuolar strands (TVSs) (Oda et al. 2009b). This study was able to describe two main types of vacuolar structures in moss cells:

-Tubular structures or TVMs (tubular vacuolar membranes) were observed to extend from the outer face of the large vacuole into the cytoplasm and between chloroplasts (fig. 7). Tubular vacuoles have already been identified by electron microscopy in *Euphorbia characias* meristematic cells (Marty 1978) and in pea root tip cells (Paris et al. 1996). The function of TVMs is still unclear but in tobacco BY-2 miniprotoplasts the tubular vacuoles appeared during expansion of the vacuole (Okubo-Kurihara et al. 2009). They might be involved in the storage of excess of membrane for later vacuolar enlargement (Okubo-Kurihara et al. 2009). In our study, the close relationship between the TVMs and the

chloroplasts suggests that the vacuoles can adapt their spatial conformation to facilitate motility of others organelles while occupying most of the cell volume (fig. 8).

-TVSs (tubular vacuolar strands) were also detected inside the large vacuole at the apex and the basal region of the cell (fig. 7). They were described in different studies as cytoplasmic tunnels within the vacuoles that serve as a route for transport of organelles such as Golgi bodies (Nebenführ et al. 1999), endosomes (Ovecka et al. 2005), and amyloplasts (Saito et al. 2005). TVSs could have many roles, such as determining the cell division site (Panteris et al. 2004) or in nuclear positioning (Goodbody et al. 1991). In moss chloronema cells, the TVSs structures might be a feature of cells with apical growth to increase the vacuole surface which interacts with the basal and apical regions of the cell.

The high mobility of vacuoles has already been observed in root hair cells and pollen tubes of seed plants (Hepler et al. 2001; Hicks et al. 2004), and also in moss chloronema (Oda et al. 2009b). Our analysis of the vacuole with FM4-64 staining confirmed its high mobility and its rearrangements (fig. 7). The vacuole was observed to interact with the plasma membrane (fig. 8), which confirms observations made by electron microscopy (Oda et al. 2009b). Such interactions with the plasma membrane may facilitate membrane or protein trafficking.

3. Model of biogenesis of artefactual AtTIP compartments

The AtTIP structures were localized outside the tonoplast and the vacuole lumen (fig. 4). Compared to other studies different observations could be made:

a) **These structures do not correspond to the Atγ-TIP bubbles described in Arabidopsis by Saito** (Saito et al. 2002). (i) In their study, the number of bubbles decreased as leaves age, whereas in our case it increased. (ii) They also showed their bubbles to be prolongations of the tonoplast, whereas we found that our structures are completely independent from the moss vacuole (fig. 7-8).

b) These structures are related. We propose a model to explain their formation (fig. 9). We found linear and vacuole-like structures, as well as intermediate structures. Older tissue showed an accumulation of these vacuole-like structures and of their intermediates. They seemed to form by a mechanism resembling *de novo* vacuole formation. This implies that AtTIP proteins may contain a signal for tonoplast formation or differentiation from the ER.

c) AtTIP proteins do not contain the targeting signal to reach the moss tonoplast. Peptide signals are responsible for targeting proteins to the correct subcellular location in plant cells. If soluble proteins lack specific information for retention or sorting to vacuoles, they will be

transported to the plasma membrane and released to the apoplast (Denecke et al. 1990b). Although the default destination within the secretory pathway for a soluble protein is secretion, the default pathway for membrane proteins is not well understood. The tonoplast has been proposed as the default destination for membrane proteins, since a truncated form of α-TIP (leaving the last 48 amino acids of the sixth TM domain) was still addressed to the tonoplast (Höfte and Chrispeels 1992). However Brandizzi et al., (2002) showed that the default pathway of single transmembrane domain proteins depended on the length of the membrane-spanning domain. For instance, the full length (23 aa) of the Transmembrane Domain (TM) of the human lysosomal protein LAMP1 was transported to the plasmalemma while the truncated versions reached only the Golgi (20 aa) or were retained in the ER (17 aa) (Brandizzi et al. 2002). In our experiment, AtTIP proteins were not correctly recognized by the moss sorting system and were not addressed to the tonoplast; however they were neither transported to the plasmalemma nor retained in the ER or in the Golgi. They accumulated in new membranes the cytosol. Are AtTIP proteins recognized as tonoplast precursors in the moss? Do AtTIP proteins contain specific signals for membrane formation?

d) **AtTIP proteins form membranes artefacts.** Another possibility is that AtTIP proteins formed artefactual structures, like the "Z membranes" observed with a fusion protein formed between the avian Infectious Bronchitis Virus M (IBVM) protein and the bacterial enzyme β-glucuronidase (GUS) in transgenic tobacco cells. IBVM protein is an integral membrane glycoprotein with three TMs which is normally retained in the ER. Overexpression of this fusion protein caused the formation of multi-layered scroll-like structures which were continuous with the ER. The concentric or spirillar configuration is probably the consequence of the oligomerization of the GUS domains in the IBVM-GUS fusion proteins (Gong et al. 1996). Nevertheless, there are differences between AtTIP-YFP and IBVM-GUS structures: (i) the normal location of IBVM-GUS was the ER and its overexpression formed structures continuous with the ER while AtTIP-YFP, instead of being addressed to the tonoplast, formed structures which were not continuous with the tonoplast (ii) AtTIP-YFP formed vacuole-like structures with a lumen whereas IBVM-GUS formed spirillar structures.

4. TIP protein evolution

In seed plants, like Arabidopsis and rice, five distinct subfamilies of TIPs can be distinguished (TIP1 to TIP5), whereas in mosses only one type (TIP6) is found (Danielson and Johanson 2008). A phylogeny of TIP sequences of different species indicated that the subfamilies TIP1 to TIP5 evolved in early vascular plant after their divergence from mosses

(Anderberg et al. 2012). Consequently angiosperms TIP proteins could have acquired new or more specialized functions. This could explain why AtTIPs were not to be correctly addressed to the endogenous moss tonoplast.

This study left open several questions. Their answers will deepen our understanding of tonoplast biogenesis and function. What are the tonoplast targeting signals in moss and in seed plants? What specialized functions did TIPs acquire during evolution of seed plants?

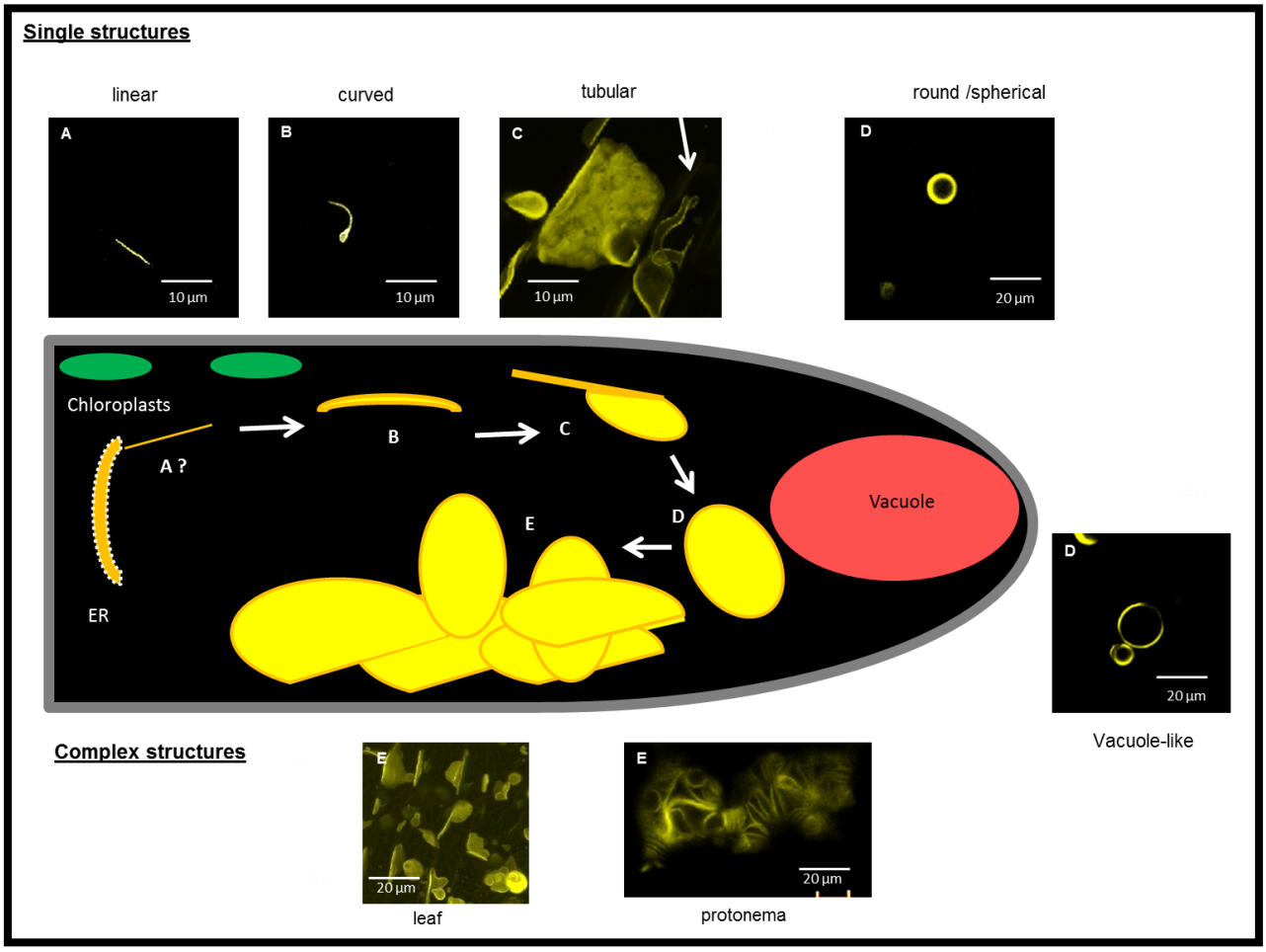

Figure 9: Model of AtTIP compartment biogenesis.

This model showed a putative mechanism of AtTIP labelled structures (white arrows). Images taken by fluorescent microscopy showed the AtTIP structures corresponding to the drawn models.

(A) Linear structures could be the first to arise from the ER possibly by tabulation forming first a linear structures with little lumen.

(B-C) The linear structures could then curve and acquire more lumen volume to form tubular structures.

(D) Further volume increase could lead to small round structures or larger vacuole-like structures

(E) Accumulation of the various structures would the form the complex structures observed in protonema and in leaf cells

IV. Material and methods

Plant culture

P. patens Gransden 2004 was cultured on BCDAT agar plates (Nishiyama et al. 2000) at 26^{o}C in discontinuous white light (16 hours/day). Protonema cultures were made in 9cm Petri dishes containing solid culture medium and overlaid with cellophane disks (W.E. Cannings, Bristol, UK). Every week, this culture was homogenized with a Polytron (Kinematica, Littau, Switzerland), resuspended on BCDAT solid culture medium. Protonema grew until 8-10 days and gametophores until 20 days.

Strain conservation and amplification

Strains are conserved as fragmented protonemal suspensions in sterile water in a refrigerator. For short-term storage, 6 days old protonemal cultures were collected in sterile water (1 plate in 5-10 mL) and fragmented it with an Ultratorrax (Polytron, 30 sec).

Moss protoplasts isolation

Protoplast were isolated from 5-6 days old protonemal cultures digested with 1% Driselase (Driselase is dissolved in 0.48M mannitol, centrifuged at 10000 rpm for 10 min. to remove debris, buffered to pH 5.6 and sterilized by passage through a 0.25 µm filter) in 0.48M mannitol (Fluka 44585, Sigma D-9515) for 30 minutes with occasional gentle mixing. The suspension was filtered through a 100 µm stainless steel sieve and left for an additional 15 min. to complete digestion, then filtered through a 50 µm stainless steel sieve and transferred to sterile 10 ml glass tubes. The protoplasts were harvested by low speed centrifugation (60g for 5 min.) and gently resuspended in 0.48M mannitol. The centrifugation step was repeated and the protoplasts were resuspended in 0.48M mannitol.

To regenerate the protoplast on a Petri dish, the protoplast were mixed with one volume of molten top layer (1.5% agar in 0.48M mannitol) and 2 ml aliquoted per 9 cm Petri dish containing solid protoplast culture medium overlaid with a cellophane disk. The protoplasts were left in darkness one night after plating and then regenerated in the light in the culture room.

Moss transformation by PEG

The protoplasts were isolated as described below. After isolation, the protoplasts were resuspended in 0.48 M mannitol. The protoplasts were centrifuged and resuspended at a concentration of 1.2 x 10^{6} /ml in MMM solution (Mannitol: 0.48 M, Magnesium chloride: 15mM, MES: 0.1%, pH 5.6 with KOH). 10-15 µg of DNA were dispensed into 14 ml Falcon tubes (maximum 30 µl, the final concentration should be between 30-50 µg/ml). 300 µl protoplast suspension were added to the DNA and gently mixed. 300 µl PEG solution (Mannitol 0.38 M, Calcium nitrate 0.1M, PEG 4000 (Serva) 33 % (w.v.) pH 8.0 with 10 mM Tris) were added to the protoplast suspension and mixed gently. The protoplasts were heat shocked for 5 minutes at 45^{o}C in water bath. The protoplasts were left at room temperature for

10 minutes with occasional gentle mixing. The sample was progressively diluted with PPNH4 recette liquid medium (5 x 300 µl and then 5 x 1 ml added at one minute intervals). The transformed protoplasts were kept overnight in darkness. The next day, the protoplasts were further cultured in liquid medium for transient gene expression assays or embedded in protoplast top layer and plated on protoplast solid medium for further selection. Each transformation sample was plated on 3-4 Petri dishes.

Stable strains expressing P6-YFP, AtGonst1-YFP, Venus-Syp61, AtTIP-YFP

To visualize vacuolar membranes in chloronema cells**,** Venus-Syp61, Atγ Tip-YFP, At∂Tip-YFP (kindly provided respectively supplied by Dr. G.P SanSebastiano, Dr Nadja Ferdermman,) were cloned using restrictions sites into the vector 35S-108-PBNRR (cut XhoI/SalI) and placed under the control of the 35S promoter. P6-YFP, AtGonst1-YFP were cloned after the Heat inducible promoter in the vector Hsp-108-PBNRR (for more details see chap annex constructs). These vectors contain 108 genomic fragments, and thus allow the targeted to be insertion into the 108 locus of *P.patens*. Polyethylene glycol (PEG)-mediated transformation was performed as described previously, and transformants were selected on the BCDAT medium supplemented with 20 $mg.l^{-1}$ G418 (Invitrogen Corporation, Carlsbad, CA, USA). The genotyping of the transgenic colonies was performed by PCR on the recombinant junctions between the 5'and the 3' regions of the genomic 108 locus and the resistance marker using the appropriate primer pairs (see annex primers)

FM4-64 dye staining

To label vacuolar membranes, protonema cells were treated with 36 µM FM4-64 (Invitrogen) dissolved in DMSO, for 3 hours. Subsequently, the cells were washed three times with fresh liquid medium with gentle agitation.

Neutral Red staining

To label acidic vacuolar lumen, protonema cells were incubated with 12.5mM Neutral Red for 20 min. Subsequently, the cells were washed three times with fresh liquid medium and incubated for 20 min with gentle agitation.

Microscopy

Images were collected with a TCS SP5 II confocal laser scanning microscope (Leica). Digital images were acquired using LAS AF (version: 2.0.0 builds 1934) and processed using ImageJ 1.41(National Institute of Health, USA). Aliquots of the protonema cell culture were transferred to a microscope slide with a coverslip window at the bottom. For simultaneous observations of AtTIP-YFP and FM4-64: they were excited by a 488 nm argon laser, and detected through a confocal unit (TCS SP5 II confocal laser scanning microscope (Leica) with a 524–546 nm band-pass filter for YFP, and a 575–625 nm band-pass filter (Olympus) for FM4-64.

Inhibitor treatments

For BFA treatment, cells were treated with 10µM Brefeldine A (Sigma-Aldrich) dissolved in DMSO, and cells were observed after 10 minutes of incubation. As control, a 1 ml suspension culture was incubated with 0.1% (v/v) dimethylsulfoxide (DMSO). The cells could be observed directly. For removal of BFA, the medium was carefully exchanged four times with fresh liquid medium.

V. Supplemental figures

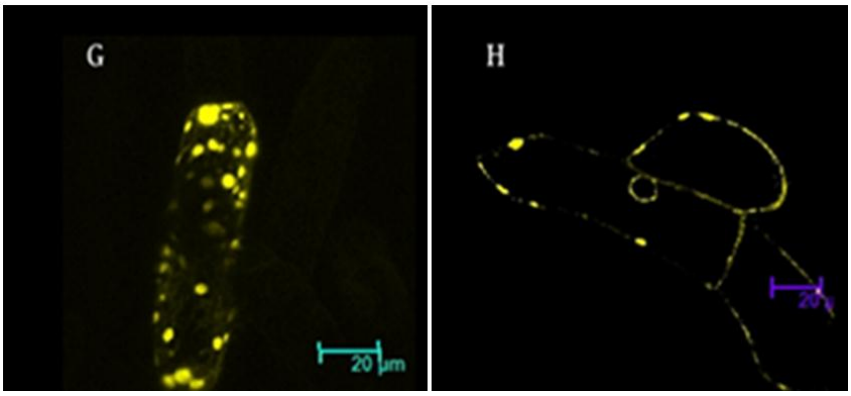

Suppl. fig. 1: Subcellular localization of a transgenic line overexpressing the ER marker.

(G) Complete Z-stack of apical chloronema from the overexpressor (P6-YFP) line shows dots with strong signal. **(H)** Section image of a cell through the nucleus showing the labelled dots.

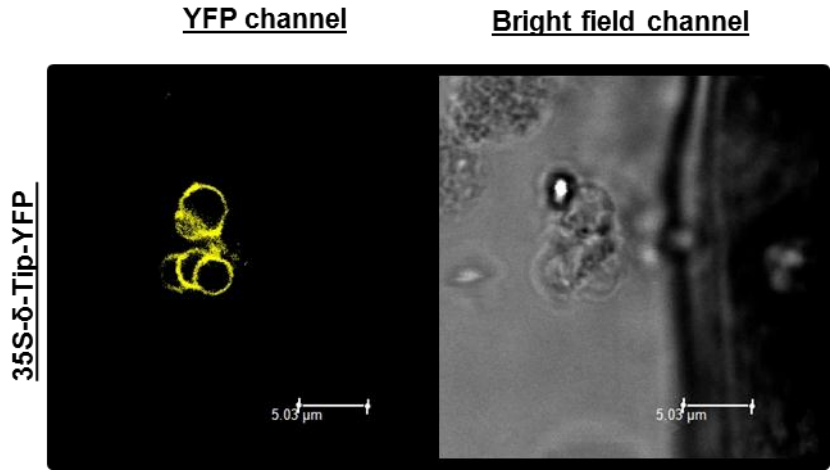

Suppl. fig. 2 : AtTIP structures are independent from the vacuole

The AtTIP-YFP structures (yellow signal) were found free in the medium after protoplasts evacuolation. Left image represents YFP channel and right image the bright field channel.

Chapter 3: Vacuole biogenesis

I. INTRODUCTION

The plant vacuoles are responsible for a variety of functions and are essential for plant growth and morphological changes during development. They contain a large variety of molecules involved in many cellular processes: hydrolytic enzymes, defense proteins, xenobiotics, osmolytes. The usual models of vacuolar biogenesis in flowering plant consider that plant cells can contain at least two types of vacuoles with distinct functions: the lytic vacuole (LV) and the protein storage vacuole (PSV) (Epimashko et al. 2004; Neuhaus and Rogers 1998; Paris and Rogers 1996; Surpin and Raikhel 2004). Depending on the physiological conditions or on the tissue type, these vacuoles fuse and form a hybrid vacuole which is commonly the central large vacuole in plant cell.

The identification of different types of vacuolar sorting signals supports this model (Jolliffe et al. 2005; Neuhaus and Rogers 1998; Vitale and Hinz 2005). These amino-acids specific peptide sequences interact with receptors which recruit cargoes to separate sorting pathways, the vacuolar sorting receptor (VSR) family (Ahmed et al. 2000; Kirsch et al. 1994; Kirsch et al. 1996; Laval et al. 2003) and the RMR family (Jiang et al. 1998; Park et al. 2005). The resulting model proposes that proteins destined to lytic vacuoles (LVs) carry sequence-specific VSDs (ssVSDs) and are sorted by VSRs while proteins bearing C-terminal VSDs (ct-VSDs) are sorted to protein storage vacuoles (PSVs) by the RMRs (Jiang et al. 1998; Park et al. 2005). In developing pea cotyledons, proteins carried to PSVs traffic via dense vesicles (Hinz et al. 1999) distinct from the CCVs that traffic in the LV pathway (Robinson et al. 1998). In tobacco (*Nicotiana tabacum*) cells, GFP fusions to the ct-VSD of tobacco Chitinase (GFP-Chi) was found in punctate structures reminiscent of PSVs, while GFP fusion of the ssVSD of barley Aleurain (Aleu-GFP) was found in the central large vacuole (Di Sansebastiano et al. 1998; Flückiger et al. 2003). In Arabidopsis, GFP-Chi and Aleu-GFP constructs were both found in the lumen of a unique central vacuole in leaves or roots (Flückiger et al. 2003). This central vacuole is consequently called hybrid vacuole (Di Sansebastiano et al. 2007; Neuhaus and Martinoia 1999; Olbrich et al. 2007b).

However it was shown that targeting to separate vacuoles may not be as clean-cut as initially postulated. Loss of function of AtVSR1 leads to secretion of storage proteins in Arabidopsis seeds (Fuji et al. 2007; Shimada et al. 2003a) and proteins with ssVSDs were found in the PSV (Brown et al. 2003; Jolliffe et al. 2004; Maruyama et al. 2006). Fluorescent proteins fused to AtTIP proteins expressed in Arabidopsis meristematic cells all labeled the

same vacuoles (Hunter et al. 2007) instead of different vacuoles as observed before by immunolabeling (Paris et al. 1996).

Presence of unique or multiple vacuoles might be explained by their biogenesis. Protein targeting from the trans-Golgi network (TGN) to the vacuoles is mediated by late endosomes, also called the prevacuolar compartment/multivesicular bodies (PVC/MVBs) (Marty 1999). Hence, the PVC/MVBs are considered as vacuole precursor (Marty 1999). Lytic vacuoles are more abundant in plant tissue and have been proposed to arise from a prevacuolar compartment that could be defined both morphologically (Paris et al. 1997) and functionally (Jiang et al. 1998). In evacuolated protoplasts, LVs can rapidly regenerate indicating that vacuole can be formed *de novo* (Di Sansebastiano et al. 2001). It has been shown that LV could be formed by autophagic uptake of cytosolic contents (Yano et al. 2007). Knock-out of a gene VCL1 (required for LV biogenesis in embryos), blocked LV biogenesis and caused an accumulation of autophagosomes. This indicates that vacuole may rise from fusion of autophagosomes (Rojo et al. 2001). Observations of vacuole biogenesis in meristematic cells are consistent with the autophagic origin of LV (Marty 1978).

In our study, we investigated the vacuole organization in moss cells. Evacuolation experiments of moss protoplasts revealed some features of the early steps of vacuole biogenesis.

II. Results

1. Most moss cells have an acidic lytic central vacuole

In flowering plant cells, the large central vacuoles can be either acidic or neutral. (Frigerio et al. 2008; Murphy et al. 2005). We investigated the vacuole types in moss by two methods: 1) staining with using the Neutral red (NR), and 2) expression of the fluorescent of LV reporter: AtAleurain-GFP. NR is a lipophilic phenazine dye membrane permeable in its unprotonated form but when protonated it becomes trapped in acidic compartments.

In moss protoplasts, NR stained the large central vacuole, i. e. an acidic lytic vacuole (fig. 1A). The same result was obtained for the large central vacuole of protonema cells (fig.1 B), and for rhizoids (fig. 1C). In contrast, leaf cells did not accumulate NR in their large central vacuole, and only small compartments were labeled which the penetration of the NR in this tissue (fig. 1C).

In order to confirm the lytic nature of the NR-labeled vacuole, we chose aleurain as reporter of the LV. Several studies showed that aleurains are sorted to LVs due to their ssVSD (Holwerda et al. 1992; Holwerda and Rogers 1993). First the endogenous *Pp*Aleurain was chosen (from 11 isoforms) with the highest expression level, as judged by the number of ESTs in the databases. We introduced by homologous recombination (HR) into its gene the coding sequence of GFP as a C-terminal translational fusion. Unfortunately, we could not detect any fluorescence in the transgenic moss. Therefore, as an alternative strategy, we used the *A.thaliana* Aleurain fused to GFP and expressed under a Hsp promoter, we addressed it by HR to a known non-coding locus (Pp-108) in the moss genome. After heat treatment, expression of this fusion protein caused an accumulation of GFP in the large central vacuole of protoplasts, chloronema cells and rhizoids (fig. 1 E, F, G). AtAleurain-GFP was thus correctly addressed to the acidic vacuole in these tissues. Consistent with their lack of NR staining, leaf cells did not show any fluorescence in large central vacuoles (fig. 1H). Comparison of moss cell images either stained with NR or expressing AtAleurain-GFP confirmed that acidic vacuoles correspond to lytic vacuoles. It also confirmed that the large central vacuole of chloronema and rhizoid cells is lytic. The absence of NR or GFP accumulation in leaf cells also indicated that they have a different type of central vacuole: neutral and not accumulating AtAleurain-GFP, presumably thus a storage vacuole.

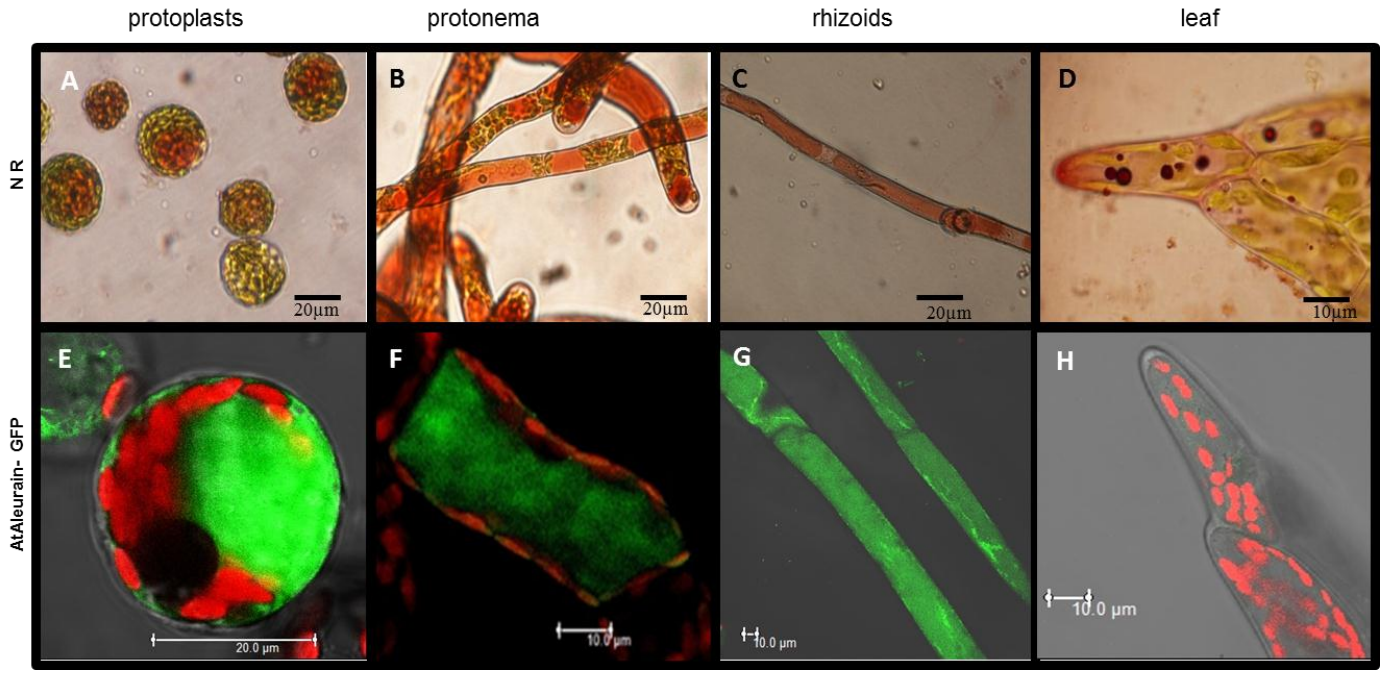

Figure 1: The large central vacuole of several cell types, but not leaf cells is acidic and accumulates a marker of the LV.

Comparison of vacuole labeling in various tissues by Neutral Red (top line) visualized by light microscopy and by AtAleurain-GFP (bottom line) visualized by confocal microscopy (red channel shows chloroplasts)

(A, E) protoplasts, **(B, F)** chloronema, **(C, G)** rhizoid, **(D, H)** leaf.

Note that the central large vacuole of leaf cells was stained by neither NR **(D)** nor AtAleurain-GFP **(H)** but NR accumulated in small compartments.

.

2. Two vacuole types can coexist in moss cells

Our previous results showed that two vacuole types can be observed in moss tissues, acidic in protonema cells and rhizoids and neutral in leaf cells. Can these two vacuole types coexist in the same moss cell? Examination of moss apical cells indicated that there could be in the same cell a vacuole accumulating NR while another vacuole was not stained (fig. 2). Similarly to *A.thaliana* and barley vacuoles, acidic and neutral vacuoles can coexist within the same moss cell.

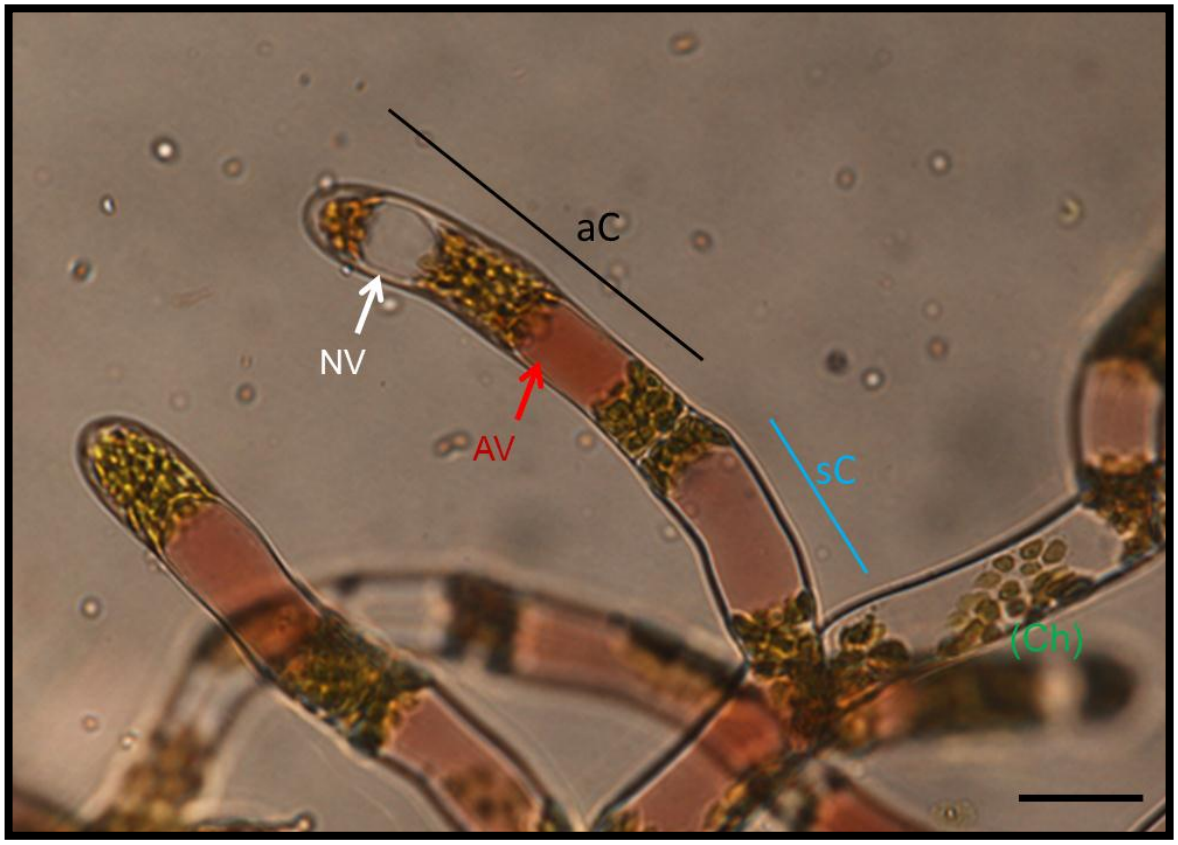

Figure 2: Detection of both neutral and acidic vacuoles in moss protonema cells.

Light microscope image of chloronema cells stained with NR.

The filament is composed by an apical cell **(aC)** and a sub-apical cell **(sC)**. Within the apical cell, two large vacuolar compartments are visible a non-acidic vacuole **(NV)** and an acidic vacuole **(AV**). Green dots are chloroplasts (**Ch**). Scale Bar = 100µm

3. The central vacuole is formed from small vacuoles in differentiated cells

Comparison of apical cells with subapical cells revealed a pattern difference. Light microscopy images revealed many small vacuoles in apical cells but mostly only one large vacuole in subapical cells (fig. 3A-B). Electron microscopic images (fig. 3C-D) also indicated that apical cells contained small vacuoles, whereas subapical cells contained a large vacuole occupying most of the cell volume. We statistically evaluated the number of vacuoles in apical, subapical and following cells (fig. 3 graph E). This confirmed that apical cells have many vacuoles while subapical cells and following cells have only one or two. These data suggest that small vacuoles, formed in (younger) apical cells, fuse to form one or two central acidic vacuoles in subapical (older) cells.

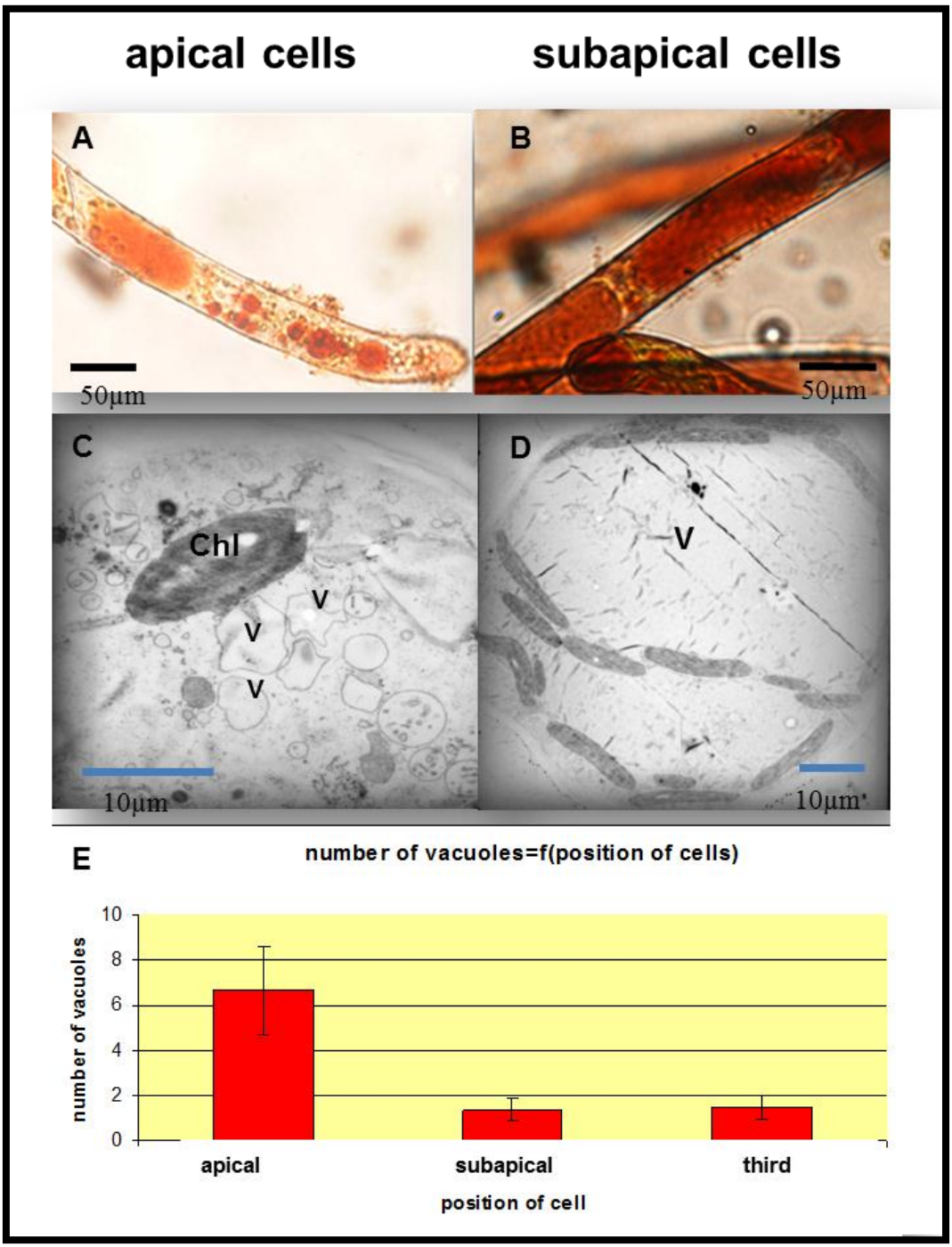

Figure 3: Vacuole formation in apical cells.

(A-B) Light microscope images of caulonema cells stained with NR and **(C-D)** Electron microscopic images. **(A, C)** Apical cells, **(B, D)** subapical cells.

(E) Statistical counting of the number of vacuoles per cell in different cell positions. Apical cells have several vacuoles whereas subapical cells, and following cells have only one or two vacuoles (number of counted filaments = 20).

4. Vacuole regeneration

The *de novo* vacuole biogenesis mechanism was investigated by starting with evacuolated protoplasts. Adapting the established evacuolation protocol for *N. tabacum* protoplasts (Di Sansebastiano et al. 2001), we evacuolated moss protoplasts was from a transgenic line expressing the tonoplast reporter AtVamp3-GFP (Oda et al. 2009b). After incubation in the lysis buffer, centrifugation allowed to expell the vacuole from the protoplasts, which remained viable. We obtained fractions containing intact vacuoles or protoplasts without vacuoles, the miniprotoplasts.

Observation by confocal microscopy of the moss miniprotoplasts, revealed that vacuole regeneration is a rapid process which only took aproximatively 3 hours (fig. 4). Representative confocal microscopic images at different time points showed the tonoplast patterns during vacuole regeneration (fig. 4). Already half an hour after evacuolation the tonoplast regenerated as filaments-like structures (fig. 4D). One hour after evacuolation, there were filaments throughout the cell volume (fig. 4E). After two hours these filaments enlarged and became independent tubules with a well defined lumen (fig. 4F). After three hours, most regenerating miniprotoplasts had recovered a large vacuole (fig. 4G).

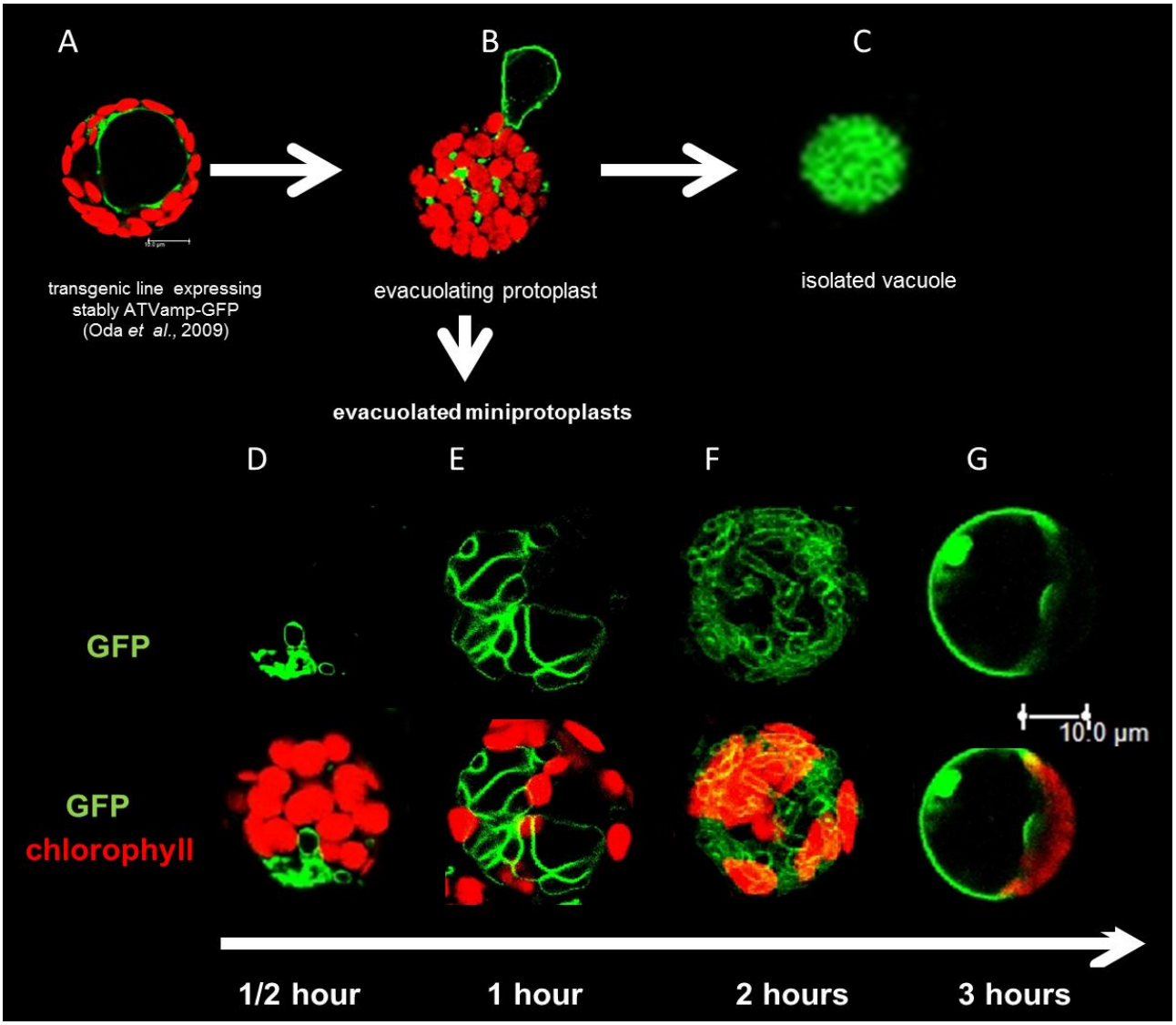

Figure 4: Regeneration of tonoplast and vacuole after protoplast evacuolation

Confocal microscopic images of protoplasts at different time points showing the localization of the tonoplast reporter Atvamp3-GFP (green signal). Chloroplasts fluoresce in red colour.

(A) Protoplast before evacuolation, **(B)** evacuolating protoplast, **(C)** isolated vacuole. **(D)** 30 minutes after evacuolation, miniprotoplasts regenerated tonoplast appearing as thin filaments. **(E)** One hour after evacuolation. **(F)** After two hours, tubular structures with lumen appeared. **(G)** Vacuole almost completely regenerated 3 hours after evacuolation.

III. Discussion

1. Does moss have different vacuoles types?

How many trafficking pathways are required to generate the vacuoles of *P.patens*? We demonstrated that two types of vacuoles can be found in chloronema apical cells: acidic and neutral (or non-acidic) vacuoles. The existence of these two vacuoles with distinct contents implies separate trafficking routes for their respective cargoes (Di Sansebastiano et al. 2001; Neuhaus and Paris 2005). In order to develop reporters for the PSV and LV, the GFP coding sequence was recombined into endogenous PpAleurain and PpChitinase genes as translational fusions. The genes had been chosen because the predicted protein sequences seemed to contain a ssVSD or a ct-VSD respectively, and available EST sequences indicated *in vivo* expression. Transgenic mosses were produced and screened. The PpAleurain-GFP was not detected anywhere. This is why we instead had to use the exogenous AtAleurain-GFP. The PpChitinase-GFP was expressed, but labeled the apoplast instead of the expected vacuoles. Production of GFP-Chi expressing moss clones is under way (see supplementary fig. 1).

Our experiments showed that most moss cells had large acidic vacuoles, in protonema cells and rhizoids (fig. 1). The targeting of the fusion protein AtAleurain-GFP to the central vacuole of protonema and rhizoids confirmed that this vacuole is a lytic vacuole. Interestingly, central vacuoles of leaf cells exhibit neither NR staining nor AtAleurain-GFP accumulation. Hence, the lytic nature of vacuole of the leaf cells was not supported. Our results instead suggest that leaf cells have a PSV. Where did the AtAleurain-GFP go in leaf cells? In fact, the same disappearance of Aleu-GFP was observed in mesophyll cells of transgenic Arabidopsis, where GFP-chi was targeted to the large central vacuole (Flückiger et al. 2003).

2. Early steps of vacuole biogenesis

Protoplast systems are useful models for the study of the secretory pathway in flowering plants (Denecke et al. 2012). By enzymatic digestion, the moss chloronema cells lose their cell wall and also become protoplasts. In order to regenerate their cell wall, they have to accelerate their protein secretion. Protoplasts can then even be evacuolated in order to observe the *de novo* regeneration of the vacuole. A previous study of vacuole regeneration in tobacco miniprotoplasts showed that large vacuoles appear 24-36 hours after evacuolation (Di

Sansebastiano et al. 2001). In contrast, moss miniprotoplasts regenerated their vacuoles within three hours. This difference in regeneration speed is probably due to the different original cell type. Indeed moss protoplasts were derived at 99% from chloronema cells (Hohe et al. 2004; Liu and Vidali 2011; Schaefer et al. 1993), while tobacco protoplasts came from mesophyll cells. The life cycle of protonema cells is quite short: chloronema cells (on average 100 μm in length) divide every 10–12 h (Cove et al. 1997). The much faster vacuole regeneration may be due to this cell being organized for a short generation time, while tobacco mesophyll cells are not prepared to divide. However these evacuolation experiments are not totally comparable since we have used a tonoplast reporter and not soluble vacuolar reporters as Di Sansebastiano et al., (Di Sansebastiano et al. 2001).

Images of vacuole regeneration at different times after evacuolation suggest that vacuoles regenerated from tonoplast "filaments", which progressively filled to form isolated tubules which then turned to vacuoles (fig. 2). Interestingly, this pattern resembles to electron microscopic images of young *A.thaliana* root cells, where vacuoles formed from filament and tubule-like structures emerging from ER (Corrado Viotti, K. Schumacher unpublished observations). This mechanism of vacuole biogenesis implies that tonoplast is formed first, and that luminal content is then targeted into these tonoplast tubules. At first they are too thin to distinguish a lumen and appear as filaments, but then enlarge and become visibly tubular and finally fuse to form a vacuole.

3. Evidence for vacuole enlargement

Vacuole regeneration in tobacco miniprotoplasts showed that in a majority of regenerated protoplasts, the central lytic vacuole remained separate from the protein storage compartments composed of small compartments. After regeneration of a lytic central vacuole, in about a third of the cells, the lytic vacuole and the protein storage compartments fused to an unique compartments (Di Sansebastiano et al. 2001). Likewise, our data indicated that in apical cells neutral and lytic vacuoles appeared to generate from distinct small vacuoles (fig. 4). As shown in subapical cells, the vacuolar pattern indicated that these small vacuoles might fuse to form a hybrid vacuole. However, we cannot exclude that apical cells inherited LV which enlarge from small pre-existing vacuoles such as in tobacco, where LVs are inherited and then enlarge in differentiating cells through a process that may involve autophagy (Yano et al. 2007).

We suppose that the features of vacuole biogenesis observed in protoplasts correspond to the early steps of vacuole enlargement process in differentiated cells. Therefore, according to our observations, a model is proposed in order to explain the vacuole biogenesis and it enlargement in moss protoplasts and protonema cells (fig. 5). This model posits that vacuole *de novo* biogenesis starts from filaments derived from the ER. The "filaments" turn into tubules and became provacuoles. Then, inherited vacuoles would enlarge by fusion of provacuoles.

The presence of tubule-like structures as vacuolar precursors is not a new idea since Marty et al., (1999) have already characterised tubule-like structures as vacuole progenitors during mitosis. The recent unpublished results (Viotti) confirm this tubule-like pattern

The ER origin of the tubule-like structure remains to be confirmed. Our model proposes that *de novo* the vacuole formation starts from ER structures that could be called provacuoles. Could prevacuolar compartments (PVC) also form this compartment? Indeed, several studies showed the PVC to be precursor of the vacuolar compartment (Mo et al. 2006; Vitale and Chrispeels 1992). Together, these results suggest that there are at least two pathways for vacuole biogenesis (Marty 1999): 1) from TGN derived PVC and 2) from ER-derived provacuoles.

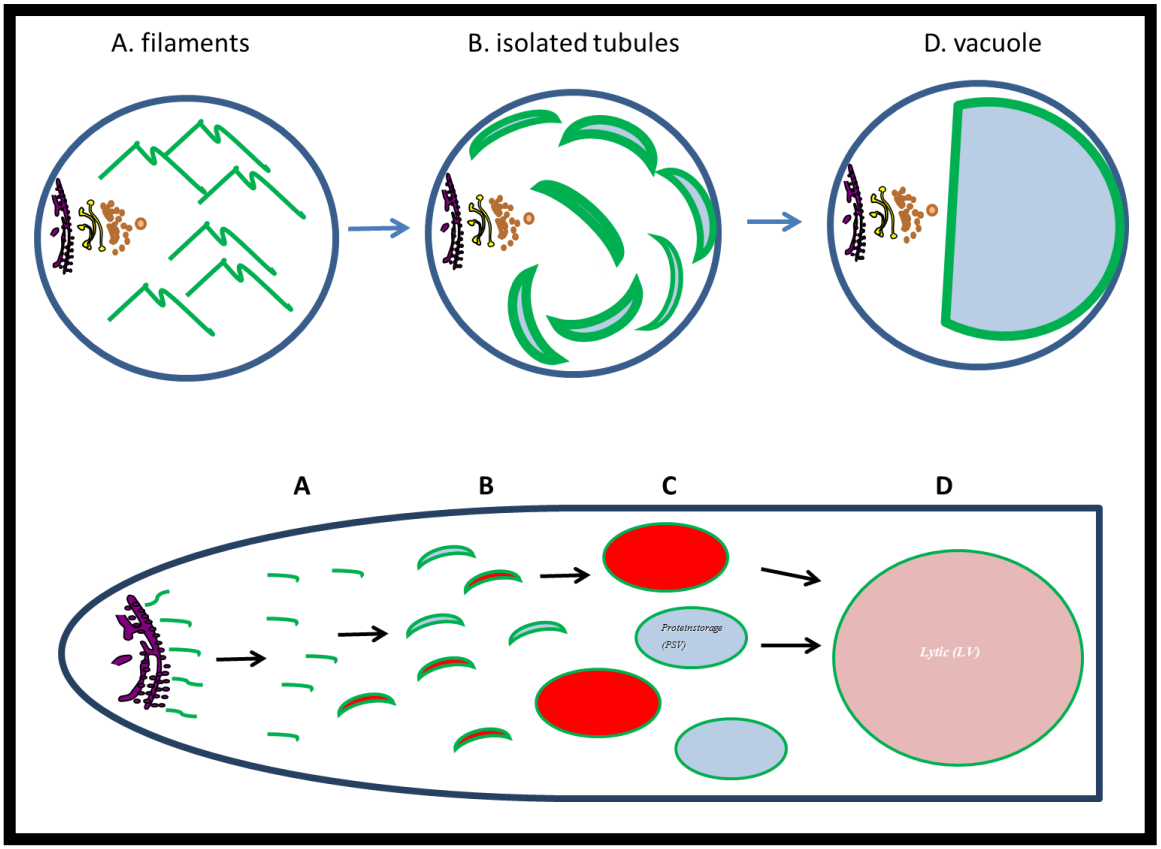

Figure 5: Model of vacuole biogenesis *de novo* in moss protoplasts and in protonema cell

(A) The tonoplast is formed from the ER as "filament" membranes (tonoplast tubes with very little lumen) where AtVAmp3-GFP is integrated (green colour)

(B) Once separated from the ER, the filaments are progressively filled with lumen (blue for neutral lumen or red for acidic lumen) to form tubules with visible lumen.

(C) Tubules continue to increase in volume to become provacuoles. The differentiation of their lumen into a lytic or neutral content could be determined by intrinsic proteins in the tonoplasts.

(D) Fusion of lytic and neutral provacuoles leads to formation of lytic and neutral vacuoles or together to form hybrid vacuoles.

IV. Material and methods

Protoplast isolation

As describes in chapter 2

Protoplasts evacuolation

Protoplast (PPs) were pelleted in 0.48M mannitol. They were resuspended in 3 ml of E. sol1 (D-Mannitol 0,5 M, $CaCl_2$ 1 mM, MES 10 mM) and in 12 ml E.sol2 (D-Mannitol 0,5 M, $CaCl_2$ 50 mM, and Hepes 0,476 g) in a ultra-centrifuge tubes. Overlay with these 3ml of E sol. 1. They were centrifuged for 45 minutes at 90,000g at room temperature in an XL-80 ultracentrifuge. The green layer contained evacuolated protoplasts (miniprotoplasts MIPs), PPs and vacuoles were put into tube in order to be centrifuged. All the green phase was diluted with 9 volumes E. sol1 and spined for 10min at 120g at room temperature in GS-6R centrifuge without deceleration setting. The supernatant was removed except the last 2ml E. sol.1 and resuspended the MIPs, PPs and vacuoles. A Percoll gradient was prepared into a centrifuge tube described as follow: 2 ml of 60% Percoll solution, overlay with 5ml of 40% solution, and finally 2ml of 20% solution. The critical step is the layering of the gradient has to be done very carefully but quickly; try to avoid mixing the consecutive layers. The Percoll gradient was overlayed with the last 2ml of E. sol1 and spined for 10min at 1000g at room temperature in GS-6R Centrifuge. MIPs should be visible as green layer on the interface between 60 and 40 % Percoll solution. They were removed carefully with 2 ml of E. sol1.

Stable transformantion to express AtAleurain-GFP.

To visualize vacuolar lumen in moss cells, hsp-AtAleurain-GFP was cloned using restrictions sites in vector 35S-108-PBNRR (cut XhoI/SalI) under the control of the Hsp promoter. This vector contains *108* genomic fragments and thus allows the fragments to be inserted into the *Pphb7* locus (see annex chapter constructs). Polyethylene glycol (PEG)-mediated transformation was performed as described by previously (Nishiyama et al. 2000), and mutants were selected on BCDAT medium supplemented with 20 mg l^{-1} G418 (Invitrogen Corporation,Carlsbad, CA, USA). The genotyping of the transgenic colonies were performed by PCR on the recombinant junctions between the 5'and the 3' genomic 108 locus and the resistance marker. These junctions were amplified with appropriate primers (see annex primers).

Confocal microscopy

Images were collected with a TCS SP5 II confocal laser scanning microscope (Leica). Digital Images were acquired using LAS AF (version: 2.0.0 build 1934) and processed using ImageJ 1.41 (National Institute of Health, USA). Aliquots of the protonema cell culture were transferred on slides with coverslip at the top for observation. For simultaneous observations of observe AtAleurain-GFP, GFP was excited by a 488 nm argon laser, and detected through a confocal unit (TCS SP5 II confocal laser scanning microscope Leica) with a 524–546 nm band-pass filter.

Staining of vacuolar lumen with Neutral Red

To label vacuolar membranes, protonema cells were treated with 12g.L-^{1}with NR (Invitrogen) for 20 min. Subsequently, the cells were washed in water or fresh PPNH4 liquid medium with liquid medium and incubated for 20min. The cells could be observed directly.

GFP-AtVamp3 line

Wild type plant expressing a fusion construct of GFP and an Arabidopsis tonoplast t-SNARE, encoded by AtVAM3/SYP22 kindly provided by the Dr. Hawesava.

VI. Supplemental figures

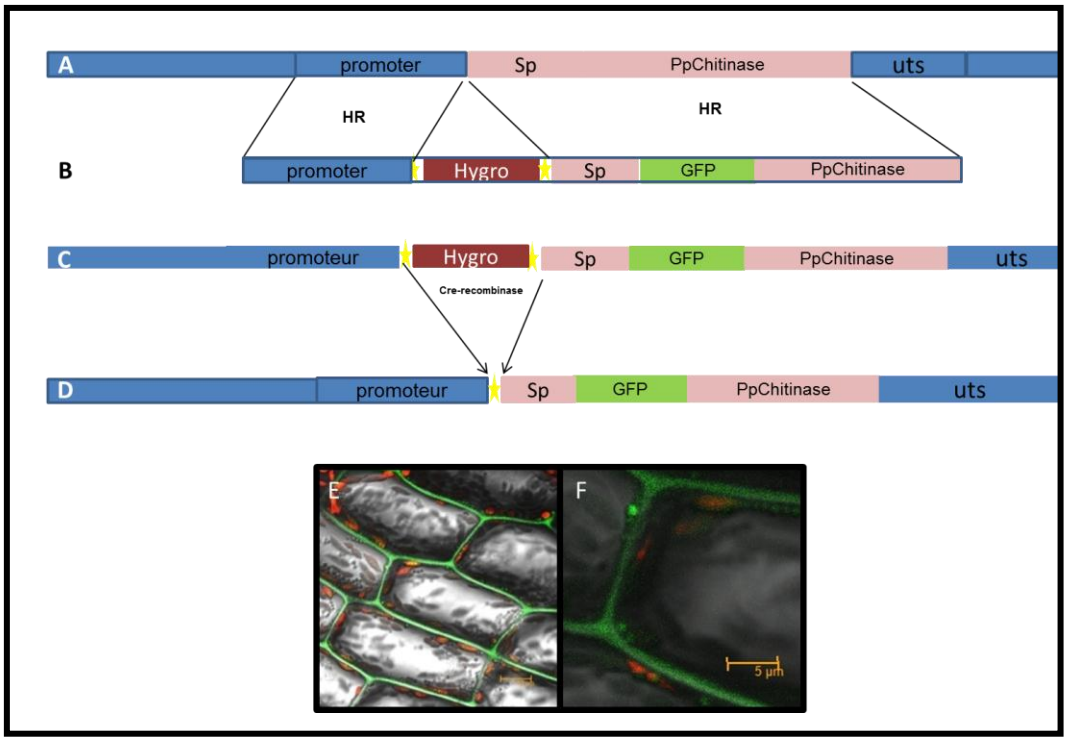

Suppl. fig. 1: Replacement vector for PpChitinase-GFP tagging in the wild type locus and it localization.

(A) Wild type locus of encoding *Pp*Chitinase (pink box) with its signal peptide (Sp).
(B) The replacement vector consists of two homologous targeting sequences the (promoter) and (the Sp + the GFP gene + PpChitinase gene sequence) flanking the Hygromycin resistance (Hygro in red) and LoxP sites (yellow stars).
(C) After transformation of the replacement vector in the moss cells, the *Pp*chitinase gene is recombined with the vector. Two homologous recombinations **(HR)** events occur.
(D) The Cre-recombinase eliminates the resistance cassette and leaves a unique lox P site (yellow).
(**E-F**) Images taken by confocal microscopy indicate that GFP accumulated in apoplast of moss leaf cells.
(**F**) Zoom showing that GFP-PpChitinase is localised in vesicles near the plasma membrane to be secreted out the cell.

Chapter 4: Characterization of complete RMR deletion mutants.

I. Introduction

Seed vacuoles are important storage compartments for the amino-acids required for early plant development. Storage and release of proteins are processes that imply numerous vacuolar transporters. During the last years, transporters implicated in many aspects of vacuolar functions have been identified and characterized. However, still little is known about their mode of action, in particular for the RMR proteins.

The coexistence of the LV and PSV was demonstrated by different studies (Di Sansebastiano et al. 1998; Jauh et al. 1998; Jauh et al. 1999). In plant, vacuolar proteins are synthesized as precursors with short peptide sequences called vacuolar sorting determinants (VSD) necessary for vacuolar targeting (Matsuoka and Nakamura 1999; Neuhaus and Rogers 1998). Different types of VSD have been described: C-terminal (ct-VSD), sequence-specific (ssVSD) and physical structure VSD (psVSD) (Vitale and Raikhel 1999). Ct-VSD were identified in the C-terminal propeptides of barley lectin (Bednarek et al. 1990), tobacco chitinase A (Neuhaus et al. 1994), and phaseolin (Frigerio et al. 1998) while ssVSD were found in the N-terminal propeptide of barley aleurain (Holwerda and Rogers 1992), or the internal propeptide of ricin sporamin (Frigerio et al. 2001). Proteins bearing ssVSD are addressed to LV (Holwerda et al. 1992; Koide et al. 1999), whereas proteins with a ct-VSD are addressed to PSV (Bednarek et al. 1990). In some tobacco mesophyll protoplasts and in certain cell types of transgenic Arabidopsis, a GFP fusion to the ct-VSD of tobacco Chitinase (GFP-Chi) was found in punctate structures reminiscent of PSVs, while a GFP fusion of the ssVSD of barley Aleurain (Aleu-GFP) was found in the central large vacuole. In tobacco protoplasts and in other cell types of the transgenic Arabidopsis, GFP-Chi was also found in the large central vacuole (Di Sansebastiano et al. 1998; Di Sansebastiano et al. 2001; Flückiger 1999).

A vacuolar receptor involved in traffic of ssVSD proteins was first identified in pea clathrin-coated vesicles (CCV) (Paris et al. 1997). This first vacuolar sorting receptor (VSR) was called BP-80 (Binding Protein 80kD) (Kirsch et al. 1994; Kirsch et al. 1996). Protease digestion of BP-80 indicated that its protease-associated (PA) domain and another part of its luminal domain are involved in binding the ssVSD of vacuolar cargo (Cao et al. 2000). *in vitro* interactions were however also found between BP-80 and the C-terminal propeptide carried by a storage protein, 2S albumins from Brazil nut (Kirsch et al. 1996).

Another putative receptor was identified by its homology to the PA domain of the VSR proteins. It was named Receptor-Membrane-RingH_2 protein (RMR) (Cao et al. 2000;

Jiang et al. 2000). The genome of Arabidopsis encodes six homologues, AtRMR1 to AtRMR6 (the original RMR is AtRMR2) (Park et al. 2005). Specific *in vitro* binding to the ct-VSD of the phaseolin was shown for the luminal domain of AtRMR1 (Park et al. 2005). In addition, AtRMR2 binds strongly to the ct-VSD of chitinase but only when its C-terminus was free, and only weakly to the ssVSD of proaleurain (Park et al. 2007). RMRs are thus likely to be receptors for storage protein.

By their subcellular localization, RMR proteins are found in strategic places. First, *At*RMR2 was originally discovered as component of the crystalloid membrane in PSV of Arabidopsis seeds (Jiang et al. 2000). Immuno-electron microscopy experiments localized RMRs in the early stacks of Golgi and in dense vesicles (DVs) (Hinz et al. 2007). In Arabidopsis protoplasts, endogenous AtRMR1 colocalized with the organelle marker DIP (Dark-induced tonoplast Intrinsic Protein) but not with a marker of PVC (Park et al. 2005). The DIP organelles were proposed to be particular prevacuolar compartments (PVC) for PSV, delivering internal proteins (Jiang et al. 2000). More recently rice OsRMR1 proteins were localized in GA, TGN, PSV and in an organelle identified as PVC for PSV (called PVCs) both in rice cultured cells and in developing rice seeds. This localization seems to be conserved since the same antibodies detected RMRs also in Golgi, TGN, and PVCs in BY-2 and in Arabidopsis cultured cells (Shen et al. 2011).

It was found that *At*RMR2 and its ligands are not dissociated at low pH (Park et al. 2007), suggesting that RMRs cannot be recycled from an acidic PVC but rather accompany their cargo proteins to PSV. Two mechanisms were proposed by Hinz *et al.* (2007) to explain the role of RMR as vacuolar receptors: (i) individual storage proteins bound to RMR proteins could act as nuclei for aggregation of storage proteins, (ii) preexisting microaggregates of storage proteins could interact with RMR proteins via surface exposed ct-VSDs. Either way RMRs could function as storage protein receptors or as assembly factors even without recycling.

The RMR proteins are composed of an N-terminal luminal domain restricted to a PA domain, a transmembrane domain, and a cytosolic tail with a RING-H2 (Really Interesting New Gene) domain, and in most RMRs a serine-rich region (missing in AtRMR 1, 5 & 6) (Park et al. 2005). The Ring-H2 domain found in RMRs is of the C3H2C3 type. Presence of this domain suggests an E3 ubiquitin ligase activity (Anandasabapathy et al. 2003; Su et al. 2009). Several studies showed a close relationship between E3 ligase activity or ubiquitination and drought stress regulation (Cheng et al. 2012; Lee et al. 2009). For example, the Ring protein RGLG2U has a E3 ligase activity and mediates ubiquitination as a signal for

proteasomal degradation of the ETHYLENE RESPONSE FACTOR53 (AtERF53), a drought-induced transcription factor in *A. thaliana*. RGLG2U has been characterized as negative regulator of the drought stress response by suppressing AtERF53 transcriptional activity in Arabidopsis (Cheng et al. 2012). Another plant protein with E3 ubiquitin ligase activity is Rma1H1 (RING membrane-anchor1 homolog1) of hot pepper (*Capsicum annuum*), a homolog of a human RING membrane-anchor protein (Lee et al. 2009). Rma1H1 was shown to be localized to the ER and to be involved in ubiquitination of proteins followed by their proteasomal degradation. This activity enhanced drought stress tolerance of transgenic Arabidopsis plants. In particular, the E3 ubiquitin ligase activity of RmaH1 played a critical role in the down-regulation of plasma membrane aquaporin levels by inhibiting aquaporin trafficking to the plasma membrane as a response to dehydration (Lee et al. 2009). Like RmaH1 and RGLG2U, RMR proteins have a Ring domain and might be involved in protein ubiquitination and degradation

The aim of this study was to characterize the function of the putative vacuolar receptors of the RMR family, by taking advantage of the efficient gene targeting system of the moss. Our aim was to delete all RMR genes, and then characterize the resulting mutants using secretory system reporters, and testing drought stress tolerance in RMR ko mutants.

II. Results

1. Identification of RMR genes in *P. patens*

To identify the *P.patens* genes for RMRs, the amino-acid sequences of RMRs from *A.thaliana* and *O.sativa* were blasted against the genome sequence of *P. patens*, using the Physcobase database (http://moss.nibb.ac.jp). Five RMR genes were found in the *P.patens* genome.

A phylogenetic tree was constructed with RMR DNA sequences without the serine rich domain (SRD) of fully sequenced genome from the dicots *Arabidopsis thaliana*, the monocots *Poplar trichocarpa, Oriza sativa, Brachypodium distachyon,* the moss *Physcomitrella patens,* and the lycopod *Selaginella moellendorffii*. The SRDs of RMR sequences are degenerated, thus they were not used to have a more accurate alignment of the RMR sequences. The *Chlamydomonas reinhardtii* RMR sequence was used to determine the root position (fig. 1). The resulting phylogenetic tree was subdivided into tree main subfamilies, one regrouping all RMRs of moss & lycopods (fig. 1 highlighted in pink), then a second comprising most of angiosperms RMRs (fig. 1 highlighted in yellow), and a third group with some angiosperm RMRs (fig. 1 highlighted in green). The lycopods RMRs are closer to the moss RMR. Both form a separate clade from the angiosperm sequences. However they appear more related to the major group of angiosperm RMRs, while there is another angiosperm group with RMRs from *Arabidopsis, Brachypodium*, *Poplar* but not *Oriza* (AthRMR1, BrachyRMR1, PoplarRMR1).

As shown in the phylogenetic tree, PpRMRs are clustered in two subfamilies PpRMR I (1&2) *vs* PpRMR II (3&4 and 5). The two subfamilies might have originated by an ancient whole-genome duplication in *P.patens* (Rensing et al. 2007). Alternatively preexisting PpRMR I and II would have been duplicated then.

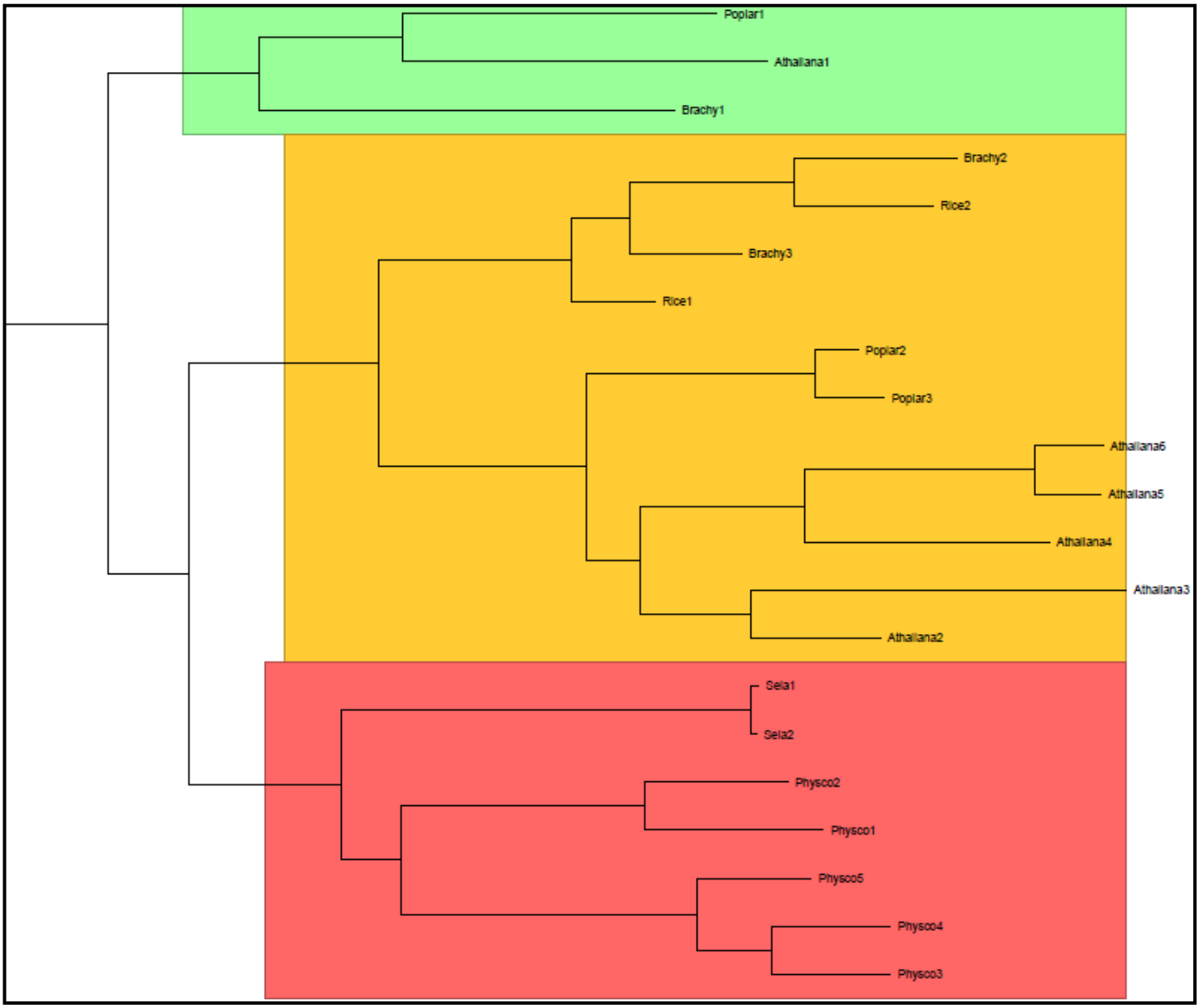

Figure 1: Phylogenetic tree of land plant RMRs

The phylogenetic tree of DNA RMR sequences (without the serine rich domain SRD) from the genomes of *Arabidopsis thaliana*, *Poplar trichocarpa* (Dicotyledons) *Oriza sativa*, *Brachypodium distachyon* (Monocotyledons), *Physcomitrella patens* (Bryophyte), *Selaginella moellendorffii* (Lycopod) was determined by the fast DNAML. The *Chlamydomonas reinhardtii* RMR sequence was used to determine the root position.

2. Generation of RMR Knock-out lines

2.1. Cloning strategy

Constructs were made for the deletion by gene targeting of each *Pp*RMR gene. They were designed to replace the wild type RMR coding sequence by a resistance cassette. As described in figure 2, genomic regions corresponding to the sequences upstream and downstream of the coding sequences of each *Pp*RMR were amplified by PCR and inserted into a bilox plasmid on either side of a Hygromycin or Neomycin resistance cassette flanked by two LoxP sites. PEG-mediated transformation of *P. patens* was carried out with these plasmids. Once inside the nucleus, the replacement vector is expected to recombine by homology at the corresponding wild type RMR locus, the resistance cassette replacing the entire coding sequence from the ATG to the STOP codons of each *Pp*RMR (fig. 2C).

Insertion at the correct locus was confirmed by PCR on genomic DNA using, for each side of the insert, primers complementary to an external target locus sequence (fig. 2C primers I and IV) and primers complementary to the resistance gene (primers II and III). The resulting PCR products testified the presence of the recombined locus in the transformant genome. There may be multiples tandem insertions of the recombination cassette. In order to eliminate the resistance cassette and possible multiple inserted copies, the Cre-lox system was used: transiently expressed Cre-recombinase in protoplasts recombines the transformed locus at Lox P sites, eliminating the resistance cassette, and leaving only a single LoxP site as a scar. After Cre-recombination, the genotype of the mutant can be tested again by PCR (fig. 2D primers I and IV) and confirms the deletion of the resistance cassette. It is however important that the excised gene has not inserted elsewhere in the genome and that no *Pp*RMR transcripts can be detected anymore in the Ko mutants.

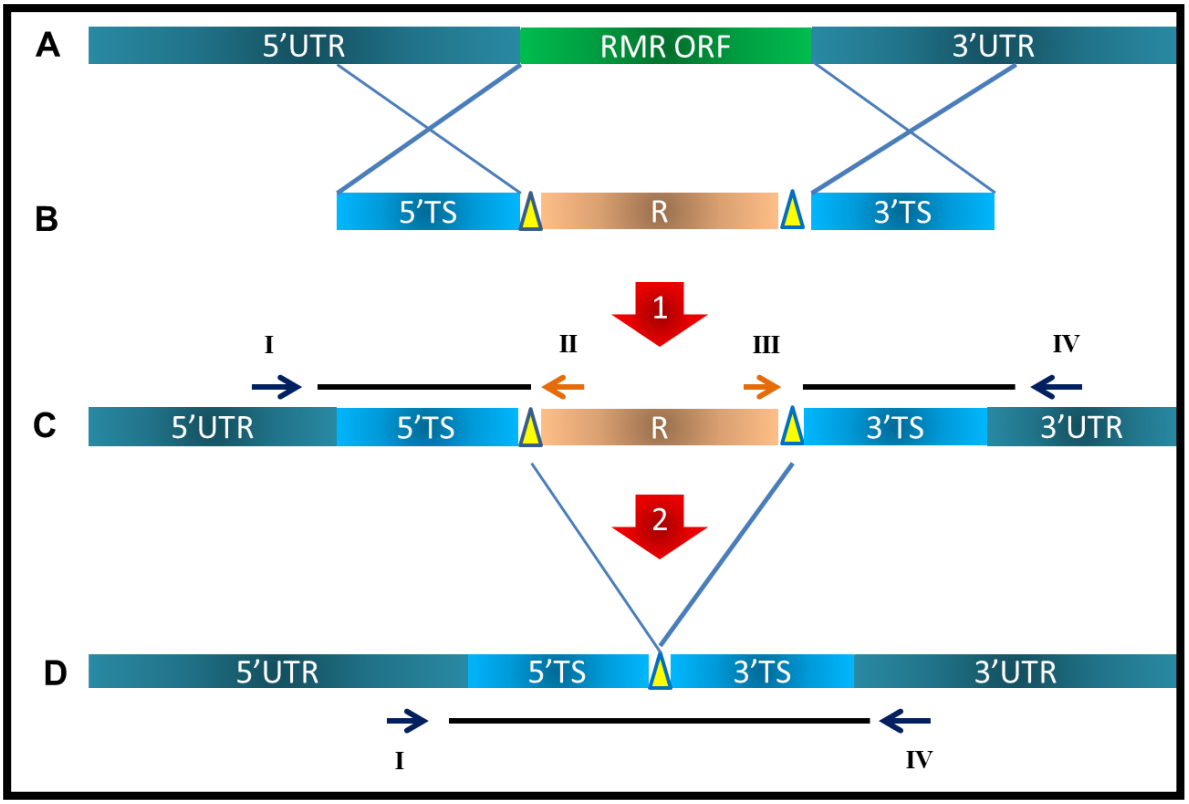

Figure 2: RMRs locus deletion by a replacement vector

(A) The RMR locus is constituted of the RMR Open Reading Frame from the ATG to STOP (green box RMR ORF) and of the UnTranslated Region at 5' and 3' (UTR dark blue boxes). **(B)** The replacement vector carries the resistance cassette (R gene orange box) between two targeting sequences (5'and 3'TS blue) which are homologous to the 5'and 3'UTR, and two LoxP sites (yellow). Gene Conversion **(arrow 1)** mediated by two homologous recombination events at 3' and 5'TS causes the replacement **(C)** of the ORF by one or several tandem repeats of the replacement cassette. Genotyping is performed by PCR using primer pairs (I & II arrows) and (III & IV arrows). PCR products of the junction between the TS and the resistance cassette are represented by a black line. **(D)** Expression of the site-specific Cre-recombinase **(arrow 2)** eliminates the resistance marker and one LoxP site. The recombined locus is free of the resistance marker leaving a single LoxP site between the two targeting sequences. The PCR product resulting from the amplification of primers I & IV confirms the deletion of ORF and resistance marker.

2.2. Simple Knock-out mutants

Knock-out mutants were generated for each *Pp*RMR genes by transforming *P. patens* protoplasts with a linear DNA replacement vector. After transformation, regenerating Neomycin or Hygromycin-resistant moss colonies had a normal growth phenotype (fig. 3). They were screened by PCR with two different primer pairs to identify positive recombination events resulting from a double homologous recombination event at the 5'and the 3'extremities of the locus. True deletion mutants of a single *Pp*RMR genes resulted in the replacement of the whole Open Reading Frame (ORF) by the resistance cassette. The results of the deletion mutant screen of the simple *Pp*RMR mutants are shown in figure 3. For each deletion mutant, the PCR reactions resulted in the expected products: 5' external UTR to resistance marker, 3'external UTR to resistance marker. After Cre-recombinase expression in these mutants genotyping showed a long 5' external UTR to 3' external UTR which revealed the complete deletion of the resistance cassette.

2.3. Multiple and complete Ko RMR mutant

In order to generate multiple RMR mutants, single RMR (1ko RMR) mutants were sequentially transformed with replacement vectors of the other RMR genes. Between each transformation step the multiple mutants were transiently transformed with the Cre-lox vector in order to eliminate each time the resistance cassette. The order of deletion was chosen according to the phylogenetic tree (fig. 1): there are two pairs of more closely related PpRMRs: 1&2 and 3&4. PpRMR5 is closer to the 3&4 pair. We first deleted one of each pair: koRMR1/4, koRMR2/4, koRMR1/3, koRMR1/5. No phenotypic change was observed in any double ko mutant (2koRMR). From the double koRMR1/3 mutant (2koRMR), we generated the triple koRMR1/3/5 (3koRMR), again without phenotypic change. We then generated the quadruple koRMR1/2/3/5 (4koRMR), still without phenotype. Finally the complete koRMR1/2/3/4/5 (5ko RMR) was generated. After each step, the recombination was confirmed by PCR using the strategy described earlier. Additionally a second control detected the RMR mRNAs (fig. 4). Indeed, in the 5ko RMR mutant no *RMR* transcripts were detected by RT-PCR (Reverse Transcriptase and Polymerase Chain Reaction) with the corresponding primers (fig. 4). In contrast, the APT (Adenosine PhosphoTransferase) transcript used as control for the RT and PCR reactions was detected in all mutant plants.

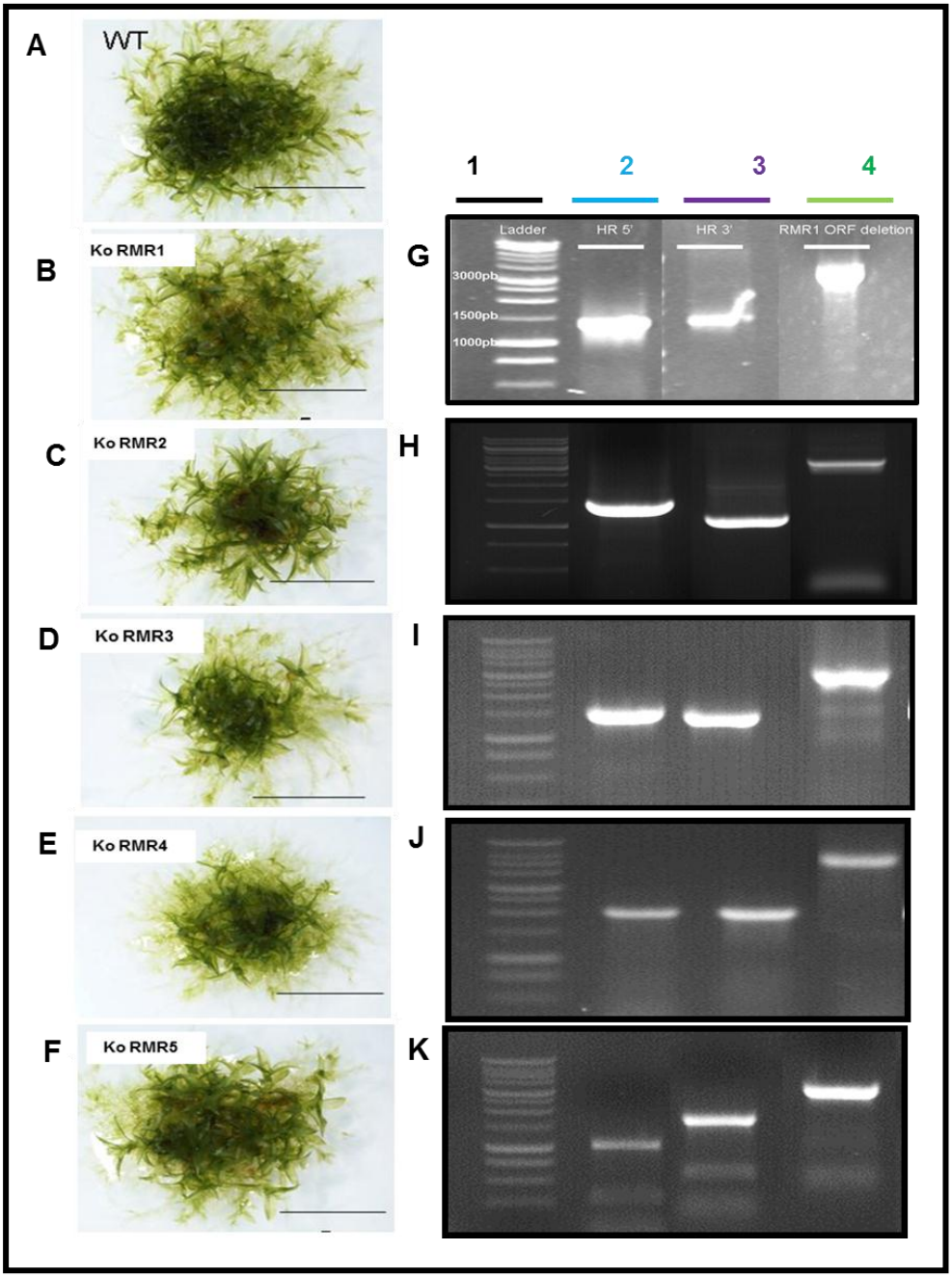

Figure 3: Simple deletion mutants of *Pp*RMR and their PCR genotyping

(A-F) Light microscopic images of WT moss and of KoRMR1, KoRMR2, KoRMR3, KoRMR4, KoRMR5 respectively. Scale Bar: 5mm

(G-K) PCR products from the genotyping, **(lane 1)** ladder, **(lane 2)** 5'recombination products, **(lane 3)** 3'recombination products, **(lane 4)** deleted locus after elimination of the resistance cassette by the Cre-recombinase.

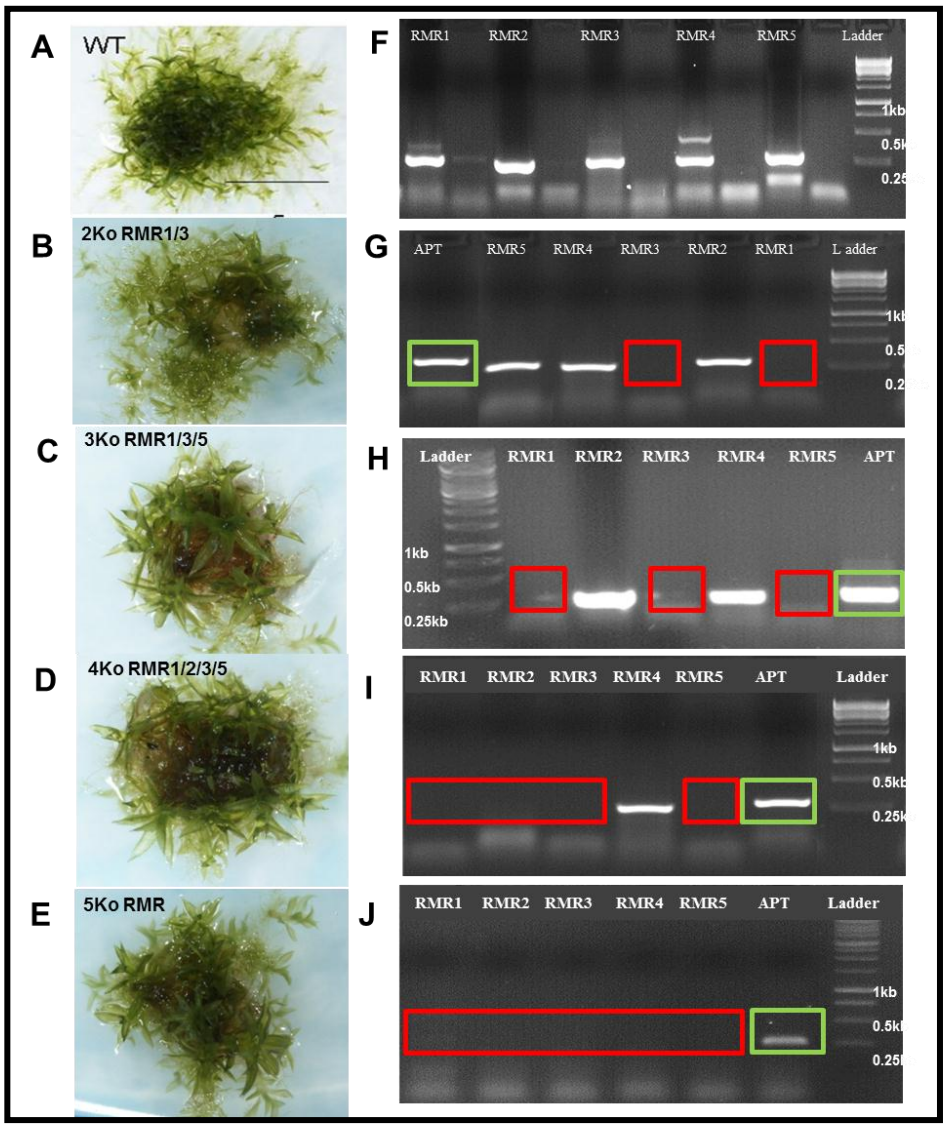

Figure 4: Multiple *Pp*RMR deletion mutants and their genotyping by PCR of the RMR transcripts

(A-E) Light microscopic images of WT and mutant plants. Scale bar: 5mm

(F-J) RT-PCR detection of *Pp*RMR transcripts. A positive control reaction assay was performed for the APT transcripts (green boxes). Length standard is a 1kb ladder with 0.25, 0.5, 0.75 fragments

(A) The wild type moss (WT). **(F)** In WT, all RMR transcripts were detected at their predicted sizes around 0.25kb.
(B) 2Ko RMR1&3. **(G)** In the 2ko plant, the missing transcripts for RMR 1 and 3 are marked by the red boxes, those for RMR 2, 4, 5 were present.
(C) 3Ko RMR1, 3&5. **(H)** In the 3ko plant, the missing transcripts for RMR 1, 3, 5 are marked by the red boxes those for RMR2, 4, appeared.
(D) 4Ko RMR1, 2, 3&5. **(I)** In the 4ko plant, the missing transcripts for RMR 1, 2, 3, 5, are marked by the red boxes those for RMR4 were present.
(E) 5Ko RMR. **(J)** All RMR transcripts were absent in the 5ko RMR plant (red box).

3. Phenotypic analysis

To closely analyse the vegetative developmental phenotypes of the mutants, single young colonies were grown to maturity for 20 days on solid minimal medium which induces gametophore development (fig. 3 and 4). The WT develops typical colonies with a dense center, densely branched protonema growing out from the colony, and the first young gametophores, the leafy shoots of moss, develop. All single knockout lines formed well developed colonies similar to the wild type. At this phenotypical level, none of the multiple *Pp*RMR loss-of-function plants showed any developmental or morphological alteration (fig. 3 and 4). Therefore, the subcellular phenotype was investigated in mutant plants. Since RMR proteins are expected to be responsible for targeting vacuolar proteins, the vacuole is the most likely changed compartment in the mutants. In a first part, the morphology of the vacuole, the ER, the Golgi, and the TGN were investigated using reporters of the secretory system in order to see if the loss of RMR function affected these intermediate and final organelles. Soluble vacuolar proteins were also expressed both in mutant and WT mosses in order to see if there was any mistargeting when RMR genes were deleted.

3.1 Vacuole characterization

We assumed that RMR proteins are vacuolar receptors in moss as angiosperms. Therefore in the absence of RMR proteins the vacuole content and/or the vacuole morphology might be affected. We compared the vacuoles in WT and in the 5koRMR mutant by Neutral Red staining to label acidic vacuoles. Images indicated that the pattern of lytic vacuoles was not modified by the loss of RMR function (fig. 5A, B). Furthermore, vacuole counts in WT and 5koRMR protonema did not show any significant difference in apical, subapical or following cells (fig. 5C). In apical cells, we counted approximately seven acidic vacuoles in WT plants *vs.* five vacuoles in the 5koRMR plant. In subapical and following cells, there were one to two acidic vacuoles in WT and in the mutant. This revealed that the complete deletion of the RMR genes did not grossly affect the vacuoles since their pattern was not disturbed (fig. 5C). As described previously in WT (Chapter 3), the presence of neutral vacuoles was also observed in 5koRMR apical protonema cells.

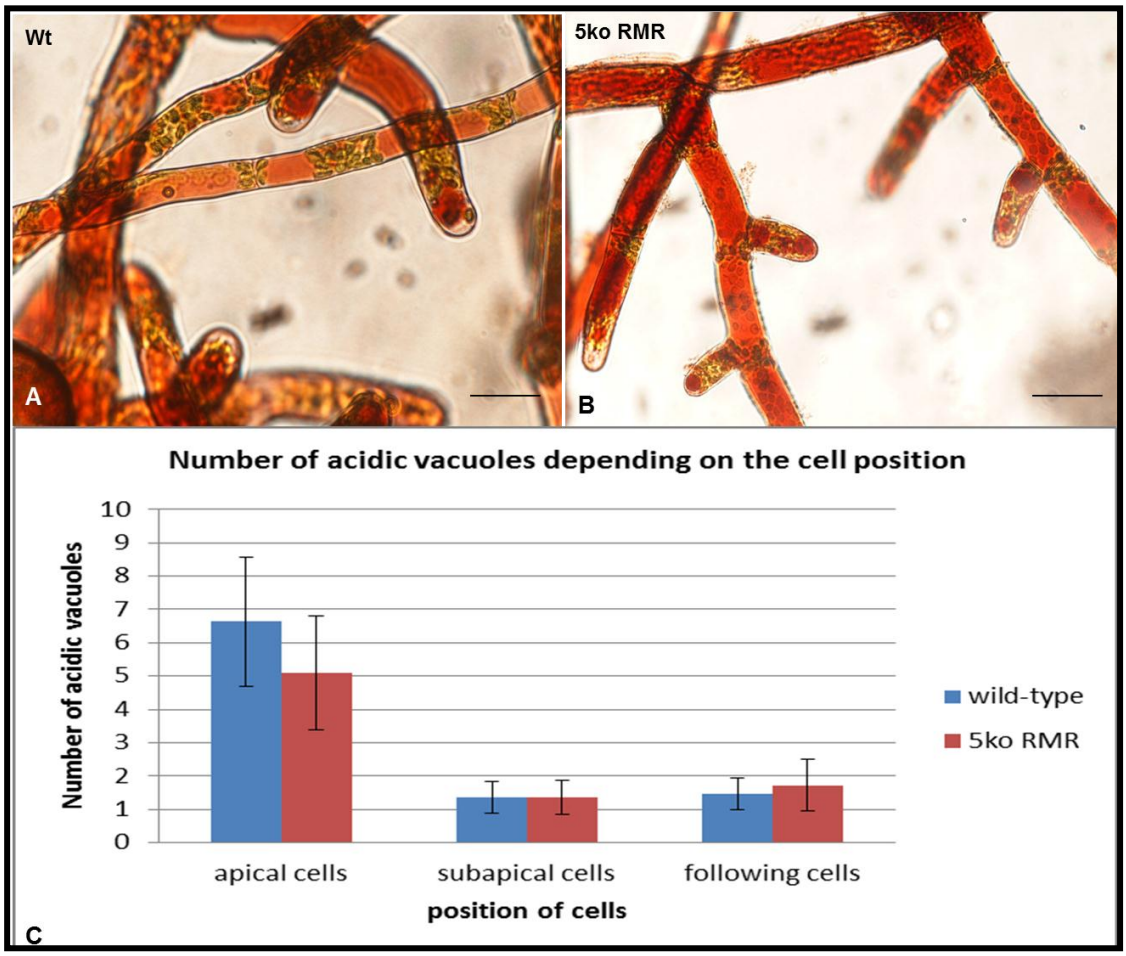

Figure 5: Comparison of Lytic vacuoles in wild-type and 5koRMR plant.

(A, B) Light microscopic images of LV in WT and 5KoRMR. Scale bar: 1mm.

(C) Quantitative assessment of vacuole number in WT (blue), and in 5koRMR protonema (red). Vacuoles were counted in 10 cells, each in apical, subapical, and following position. Errors bars indicate that the difference between WT and 5koRMR protonema was not significant.

3.2 Subcellular characterization

3.2.1. Soluble vacuolar proteins localization in full RMR mutant

The first expected effect of the loss of RMR function as vacuolar receptors is that soluble vacuolar proteins will fail to be transported to the vacuole. This can be tested for soluble vacuolar proteins of the lytic and storage vacuoles. Proteins bearing an ssVSD such as the one from barley aleurain are addressed to LVs (Holwerda et al. 1992; Koide et al. 1999), whereas proteins with a ct-VSD such as the one found in tobacco chitinase A are addressed to PSVs (Bednarek et al. 1990; Di Sansebastiano et al. 1998; Di Sansebastiano et al. 2001).

P. patens has genes for both chitinases and aleurain-related proteases. We selected one gene for each protein family, based on the presence of a putative VSD and on the number of available EST sequences as a marker of gene expression in moss. These two genes were tagged with a GFP-encoding sequence in order to obtain expression of PpAleurain-GFP or of a GFP-PpChitinase under the endogenous promoters. However we could not detect any fluorescence in the PpAleurain-GFP strain. The GFP-PpChitinase strain was fluorescent, but the reporter was unexpectly detected in the apoplast (see supplemental fig. 1 chap2).

For this reason, heterologous GFP reporters were used based on the full length aleurain from *A.thaliana* and the C-terminal VSD from bean phaseolin (AFVY). The fluorescent vacuolar reporter AtAleurain-GFP was expressed transiently in mutant and in WT and in 5koRMR mutant protoplasts (fig. 8). In WT protoplasts, AtAleurain-GFP was localized in the large central vacuole. Comparison of images taken 72 hours after the transformation did not reveal any mistargeting of the lytic vacuole reporter in protoplasts of the 5koRMR mutant. This observation indicates that RMRs are probably not involved in targeting of AtAleurain-GFP, since it is still correctly targeted to the central vacuole.

In order to develop a PSV reporter, reporters are under construction to test the implication of RMR proteins in ct-VSD addressing to PSV.

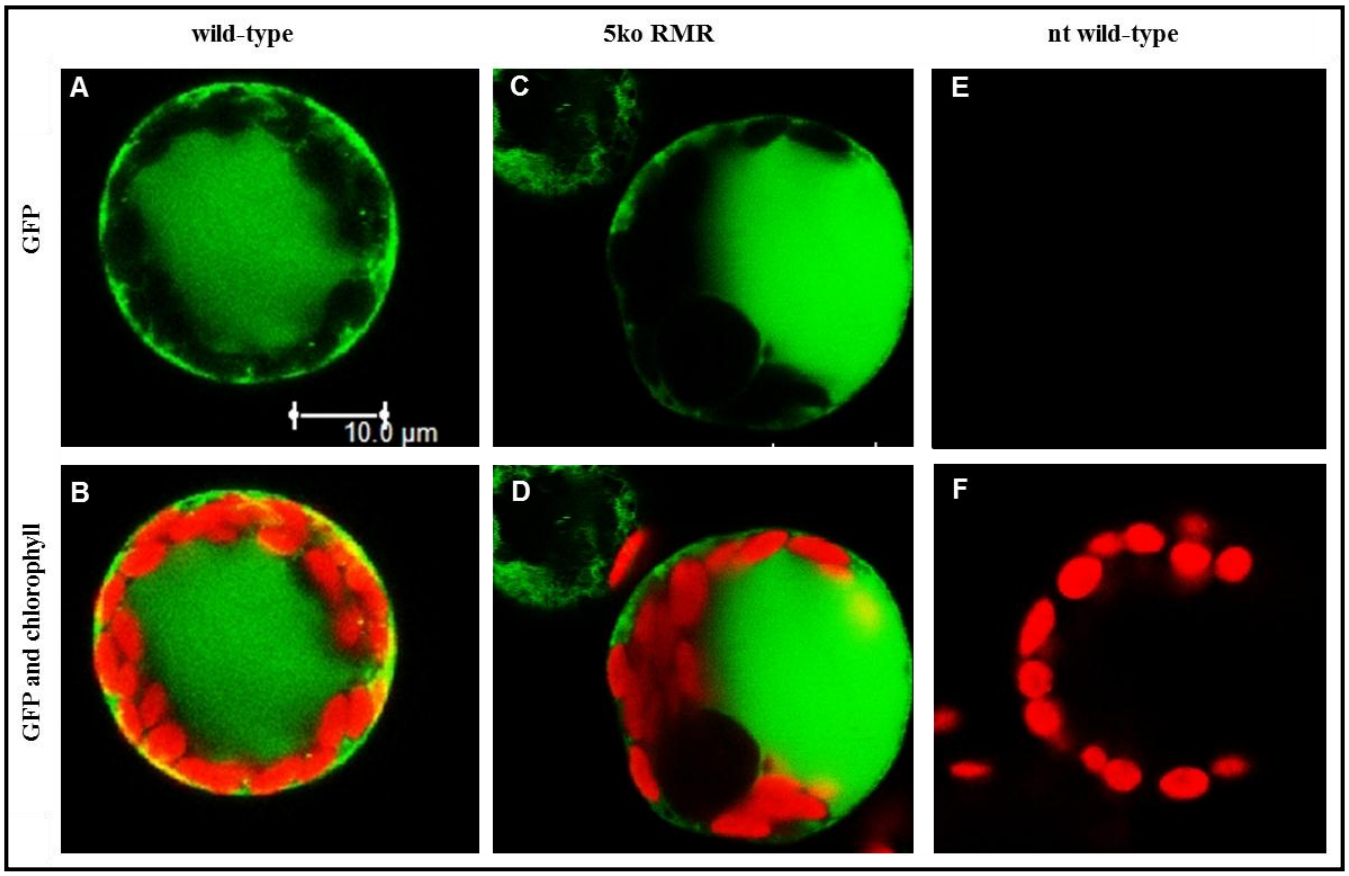

Figure 6: Lytic vacuole reporter labelled the central vacuole in wild-type and 5ko RMR plants

Confocal microscopic images of protoplasts transiently expressing the LV reporter AtAleurain-GFP (green signal) 72hours after transfection. Red channel is chlorophyll.

(A, B) Wild-type protoplast, **(C, D)** 5ko RMR protoplasts, **(E, F)** non transformed control protoplast

3.2.2. The ER and Golgi phenotypes in the full RMR mutant

The loss of function of all RMRs might affect other organelles of the secretory system pathway to the vacuole, due to RMR cargo accumulation or mistargeting. In Arabidopsis AtRMRs where localized in ER and in Golgi organelles (Hinz et al. 2007 ; Occhialini PhD thesis). We thus expected that if *Pp*RMRs were normally localized in the ER and/or the Golgi, then abnormal accumulation of RMR cargoes could perturb ER and/or Golgi morphology. Reporters of these organelles were used to test this hypothesis. Fluorescent ER and Golgi reporters were stably transformed into WT and 5koRMR plants. Confocal images of apical chloronema and of leaf cells showed that the ER reporter was localized in a similar reticulated web in both WT and 5koRMR mutant (fig. 7). Close examination of the transformed lines did not reveal abnormal fluorescent structures such as swollen ER bodies or modified form of the ER membrane. Confocal images of the Golgi label in 5koRMR mutants and WT also showed an identical punctate pattern (fig. 7). Therefore, the loss of function of all RMRs in *P.patens* did not affect either ER or Golgi morphology, indicating no abnormal protein accumulation, which could have distorted organelle morphology.

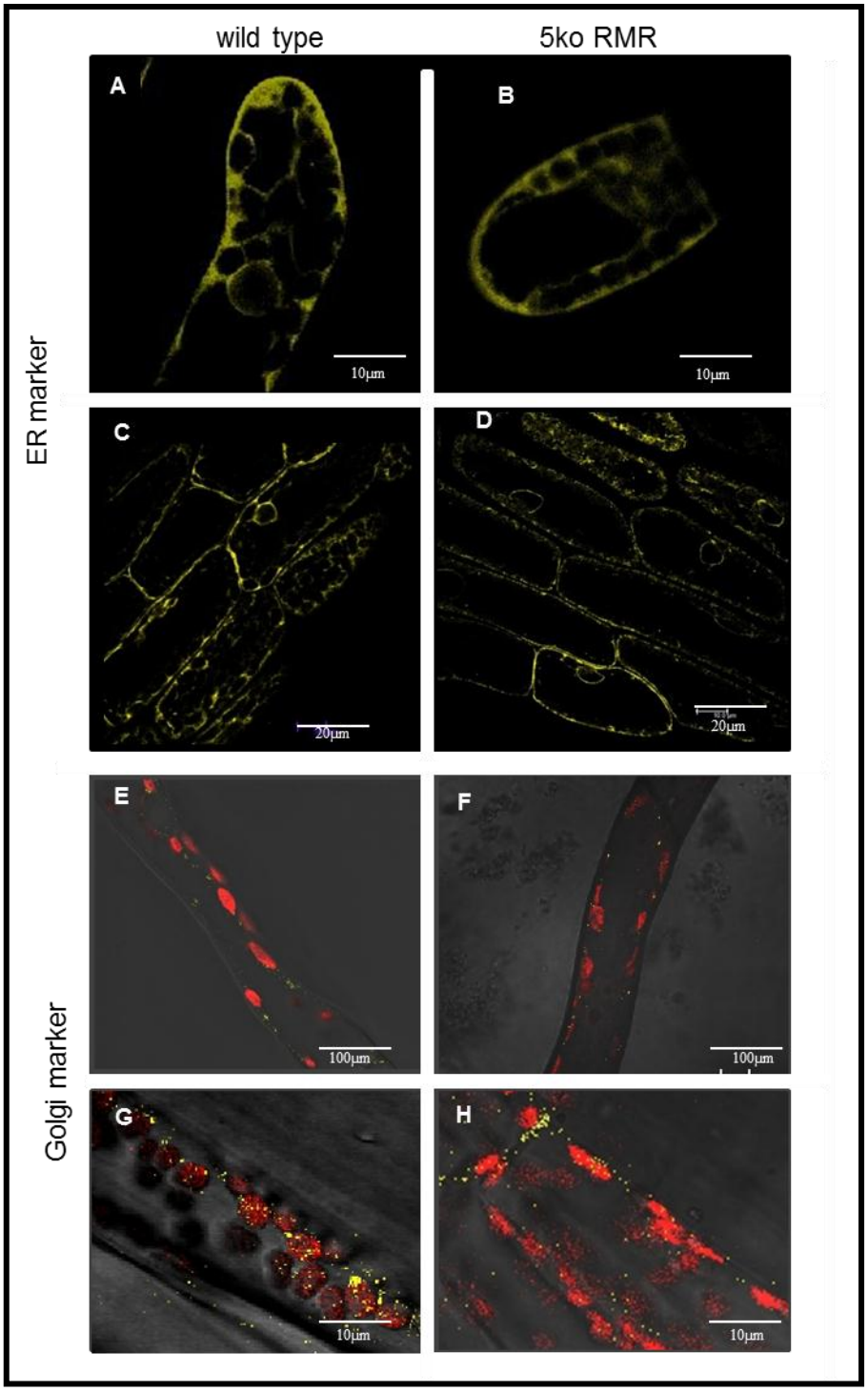

Figure 7: ER and Golgi markers in wild-type and 5ko RMR protonema and leaf cells

(A-D) The ER reporter P6-YFP localized in a similar reticulated web (yellow signal) in the WT apical chloronema **(A)** and leaf cells **(C),** and in 5ko RMR chloronema **(B)** and leaf cells **(D).**

(E-H) For the Golgi label the confocal YFP images were combined with the red channel showing the chloroplasts (red). The Golgi reporter AtGonst1-YFP localized in similar small dots (yellow signal) in the WT subapical caulonema **(E),** and leaf cells (**G),** and in 5ko RMR subapical caulonema **(F),** and leaf cells **(H).**

3.3. Drought stress responses

RMR proteins have a Ring-H2 domain and could have an E3 ubiquitin ligase activity contributing to the vacuolar targeting or to proteasomal degradation. To test this hypothesis single, triple, quadruple and total RMR deletion mutants were subjected to a dehydration stress to determine their capacity to cope with severe water loss. *in vitro* cultured *P. patens* culture were exposed for 24 hours to dehydration following a published protocol (Khandelwal et al. 2010). The aim is to determine if the protonema culture is able to recover from complete desiccation. Pretreatment of plants with the phytohormone abscisic acid (ABA) is known to enhance their tolerance to severe desiccation. ABA is known to protect seeds from water stress by activating transcription factors such as ABI3 (Khandelwal et al. 2010). WT and mutant mosses were first subjected to a pretreatment with 0.25 or 50 µM ABA for one day. Plants were then dried on open petri dishes for 24 hours in the sterile hood then rehydrated by floating on tap water. The rehydrated plants were then transferred to fresh medium plates and cultivated under standard growth conditions. Photographs were taken after 10 days recovery. The WT moss was not able to recover from the drought stress without pretreatment whereas it recovered completely after ABA pretreatment. Moss mutants were tested under the same conditions, and as the WT they were not able to recover without ABA pretreatment. When pretreated with ABA (25 and 50µM), WT and koRMR mutants recovered partially and/or completely. The recovery was more efficient with 50 µM of ABA. Inspection under a binocular indicated that 5ko RMR plant recovered as well as the WT and no bleached areas could be observed (fig. 9B, C). Surprisingly, the quadruple RMR deletion mutant (4koRMR = koRMR1/2/3/5), the triple RMR deletion mutant (3koRMR = koRMR1/3/5) and the simple RMR deletion mutant (1koRMR = koRMR4) recovered less well and presented bleached areas. The experiment was repeated once and the differences in recovery were not linked to any particular line of RMR mutant. The differences could be due instead to variations in inoculum densities. Therefore no significant difference in drought stress sensitivity was detected in any of the tested RMR deletion mutants.

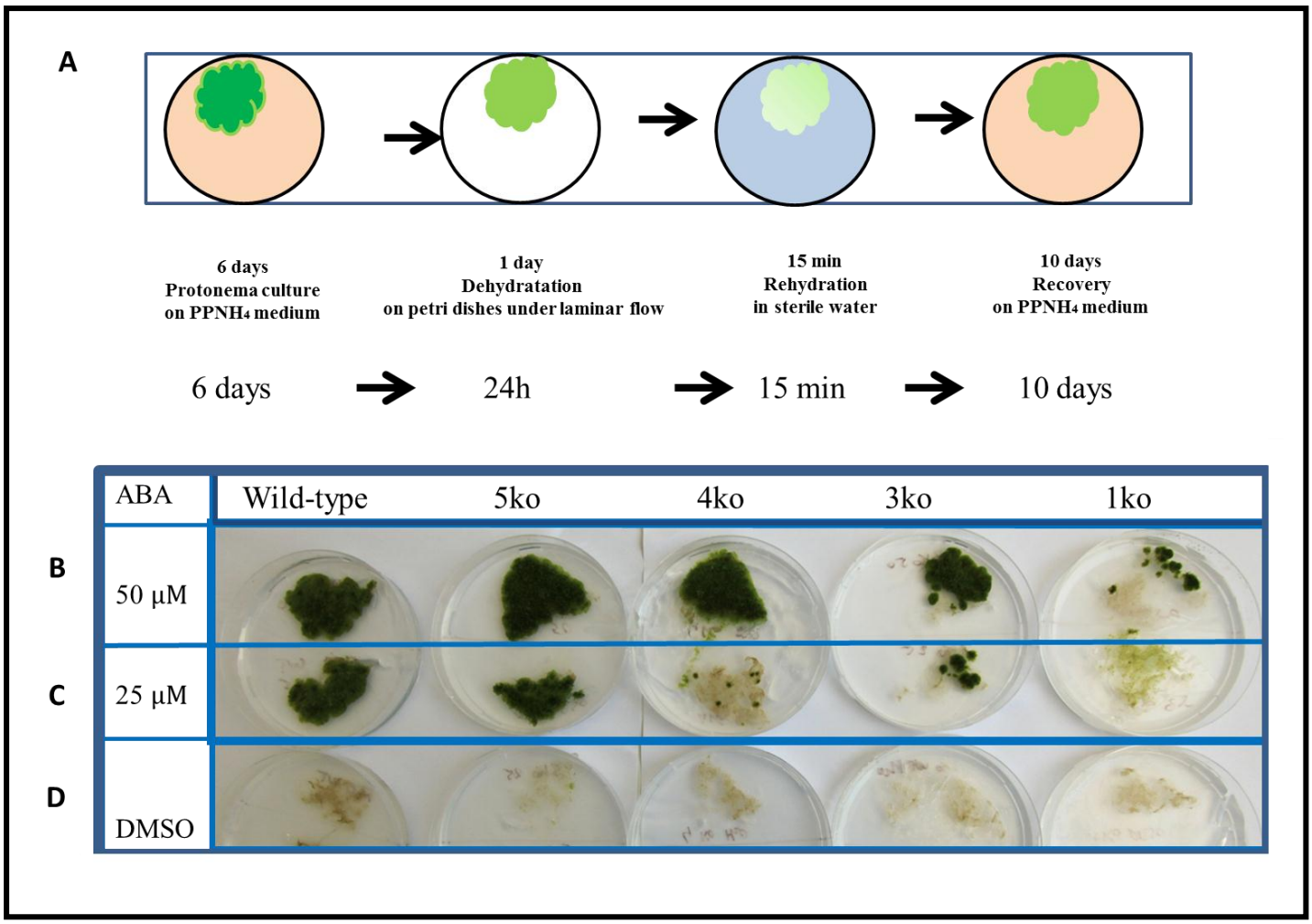

Figure 9: Drought stress response of the ko RMR and the wild-type cultures

(A) The experimental setup: plants (5koRMR, 4koRMR, 3koRMR, 2koRMR, 1koRMR) were transferred onto $PPNH_4$ medium supplemented with ABA for 1 day. Tissue cultures then were dried for 24 hours on petri dishes without medium under sterile laminar flow. Plants were rehydrated for 15 min in sterile tap water and transferred onto fresh medium for recovery.

(B-D) Images of culture tissue taken after 10 days of recovery. **(B, C)** Plants pretreated with 50 and 25µM, WT and KoRMR mutants recovered partially and/or completely. **(D)** The control plants were treated with DMSO (Dimethyl-sulfoxide).

III. Discussion

Gene families are difficult to analyse genetically, because single mutants may have no phenotype and combining multiple mutants by crossing takes very long time. In angiosperms, it is not yet possible to eliminate or replace target genes. This is why the moss *P.patens* has become a powerful complementary model system for plant studies. Single mutants of RMR genes have no phenotype in *A.thaliana*, which has six genes, two of which are even in tandem in a single locus. In the moss system, generation of targeted mutants is possible. This is why we chose to delete all five RMR genes in *P.patens.* The RMR genes were deleted sequentially. After each step the plants did not reveal any phenotypes or altered morphology. The challenge of this work was to detect more subtle phenotypes in such mutants. Different hypotheses were investigated in order to determine possible pathways where RMR family proteins are involved.

1. Phenotypic analysis

Morphologic analysis of the RMR mutants revealed a normal development of all tissues: protonema and gametophytic tissues and their growth were not delayed under normal conditions. Therefore based on this fact, the putative phenotype of these mutants must be minor and not deleterious for the normal plant development. The first obvious conclusion is that the PpRMR family is not necessary for the function or localization of key proteins involved in tissue development under normal conditions. Are PpRMRs required for stress responses?

2. Stress response

Vacuoles are also essential for resistance to drought stress (Apse et al. 1999; Suga et al. 2002). A close relationship between proteins with E3 ubiquitin ligase activity and the drought stress regulation has been observed (Cheng et al. 2012; Lee et al. 2009). RMRs have a Ring domain with a putative E3 ubiquitin ligase activity (Joazeiro and Weissman 2000; Wang et al. 2011). How would the mutants react under drought stress conditions? Comparison with two human RMR paralogues (proteins also having the PA-TM-RINGH_2 organization) suggested two hypotheses:

1) PpRMRs could act like GRAIL (gene related to anergy in lymphocytes), a transmembrane RING finger ubiquitin E3 ligase which targets proteins for degradation by the 26S proteasome pathway, without involvement of its PA domain (Su et al. 2009).
2) PpRMRs could act like RNF13 (Ring finger protein 13), which ubiquitinates key nuclear proteins in response to signals received at the plasma membrane via interaction with its PA domain (Bocock et al. 2010).

We supposed that PpRMRs could be required under drought stress response. To test this hypothesis, RMR deletion mutants were subjected to dehydration stress to determine their capability to cope with severe water loss. All mutants recovered as the WT, no drought stress sensitivity was detected in the RMR deletion mutants. Therefore PpRMRs are not necessary for the survival and recovery mechanisms induced by the ABA pretreatment. However, we can't exclude that RMRs could be involved in the drought stress response. A changed survival threshold of the mutants could have been detected using different drought stress times. Other types of stress responses could also be tested in the future, such as salt or heat stress.

3. Vacuolar organization

Investigation of the 5koRMR mutant cells indicated that the vacuolar organization was not modified by the RMR loss of function. This suggests that the PpRMR family is not necessary for the formation of vacuoles. However, the vacuole regeneration in RMR mutants needs still to be investigated and compared to WT vacuole biogenesis (see chapter 3).

4. Secretory systems reporters

We also examined the effect of RMR deletion on ER and Golgi. An altered morphology of these organelles could be caused by the accumulation of RMR cargoes in the complete 5ko RMR mutant. The ER and Golgi pattern was observed on 5ko RMR strains. No obvious differences were observed in the mutant compared to the wild-type. According to our results, the ER and the Golgi were thus not affected by the RMR loss of function.

The subcellular phenotype was investigated with soluble reporters of the vacuole but so far only a reporter for the lytic vacuole was tested, AtAleurain-GFP. A PSV reporter, the RFP-AFVY is under construction and will be tested in the 5koRMR deletion mutant. Its expression in WT and the 5koRMR will hopefully show us the implication of RMR proteins in the targeting of the ct-VSD proteins. Without specific targeting sequence, the default

pathway of a soluble protein is the secretion into the apoplast (Denecke et al. 1990b). In our study, AtAleurain-GFP was still addressed to the LV in the 5ko RMR deletion mutant. Our results showed that RMRs are not involved in the targeting of ssVSD proteins to the vacuole, which is probably done by members of the VSR family. This result is consistent with previous studies, in flowering plants, which showed that AtRMR1 binds strongly to the ct-VSD of chitinase and only weakly to the ssVSD of proaleurain (Park et al. 2007). Moreover, structural evidence indicated that the PA domain of VSR is involved in binding the ssVSD of vacuolar cargo (Cao et al. 2000). Therefore, our experiment indicated that RMRs are not vacuolar receptors for ssVSD proteins. However this conclusion is not clean-cut because we cannot exclude, the involvement of a rescue pathway activated when RMRs are defective.

5. A rescue pathway?

Different pathways to the vacuole have been described in plant cell (Bednarek et al. 1990; Frigerio et al. 1998; Holwerda et al. 1992; Koide et al. 1999; Neuhaus et al. 1994; Neuhaus and Rogers 1998). Different working hypotheses were investigated in order to determine the pathways where RMR family proteins are involved. Indeed, the absence of phenotype could be explained by the presence of a default pathway which might be active in absence of RMRs. Additional experiments are necessary to answer some important questions.

Will various ct-VSD proteins be mistargeted in 5koRMR mutants? Do PpVSR proteins constitute rescue pathways for vacuolar proteins? Considering the role of RMR as PSV vacuolar receptor, at least a mistargeting of the fluorescent ct-VSD reporter will be expected in RMR deletion mutants. However, we cannot exclude that ct-VSD proteins are directed to the vacuole *via* other vacuolar receptors like VSR. In fact, it has been demonstrated that insertion mutants of *A.thaliana* in which expression of AtVSR1, (one of the seven members of the BP-80 family) was suppressed, disturbed the sorting of the two major classes of *A.thaliana* storage proteins (2S and 11S) leading to their partial secretion in the apoplast (Shimada et al. 2003b). In order to investigate the role of VSR in RMR deletion mutants, the activity of VSR have to be compared between the wild-type moss and the RMRs deletion mutants. Is there any interaction between RMR cargoes and PpVSRs in the WT or in the 5koRMR mutants?

IV. Material and methods

Plant culture

As described in chapter 2

Establishment of stable transformants expressing P6-YFP, AtGonst1-YFP.

To visualize ER and Golgi membranes, P6-YFP, AtGonst1-YFP (fragment respectively supplied by Dr G.P Di Sansebastiano were cloned using restrictions sites in vector Hsp-108-PBNRR (cut XhoI/SalI) under the control of the Heat shock promoter (Hsp) promoter. The target vector contains *108* genomic fragments and thus allows the fragments to be inserted into the *108* locus. HSP-P6-YFP, HSP-AtGonst1-YFP were transformed by Polyethylene glycol (PEG)-mediated as described by Nishiyama et al. (Nishiyama et al. 2000) .Transformants were selected on BCDAT medium supplemented with 20 mg l –1 G418 (Invitrogen Corporation, Carlsbad, CA, USA). The genotyping of the transgenic colonies were performed by PCR on the recombinant junctions between the 5'and the 3' genomic 108 locus and the resistance marker. These junctions were amplified with appropriate primers (see in annex primers).

Staining of vacuolar membranes with Neutral Red

To label vacuolar membranes, protonema cells were treated with 25 mMol Neutral Red (Invitrogen) for 20 min. Subsequently, the cells were washed three times with fresh liquid medium and incubated for 20 min. The cells could be observed directly.

Microscopic observations

Images were collected with a TCS SP5 II confocal laser scanning microscope (Leica). Digital images were acquired using LAS AF (version: 2.0.0 build 1934) and processed using Image J 1.41(National Institute of Health, USA). Aliquots of the protonema cell culture were transferred on to lame observation with coverslip window at the bottom. For simultaneous observations of observe YFP**,** GFP were excited by a 488 nm argon laser, and detected through a confocal unit (TCS SP5 II confocal laser scanning microscope (Leica) with a 524–546 nm band-pass filter for YFP, and a 395- 475 nm band-pass filter (Olympus) for GFP. Bright-field and epifluorescent cell images were recorded with a CCD camera (Nikon DXM1200).

Genes for RMRs in *P. patens*

Amino-acid sequences of RMRs in *A. thaliana and O. sativa* were obtained from the DDBJ, EMBL, and Genbank databases (http://www.ncbi.nlm.nih.gov/). DOE Joint Genome Institute (JGI) P. patens ver. 1.1 database (http://genome.jgi-psf.org/Phypa1_1/Phypa1_1.home.html) was used for searching for *P. patens* RMRs.

Plasmid construction for generation of the knockout lines

Plasmids pBlue script with a two lox P sites flanking a resistance cassette (a NPTT cassette or Hygromycin cassette) was used to clone the targeting sequences. The 5‘and the 3’genomic region (targeting sequences) for each PpRMR were amplified from wild type genomic DNA by PCR using following primers (see in the annex primers). Following the strategy explained in the figure 2, the targeting sequences were cloned into the bilox pBluescript plasmid described below.

Phylogenetic tree

A phylogenetic tree was constructed with RMR DNA sequences without the serine rich domain (SRD) of genome from *Arabidopsis thaliana*, *Poplar trichocarpa*, *Oriza sativa*, *Brachypodium distachyon, Physcomitrella patens, and Selaginella moellendorffii*. Sequences were aligned using ClustalΩ program (http://www.ebi.ac.uk/Tools/msa/clustalw2/). The phylogeny was calculated by maximal likelihood using the fast DNAML and the tree figure was constructed using Figtree software (http://tree.bio.ed.ac.uk/software/figtree/).

Generation of the deletion mutant lines

Prior to transformation, the knock-out plasmids were linearized by the corresponding enzymes (see annex). Linearized constructs were transformed into protoplasts using PEG and heat shock following a moss transformation protocol described in chapter annex.

RT-PCR

Total RNA was isolated from protonemata cells of the wild-type and disruptant lines using the RNeasy Plant Mini Kit (Qiagen GmbH, Hilden, Germany). After treatment with DNase I, first-strand cDNAs were synthesized from total RNA with the oligo-dT primer and the RNA PCR Kit AMV Ver. 3 (Takara Bio Inc., Shiga, Japan). Quantitative RT-PCR was performed with the LightCycler real-time PCR machine (Roche Diagnostics GmbH, Mannheim, Germany) and a SYBR Primescript RT-PCR kit II (Takara Bio Inc.). The primer pairs used for quantitative RT-PCR were reporter in annex primers. Isolations of RNA was repeated three times. The quantitative RT-PCR assays were repeated four times for each RNA sample.

Drought stress assay

Protonema suspensions on plates were pretreated with 25 µM or 50 µM ABA (Abscisic acid, sigma Aldrich): the cellophane carrying the moss cultures tissue cultures were transferred onto PPNH4 medium supplemented with ABA for 1 day. Then, they were dried under laminar flux for 3 days in petri dishes without medium. Tissue cultures were rehydrated for 1 hour in sterile tap water and transferred onto PPNH4 medium for recovery. Photographs of the cultures were taken after 10 days recovery on PPNH4 medium. The control plants were treated with 50 µM, DMSO (Dimethyl-sulfoxide).

General discussion and outlook

1. Moss secretory system

1.1. The development of the moss reporters

Secretory system reporters were developed in order to achieve two main goals: general study of the moss secretory system and the characterization of moss mutants. Two main strategies were employed: heterologous reporters from Arabidopsis, and homologous reporters (genes tagged in situ by fluorescent proteins). Proteins *in situ* tagged were unfortunately either not fluorescent (*Pp*Aleurain-GFP) or not at the desired location. Indeed GFP-*Pp*Chitinase fluoresced well but it was addressed to the apoplast instead of the vacuole. Chitinases are expressed in most plants tissues of in both the vacuole and the apoplast (Neuhaus 1999). The tagged *Pp*Chitinase had been chosen for its putative ct-VSD signal, which was thus mistaken. In contrast, heterologous reporters already used in Arabidopsis could be expressed in moss under a controlled promoter (Hsp promoter) and showed mostly the expected localization.

1.2. Use of heterologous reporters

Expression of secretory system reporters showed that some heterologous reporters from seed plants are correctly recognized and addressed to their target compartments also in the moss secretory system. Transgenic lines expressing P6-YFP (ER), AtGonst1-YFP (Golgi), Venus-Syp61 (TGN), GFP-AtVAMP3 (vacuole) showed a similar pattern as previously described in other plant models (Baldwin et al. 2001a; Fukuda et al. 2000; Oda et al. 2009b; Peremyslov et al. 2004). These results revealed that: 1) ER, Golgi and TGN, vacuole organelles of the moss secretory system have a similar organization compared to seed plants organelles, 2) The protein‘s specific targeting signals were properly recognized by the moss secretory system.

However, it would be wrong to think that all moss organelles have identical functions as seed plant organelles. Our study revealed one of the differences of the moss model: Targeting the vacuole with two different heterologous reporters, GFP-AtVAMP3 and AtTIP-YFP (Hunter et al. 2007) revealed their different localizations in moss cells. AtTIP-YFP proteins were localized in membrane structures distinct from ER and from the vacuole,

indicating that AtTIP-YFP do not contain the proper tonoplast targeting signals (TTS) by moss sorting machinery, but are also not addressed by a default pathway to the plasmalemma. Indeed, *P.patens* thus stands at an interesting phylogenetic distance from flowering plants to provide informations on the evolution of seed plant organelles.

2. Vacuole biogenesis

2.1. Vacuole regenerates from tubule-like structures

The different experiments performed in this thesis gave us some ideas about *de novo* vacuole biogenesis. After evacuolation, protoplasts regenerated their vacuole from small vesicles in *N. tabacum* miniprotoplasts (Di Sansebastiano et al. 2001) while in moss protoplasts, we showed that vacuole regeneration from tubules, which were progressively filled to become provacuoles. This difference could be due to the nature of the reporter used in the two studies: Di Sansebastiano et al., (2001) used soluble vacuolar reporters whereas we used a tonoplast reporter. Therefore, our study has detected the very early steps of vacuole development starting with the biogenesis of the tonoplast before soluble proteins start to accumulate in the lumen. This model is supported by two other results:

1) A tubule-like origin of vacuoles was also shown by electron microscopy on *A.thaliana* roots (unpublished results, Viotti).

2) The artefactual structures formed by AtTIPs in moss cells also started from tubule-like then appeared to fill, even if they did not eventually become incorporated in the moss vacuole.

2.2. One or several vacuole types?

In protonema and rhizoids subapical cells, there are only one or two large LV. In apical cells, the central large appears to form by the fusion of smaller vacuoles. Moreover we showed presence of two small vacuoles types; the acidic and the non-acidic “neutral” vacuoles. There are two possibilities for moss:

1) The neutral vacuole is a second type of vacuole (PSV) as described by the current model of vacuole biogenesis in flowering plant; with content and functions distinct from the

LVs. This implies that separate trafficking must exist in order for the distinct cargoes to reach the correct vacuole (Di Sansebastiano et al. 2001; Neuhaus and Paris 2005).

2) Neutral small vacuoles are immature vacuoles which will later become incorporated into the central LV.

These two possibilities are not exclusive. They are both consistent with previous studies in Arabidopsis roots: the LV reporter (Aleu-GFP) was sorted to the lytic central vacuole in immature, still elongating, root cells while the PSV marker (GFP-Chi) remained separate from the large central vacuole in small PSV compartments until the cell finished to elongate. After complete differentiation of these cells, both vacuolar reporters Aleu-GFP and GFP-Chi reached the same vacuoles (Flückiger et al. 2003). Our observation in moss could also indicates that neutral vacuoles are PSV, which form separately from the LV, fuse with the large central vacuole at the end of cell maturation. Therefore the presence of different vacuole types depends of the maturation stage. To test these possibilities we definitively need specific markers of the PSV. Many questions wait for an answer: Are neutral vacuoles really PSV? Do tonoplast of LVs and PSVs regenerate separately in the moss miniprotoplasts system?

3. Are RMRs vacuolar receptors?

3.1. Putative destinations of the RMRs cargoes in the PpRMRs ko mutant

Growth size and tissue development of RMR deletion mutants did not reveal any morphological phenotype. Neither the ER, nor the Golgi structures were affected by loss of function of the RMR family. Therefore, in the absence of RMRs, cargoes did not massively accumulate in the ER or in the Golgi. In contrast in *A. thaliana*, ko mutants of GSH2, the enzyme converting γ-glutamylcysteine (γ-EC) to glutathione (GSH), exhibited γ-EC hyperaccumulation. These mutants lost the typical polygonal endoplasmic reticulum (ER) network and accumulated swollen ER-derived bodies (Olbrich et al. 2007a). We cannot exclude that the putative accumulation of RMR cargoes is not detectable via our fluorescent reporters. However, while they did not accumulate in the ER or in the Golgi, RMR cargoes could have two other destinations:

1) They could be secreted out of the cell into the periplasm, which is the default pathway for soluble proteins (Denecke et al. 1990a; Neuhaus et al. 1991b).

2) They could be sorted by a rescue pathway (see below).

3.2. RMRs are not a major actors of the protein targeting to the vacuole

Since no phenotype was detected in complete deletion mutant, RMR proteins are not major actors of the protein targeting to the vacuole. Different arguments support it:

1) RMRs loss of function did not disorganize the plant development neither the secretory system organisation nor the vacuole organization. If RMR proteins were a major actors of the protein targeting to the vacuole, several proteins would be affected, and among them important protein for plant development.

2) The response to a severe drought stress was not altered.

3) The RMR family is not involved in addressing ssVSD proteins to the vacuole since AtAleurain-GFP was not mislocalized in the quintuple RMR deletion mutant.

3.3. Perspectives

This thesis leaves many questions unanswered. Perspectives for the continuation of my PhD work are summarized in the figure 1. Our results showed that the ssVSD- fluorescent protein (ssVSD-FP) was not mistargeted, therefore PpRMRs are not involved in ssVSD sorting, which confirms previous studies (Park et al. 2007) (fig. 1, #1). The outcomes are conditioned by the next future experiment, which is the expression of ct-VSD fluorescent proteins (Ct-VSD-FP) in the 5koRMR mutants. Depending on the future results, different strategies could be considered:

1) If the Ct-VSD-FP will be mistargeted, this will confirm that PpRMRs are PSV vacuolar receptor. Deeper investigation of this phenotype on the 1ko, 2ko, 3ko, 4ko RMR mutants will be performed. The deletion of how many RMR genes will cause the mistargeting? Then a complementation experiment of the 5ko RMR mutants with an AtRMR sequence could be envisaged to verify the conservation of RMR functions (fig. 1, #2-2a).

2) If the Ct-VSD fluorescent protein will not be mistargeted (2b):

(i) The first possibility is that PpRMRs are not PSV vacuolar receptors but have another function in cells. This possibility can be investigated with an overexpression of PpRMR proteins in new mutants (fig. 1, #2-2b-3).

(ii) The second possibility is that PpRMR is still vacuolar receptor but Ct-VSD-FP is not the good PpRMRs cargo (fig. 1, #4-4a) and then we'll have to search for PpRMRs cargoes (fig. 1, #5). To identify new PpRMRs targets comparison of the WT with the 5koRMR secretome (fig. 1, #5a) would reveal a presence of mistargeted RMR cargoes. Another possibility would be to perform a TAP-TAG (Tandem Affinity Purification) experiment in order to identify the PpRMRs cargoes and/or partners (fig. 1, #5b). These new PpRMRs cargoes would be identified by mass spectrometry (fig. 1, #6). Finally, these new identified PpRMRs cargoes could be tagged and colocalized with our secretory system reporters in the WT and in the 5koRMR. The normal route of the RMR cargoes in the wild-type and their modified route in the 5ko RMR would be then precisely traced (fig. 1 #7-8).

(iii) The third possibility is that PpRMRs are PSV vacuolar receptors and there is a rescue pathway via the VSR proteins (fig. 1, #4a). Then a BiFC (Bimolecular Fluorescence Complementation) experiment could be performed to investigate PpVSR/Ct-VSD-FP interaction in the WT (fig. 1, #4b). The presence of a rescue pathway would be confirmed if this interaction will be modified in the 5koRMR mutant (fig. 1, #4c). If no evidences show presence of rescue pathway by PpVSR (fig. 1, #4d) a new strategy can be considered, for example: to research new PpRMRs cargoes (fig. 1 , #5-7-8).

To conclude: All these future experiments should answer questions such as:

- Are PpRMRs vacuolar receptors for Ct-VSD proteins? Then PpRMRs would have the same function in Bryophytes and in Angisosperms.
- Are PpRMRs vacuolar receptors for another type of proteins? Then we have to identify the PpRMR cargoes
- Do PpRMRs have another role in the secretory system? Then angiosperm RMRs would have evolved a specialized role in PSV targeting after their divergence from moss.

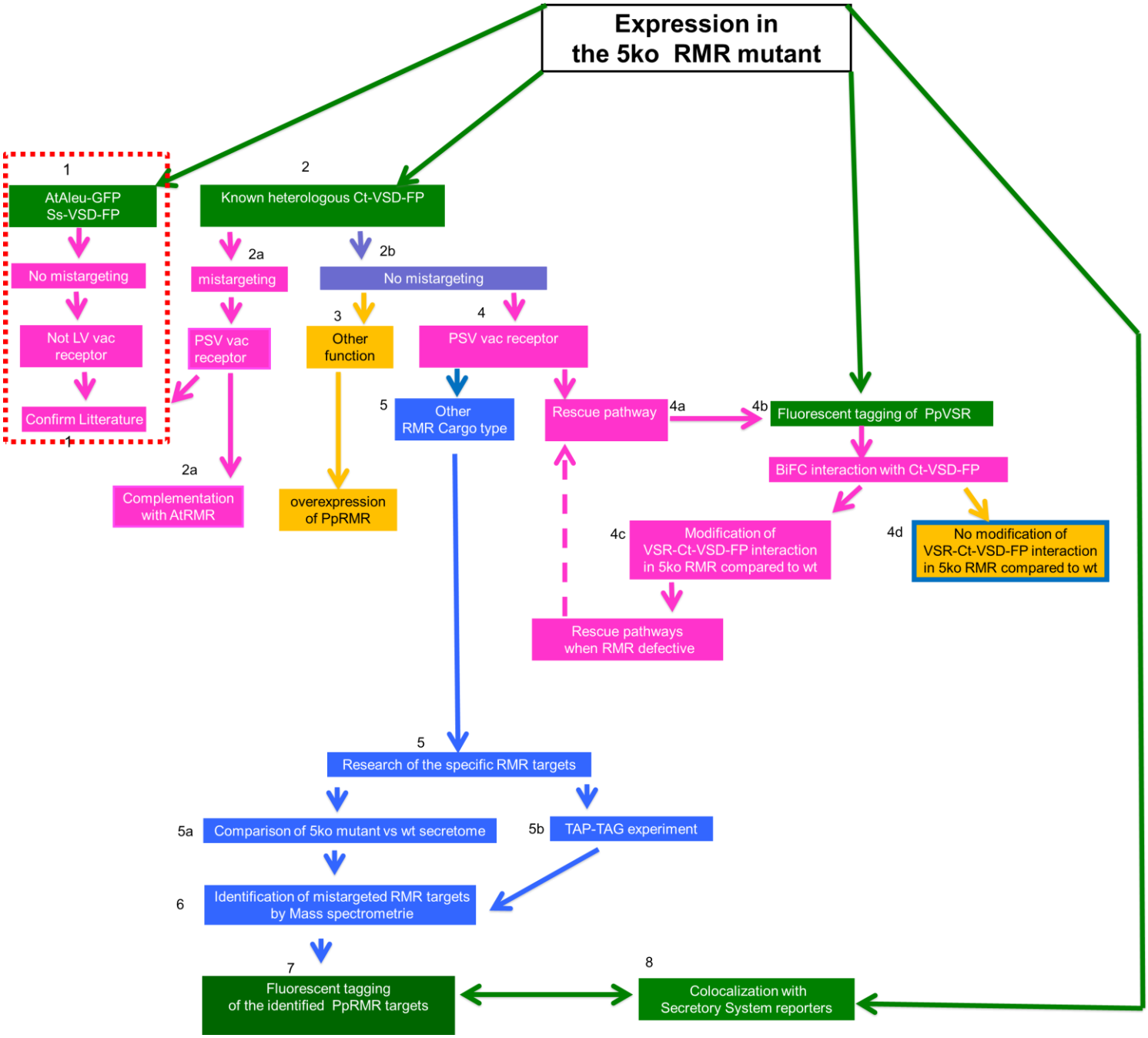

Figure 1: Working strategy for the further functional characterization of the 5 ko RMR

Red box: already performed experiments

Green boxes: protein of interest fused to a fluorescent protein.

Pink boxes: expected results if PpRMR are vacuolar receptors

Orange boxes: expected results if PpRMR are not vacuolar receptors

Blue boxes: expected results if PpRMR are not vacuolar receptors for Ct-VSD but are involved in vacuolar targeting of proteins with some other type of VSD

Annex

1. Materials

1.1. Plant material

Physcomitrella patens
(*Funariaceae*, Bryophytes), the Grandsen strain was provided by D.Cove (Leeds University, UK).

P. patens growth conditions
The standard conditions for *P. patens* in the lab are as follows: Cultures are grown in the culture room at 26 ± 2 °C in discontinuous white light (16 hours / day). Light is provided by fluorescent tubes Sylvania GRO-LUX WS at quantum irradiance of 50 to 80 µmol·m^{-2}·s^{-1}, and with a red-far-red ratio of 1.2. Protonema is cultured in 9 cm Petri dishes containing solid culture medium and overlaid with cellophane disks (W.E. Cannings, Bristol, UK). The cellophane disk is not necessary but facilitates subsequent observations and collection of material.

P. patens sporogenesis
Moss are grown in Magenta boxes or in culture glass tubes on minimal medium (PP-NO_3 without glucose). Cultures with well differentiated gametophores are irrigated with sterile water and transferred at 17°C in illuminated temperature-controlled growth chambers (Polytron, Weiss Technik AG) for three weeks to induce gametogenesis. Sporophyte development is further completed under standard conditions and the maturation is followed visually.

1.2 Bacterial strains

Escherichia coli XL-1 Blue (recA1, endA1, gyrA96, thi-1 hsdR17 (rk^-, mk^+), supE44, relA1, λ^-, lac^-) were grown in LB medium (0.5% NaCl; 0.5% (w/v) yeast extract; 1% (w/v) bacto-tryptone in H_2O). For liquid cultures, *E.coli* was grown at 37°C shaking at 200 rpm. For cultures on solid medium, LB agar (LB medium plus 6% Agar) was used. Specific antibiotics (50 µg/ml kanamycin; 50 µg/ml Ampicillin) were added in the medium in order to select bacteria carrying specific plasmids.

2. Methods

2.1. Methods related to plants

2.1.1. Strain conservation and amplification

Strains are conserved as fragmented protonema suspensions in sterile water at 4°C. These suspensions remain viable for several years. For short-term storage, 6 days old protonemal cultures are collected in sterile water (1 plate in 5-10 mL) and fragmented with an Ultratorrax (Polytron, 30 sec. at position 4). Strains can also be stored for several months in the refrigerator as colonies on a Petri dish sealed with parafilm. This provides a convenient way for medium term storage of strains without fragmentation (i.e. directly from the culture room).

2.1.2. In vitro plant culture

Plates were inoculated with a freshly fragmented suspension. For long term storage, the suspension was filtered after fragmentation. Fragments of protonema that were retained on the filter were collected with a forceps and resuspended in sterile water. A piece of the colony can be directly inoculated on PP NH4 plate.

Table: composition of PPNH4 medium (Ashton et al., 1979)

Macroelements: $CaNO_3 \cdot 4H_2O$ 0.8 g/l $MgSO_4 \cdot 7H_2O$ 0.25 g/l $FeSO_4 \cdot 7H_2O$ 0.0125 g/l
Microelements Micro elements $CuSO_4 \cdot 5H_2O$ 0.055 mg/l $ZnSO_4 \cdot 7H_2O$ 0.055 mg/l H_3BO_3 0.614 mg/l $MnCl_2 \cdot 4H_2O$ 0.389 mg/l $CoCl_2 \cdot 6H_2O$ 0.055 mg/l KI 0.028 mg/l $Na_2MoO_4 \cdot 2H_2O$ 0.025 mg/l
Phosphate buffer Dissolve 25 g KH_2PO_4 in 100 mL water and titrate to pH 7 with 4M KOH to make a 1000x stock. Autoclave and add 1 ml per litre of medium.
NH4 tartrate 500 mg/l
Glucose 5 g/l
Antibiotics: for Neomycin or Hygromycin resistance, supplement with 40 mg/L G-418 or 25 mg/L Hygromycin B, respectively

-.

2.1.3. Moss protoplasts isolation

The protoplasts were isolated from 5-6 days old protonema culture digested with 1% Driselase in 0.48M mannitol (Fluka 44585, Sigma D-9515) for 30 minutes with occasional gentle mixing. (Driselase was dissolved in 0.48M mannitol, centrifuged at 10'000 rpm for 10 min to remove debris, buffered to pH 5.6 and sterilised by passage through a 0.25 µm filter). The protoplast suspension was filtered through a 100 µm stainless steel sieve and left for an additional 15 minutes to complete digestion, then filtered through a 50 µm stainless steel sieve and transferred to sterile 10 ml glass tubes. The protoplasts were harvested by low speed centrifugation (60 g for 5 min) and gently resuspended in mannitol 0.48M. The centrifugation was repeated and the protoplasts were resuspended in 0.48M mannitol.
The yield was usually about 10^6 viable protoplasts per initial culture plate. To regenerate the protoplasts on a Petri dish, the protoplast were mixed with one volume of molten top layer and aliquots of 2ml per 9 cm Petri dish containing solid protoplast culture medium were plated over a cellophane disk. The ideal concentration for good regeneration is 10'000-30'000 protoplasts per Petri dish. The protoplasts were then left in darkness one night after isolation and then regenerated in the light in the culture room.

2.1.4. Moss transformation by PEG

The protoplasts were isolated following the described method below. After isolation, the protoplasts were resuspended in mannitol. The protoplasts were then centrifuged and then resuspended at a concentration of 1.2 x 10^6/ml in MMM solution (mannitol: 0.48 M (8.5%), magnesium chloride: 15mM, MES: 0.1%, pH 5.6 with KOH). 10-15 µg of DNA were dispensed into 14 ml Falcon tubes (maximum 30 µl, the final concentration should be between 30-50 µg/ml). Then, 300 µl of protoplast suspension were added to the DNA and mixed gently. 300 µl PEG solution (mannitol 0.38 M (7 %), calcium nitrate 0.1M, PEG 4000 (Serva) 33 % (w.v.) pH 8.0 with 10 mM Tris) were added to the protoplast suspension and mixed gently. The protoplasts were heat shocked for 5 minutes at 45^{o}C. Then the protoplasts were left at room temperature for an additional 10 minutes with occasional gentle mixing. The sample was progressively diluted with PPNH4 moss liquid medium (5 x 300 µl and then 5x 1ml added sequentially every minute). The transformed protoplasts were kept overnight in darkness. The next day, protoplasts were cultured in liquid medium for transient gene expression assays or were embedded in protoplast top layer and plated on protoplast solid medium for further selection. For the selection, each transformation sample was plated on 3-4 Petri dishes.

2.2. Methods related to nucleic acids

2.2.1 Extraction of plasmid DNA

A single bacterial colony was inoculated into 5 ml of LB medium containing the adequate antibiotics. The culture was then incubated overnight at 37°C with shaking (250 rpm). The day after 1.5 ml culture was centrifuged at 20'000 g in order to pull down bacterial cells. The pellet was resuspended in 150 µl resuspension buffer P1 (50 mM Tris-HCl pH 8; 10 mM EDTA; 100 mg/ml RNase). 150 µl of lysis buffer P2 (200 mM NaOH; 1% SDS) were then added and the sample was gently mixed a few times. The sample was incubated for 5 minutes at room temperature and 150 µl equilibration buffer P3 (3M NaOAc pH 5.5) were then added. The sample was gently mixed and incubated for few minutes on ice. The samples were then centrifuged for 15 minutes at 20'000 g in order to precipitate the bacterial lysate. The supernatant containing plasmid DNA was transferred into a new Eppendorf tube and 0.7 volumes of isopropanol were added. The tube was centrifuged at 20'000 g for 30 minutes. The DNA pellet was then washed once with 70% ethanol. Finally the pellet was dried and resuspended in an adequate volume sterile H_2O. Isolation of plasmid DNA for sequencing was performed using the NucleoSpin plasmid kit (MACHEREY-NAGEL) as indicated in the provider's protocol. Isolation of plasmid DNA from *E.coli* in a big-scale was performed using the NucleoBond Xtra Midi Plus kit (MACHEREY-NAGEL) as indicated in manufacturer's instructions.

2.2.2 Extraction of genomic DNA from P. patens

Eppendorf tubes were used to collect moss tissue. The tissue was powdered using a small pestle and then 400 µl extraction buffer (200 mM Tris-HCl pH 7.5; 250 mM NaCl; 25 mM EDTA; 0.5% SDS) were added. The tube was mixed for 5 minutes using a vortex and then centrifuged for 5 minutes at 15'000 g in order to eliminate cell debris. 300 µl supernatant were mixed with an equal volume of isopropanol. The tube was incubated at room temperature for 10 minutes and then centrifuged for 30 minutes at 15'000 g. The DNA pellet was washed once with 75% ethanol. Finally the DNA was resuspended in an adequate volume of sterile H_2O.

2.2.3 Extraction of total RNA from P. patens

Moss protonema material was collected and immediately frozen in liquid nitrogen. The tissue was then ground in liquid nitrogen using pre-cooled mortar and pestle. The tissue was transferred to a Rnase-free 2ml Eppendorf tube pre-cooled in liquid nitrogen. 500 µl plant RNA purification reagents (Invitrogen) were immediately added. The tissue was resuspended by mixing using a vortex and then incubated for 5 minutes at room temperature. The tube was centrifuged for 2 minutes at 15'000 g in order to eliminate cell debris. The supernatant was then transferred into a new Eppendorf tube (RNase free). 100 µl 5M NaCl was added and then the tube was gently mixed. 300µl chloroform was added and the tube was mixed 3-4 times by invertion. The tube was centrifuged at 15'000 g for 10 minutes at 4°C. The aqueous phase was

transferred to a new Eppendorf tube (RNase free) and one volume of isopropanol was then added. The tube was incubated for 10 minutes at room temperature and then centrifuged at 15'000 g for 30 minutes at 4°C. The supernatant was discarded and the pellet was washed once with 75% ethanol. The pellet was then resuspended in an appropriate volume of RNase-free H_2O. Finally the total RNA was treated with DNase (Promega) in order to eliminate contaminant genomic DNA and then quantified using a Nano-Drop spectrophotometer.

2.2.4 Inverse transcription

The cDNA was synthesised from the moss RNA extract. 1 µg total RNA extract was transferred to a 1.5 ml Eppendorf tube (RNase-free). Then, 1 µl oligo-dT primer and 1 µl 10 mM dNTP were added. The volume was adjusted to 11 µl using an adequate volume of RNase-free H_2O. The tube was incubated at 70°C for 5 minutes and then for 1 minute on ice. 12 µl mix [5 µl 5X transcriptase buffer; 1 µl 0.1 M DTT; 0.5 µl SuperScript III RT (Promega); 5.5 µl RNase free H2O] was added to the tube. The reverse transcriptase reaction was performed at 50°C for 1 hour. Finally the tube was incubated for 15 minutes at 70°C in order to inactivate the reverse transcriptase and transferred to ice. The single strand cDNA was used to amplify *Pp*RMR sequences using specific pairs of primers.

2.3. Cloning techniques

2.3.1 PCR polymerase chain reaction

PCR reactions were performed combining the following components in a nuclease-free micro-centrifuge tube: buffer (final concentration 1x); 0.2 mM for each dNTP; 0.1-1 µM forward primer; 0.1-1 µM reverse primer; 1.25 Unit DNA polymerase (Promega); 100-500 ng DNA template; H_2O to a final volume of 50 µl. The reaction was performed in a thermal cycling machine (Biometra).

2.3.2 Digestion of plasmid DNA

Restriction enzyme digestions were performed mixing the following components in a 1.5 ml sterile Eppendorf tube: 0.2-1.5 µg substrate DNA; restriction buffer (final concentration 1x); BSA (final concentration 0.1 µg/µl); 0.5 units of restriction enzyme (usually Promega); H_2O to a final volume of 20µl. The digestions were performed for 1-4 hours at 37°C.

2.3.3 DNA electrophoresis

DNA electrophoresis was performed using a Bio-Rad apparatus. Agarose gels were prepared with 0.7-2.5% of agarose (depending on the size of DNA fragments) in 0.5x TBE and using Ethidium Bromide as a DNA dye. DNA samples were separated in agarose gel at 90-95 Volt whereas they were separated at 120 Volt in a big agarose gel. The DNA was visualized under UV light using a GEL-DOC system from Bio-Rad.

2.3.4 DNA purification and precipitations

The DNA was extracted from the agarose gel with a cutter. The DNA was extracted using the Wizard SV Gel and PCR Clean-Up system (Promega) as indicated in the provider's protocol. The DNA was precipitated with 1/10 the volume sodium acetate (NaAc) 3M and 2 volumes ethanol. The samples were incubated at -80°C for 10 minutes in order to precipitate the DNA. They were centrifuged for 20 minutes at -20°C and DNA pellets were then washed once with 70% ethanol. Finally, samples were dried and then resuspended in an adequate volume of sterile H_2O.

2.3.5 Ligation of a fragment into a plasmid

DNA ligase reactions were performed mixing the following components in a 1.5 ml sterile Eppendorf tube: 100 ng vector DNA; 17 ng insert DNA; 10x ligation buffer (final concentration 1x); 0.1-1 u T4 DNA ligase (Promega); and H2O to a final volume of 10 µl. The reactions were performed overnight at 4°C or for few hours at 14°C.

2.3.6 Transformation of E.coli by heat-shock

Competent *E.coli* cells were thawed on ice and then placed on pre-cooled 1.5 ml Eppendorf tube containing 1ng purified plasmid or 10µl ligation mixture (approx. 200ng). Cells were incubated for 15-20minutes on ice. They were then incubated for 90 seconds at 42 °C and immediately back on ice for 2 minutes. 1ml liquid LB-medium without antibiotics was added and bacteria were then incubated for 1 hour at 37 °C under shaking. Finally, the bacterial culture was plated on a petri dish containing selective LB-medium and grown at 37 °C overnight.

2.3.7 Preparation of heat-shock competent E.coli cells

5 ml selective LB medium (25 µg/ml tetracycline) was inoculated with a single *E.coli* colony and then incubated at 37 °C overnight under shaking. The day after this preculture was diluted in 500 ml of fresh liquid LB medium and incubated at 37 °C under shaking. The culture was grown until the OD_{600} reached 0.5, which represents the exponential phase of bacterial growth. Cells were then put on ice and recuperated by centrifugation at 5000 g for 15 minutes at 4 °C. From this step on the cells were kept cold throughout the preparation. The bacterial pellet was resuspended in 32 ml RF1 buffer (100 mM KCl; 30 mM $MnCl_2$; 30 mM K-acetate pH 7.5; 10 mM $CaCl_2$; 15% glycerol; pH 5.8 adjusted with acetic acid) and then left for 20 minutes on ice. Cells were recuperated by centrifugation at 5000 g for 15 minutes at 4 °C and the resulting pellet was resuspended in 8 ml RF2 buffer (10 mM MOPS pH 6.8; 10 mM KCl; 50 mM $CaCl_2$; 15% glycerol; pH 6.8 adjusted with NaOH). The suspension of competent bacteria was incubated for 20 minutes on ice. Finally, 100 µl aliquots were pipetted and then frozen in liquid nitrogen. Tubes were stored at -80 °C.

3. Annex primers

Primer names	Knock-out vectors	Use
	pBNRR RMR28 ko = koRMR1	
C31	ATCTCGTACCCCTTGTCAG	clonnig
C51	CTCGCCTCCCACTTTCAACCTTC	clonnig
C32	TGTTCCCTGCCAGTAGAT	clonnig
N51	CAAAGGATATCAAGCAATGAC	clonnig
N32	GAGACACGAAACGAAGAGTG	clonnig
N52	ACATAGAAACACCACCACACAACA	clonnig
N31	ATATCTCGCCTTCCATATCC	clonnig
C52	CTCGAGTGAGGAGCTGGAAGATG	clonnig
RMR28 Nter fw	GCGGCGCCTACTTGCACAACAGTG	*genotyping*
RMR28 Nter rv	GAAGCAATCGACTTTCCAG	*genotyping*
	pBHRR RMR58 ko = koRMR2	
RMR58 Nter fw	ATCGATGCAGCATAAAGTCGCG	clonnig
RMR58 Nter rv	GCAAACATCCGTAAAAGGC	clonnig
RMR58 Cter fw	GCCACCACAGTAGTATTTCACAG	clonnig
RMR58 Cter rv	TGATGCTCACCATATCGTTC	clonnig
RMR58 5'g REC	CAGCCAGCCATCTATCCATCT	*genotyping*
RMR58Cter Rev	TGATGCTCACCATATCGTTC	*genotyping*
	pBNRR RMR282 ko = koRMR5	clonnig
RMR282 Nter fw	GCGCGCGAATTCATGGACTGTGTACTCCGCTC	Clonnig- *Genotyping*
RMR282 Nter rv	GCGCGCACTAGTCACGACCGTGGAACGGTTGA	clonnig
RMR282 Cter fw	CGGCTGTTCTCGCTACTGCTTTCTTTGTGCG	clonnig
RMR282 Cter rv	ACATTGCAAGCAGCGAGATAAACGAAACCGCC	Clonnig- *Genotyping*
	pBNRF RMR81 ko = koRMR3	clonnig
RMR81 Nter fw	TTGTCTCCAACAGTGTAGTCTTCAAGGC	clonnig *Genotyping*
RMR81 Nter rv	GCTCAGGCTCTTACCTTGCGCTCACAAGTTTCATGC	clonnig
RMR81 Cter fw	TGACGCACAATCCCACTATCCTTCGCA	clonnig
RMR81 Cter rv	TGTAGAGAGAGACTGGTGATTTC	clonnig *Genotyping*

	pBHRR RMR88 ko = koRMR4	
RMR88 Nter fw	CAATGACAAGCTCCAAATGC	Clonnig- *Genotyping*
RMR88 Nter rv	TTGTGTCACCACGATCAGGT	clonnig
RMR88 Cter fw	CTCGAGTCCAATTCCCAGAGATCATC	clonnig
RMR88 Cter rv	CCAATATCCCAAAACAATGC	Clonnig- *Genotyping*
Cam Prorev	GTGTCGTGCTCCACCATGT	*genotyping*
TerF3	CGCTGAAATCACCAGTCTCT	*genotyping*
	Knock-in Vectors	
	pBHRF-GFP-*Pp*Chitinase	
PpChid5'TS fW	CCGAATTACCTCTCACTTTG	clonnig
PpChid5'TS rv	CGTACGCCCCTTCCTCGTACTCTATC	clonnig
PpChid3'TS fW	GGCGCCAGTTGTGGGGTTGATTGCTG	clonnig
PpChid3'TS rv	CCATCTGGGAAGTTTACCTTG	clonnig
eGFP3'TS fw	GCGCGCACGGACGCAAGGGATACCCATACGACGTCCCA	clonnig
eGFP3'TS rv	GCGCGCCTCCTCCTCCTCCCTTGTACAGCTCGTCCATGC	clonnig
Chi-3'TS cre	TCCCAGAATTGCTGTAGATG	*Genotyping*
Chi-5'TS cre	CAACAAGTCCTGCTTCAGAG	*Genotyping*
	pBHRF-*Pp*Aleurain-mcherry	
CTer-aleufw	TTCGAATTGTACGTCAACTAA	clonnig
CTer-aleurv	CCCGGGCACATCAACATTCGCA	clonnig
UTSaleu2ndFw	GGCCGCACTAGTATTATTTCCCCATCGAC	clonnig
UTSaleu2ndrv	CGCGCGACTAGTTTTGTTCATTGTACTTGTAGTTTG	clonnig
FPaleu mcherryfw	CCCGGGTACCCATACGACGTCCCAG	clonnig
FPaleu mcherryRV	CCCGGG CTCGAG TTA CAGATCttcttcagaaataag	clonnig
	Heterologous reporters	
	Pbnrr108	
Sa108gen5'FW	GGACGCCAATTACAAAGCAAC	*genotyping*
YFP rev	AGCAAAGACCCCAACGAGAA	*genotyping*
108.3'	GCTGAAATCACCAGTCTC	*genotyping*
Cam Prorev	GTGTCGTGCTCCACCATGT	*genotyping*
TerF3	CGCTGAAATCACCAGTCTCT	*genotyping*

	CDNA primers	
28 Cdna fw	ATCCAGATGGTGGTGAG	cDna
28 Cdna rv	GCATAATTTAGGATCCACCAGGTC	cDna
58 Cdna fw	TGGCGAAAAGCTGAGGTT	cDna
58 Cdna rv	AGTAGTTTCGTCCGGTGAAGC	cDna
81 Cdna fw	GCATAGATCAGTGGCTACTCACGCGGA	cDna
81 Cdna rv	AAGTTAACACAGATCTTCTCCCGA	cDna
88 Cdna fw	TAGAGGACTATGAGAGCGGACAA	cDna
88 Cdna rv	AGAGCCTACAGGTGAGGTTGAG	cDna
282 Cdna fw	ATCTGAAGGCGATGATTGGAT	cDna
282 Cdna rv	TGCGACTCTTACCTTGTCAGC	cDna

Table 1: List of the primers used

4. Annex: plasmids and constructs

4.1. Cloning vectors

-The plasmid Pgemt-T easy (from Promega) with gene for ampicillin resistance.

-The plasmid pGREEN0229 with the 35S promoter and terminator cloned into XhoI/SacI (MCS) sites presents in the LacZ gene.

-The plasmid pBNRR is a pbluescript with 2 LoxP sites flanking a resistance cassette NTPP or cassette NTPP for N or Hygromycine for H (pBHRR).it exist the versions pBHRF, pBHRF were the direction of the resistance cassette ORF is inversed.

-The plasmid pBNRR-108 is the pBNRR plasmid describes below. 5'TS Pp108 locus and 3'TS Pp108 locus were used as targeting sequences and cloned before and after the resistance cassette.

-The plasmid pBNRR-108-Hsp-Ter35S is the pBNRR-108 plasmid describes below with additional Hsp promoter and 35S terminator were cloned upstream the resistance cassette.

4.2. Knock-out vectors

pBNRR RMR28 ko = koRMR1
The 5' and 3'targeting sequence (TS), respectively upstream and downstream the open reading frame) of PpRMR1 were amplified by PCR using the following primers: N51fw/N31rv for 5'TS and C51fw/C52rv for 3'TS. The resulting fragment was subcloned in pGEMT enzymes and cut using as an AscI/speI for 5'TS and XhoI/XbaI fragment. The fragments were then cloned into pBNRR plasmid using the restriction enzymes cited. Finally before the plant transformation the vector is linearized as a AscI/XbaI fragment

pBHRR RMR58 ko = koRMR2
The 5' and 3'targeting sequence (TS), respectively upstream and downstream the open reading frame) of PpRMR1 were amplified by PCR using the following primers: RMR58 Nter fw/RMR58 Nter rv for 5'TS and RMR58 Cter fw/RMR58 Cter rv for 3'TS. The resulting fragment was subcloned in pGEMT enzymes and cut using as an MluI/speI for 5'TS and HindIII/XhoI fragment. The fragments were then cloned into pBNRR plasmid using the restriction enzymes cited. Finally before the plant transformation the vector is linearized as a MluI/XhoI fragment.

pBNRF RMR81 ko = koRMR3
The 5' and 3'targeting sequence (TS), respectively upstream and downstream the open reading frame) of PpRMR1 were amplified by PCR using the following primers: Nter fw/RMR81 Nter rv for 5'TS and RMR81 Cter fw/RMR58 Cter rv for 3'TS. The resulting fragment was subcloned in pGEMT enzymes and cut using as an NspV/XhoI for 5'TS and

speI/ClaI fragment. The fragments were then cloned into pBNRR plasmid using the restriction enzymes cited. Finally before the plant transformation the vector is linearized as a NspV/ClaI fragment.

pBHRR RMR88 ko = koRMR4

The 5' and 3'targeting sequence (TS), respectively upstream and downstream the open reading frame) of PpRMR1 were amplified by PCR using the following primers: RMR88 Nter fw/RMR58 Nter rv for 5'TS and RMR88 Cter fw/RMR88 Cter rv for 3'TS. The resulting fragment was subcloned in pGEMT enzymes and cut using as SpeI/ /NsiI for 5'TS and HindIII/XhoI fragment. The fragments were then cloned into pBNRR plasmid using the restriction enzymes cited. Finally before the plant transformation the vector is linearized as a HindIII/NsiI fragment.

pBnRR RMR282 ko = koRMR5

The 5' and 3'targeting sequence (TS), respectively upstream and downstream the open reading frame) of PpRMR1 were amplified by PCR using the following primers: RMR282 Nter fw/RMR282 Nter rv for 5'TS and RMR282 Cter fw/RMR282 Cter rv for 3'TS. The resulting fragment was subcloned in pGEMT enzymes and cut using as XhoI /NspV for 5'TS and SpeI/NsiI fragment. The fragments were then cloned into pBNRR plasmid using the restriction enzymes cited. Finally before the plant transformation the vector is linearized as a NsiI/NspV fragment.

4.3. Knock-in Vectors

pBHRF GFP-PpChitinase

The fragment N-terminal sequence *Pp*Chitinase as the 3'TS and an untranslated sequence as 5'TS were amplified by PCR by the following primer: (PpChid5'TS fw/PpChid5'TS rv) for the 5'TS and (PpChid3'TS fw/ PpChid3'TS rv) for the 3'TS and cloned separately in pgreen vector. The GFP sequence was amplified by PCR by the following primer: (eGFP3'TS fw/ eGFP3'TS rv) and also cloned in pgreen vector. The GFP fragment was cut by BsshII and cloned in Nter-Ppchitinas-pgemt using the same restriction site. The 5'TS was cut and cloned by Nar/Nsi. Then Nter-Ppchitinase was cut by HindIII/SunI and cloned in pBHRF using the same restriction sites. Finally before the plant transformation the vector is linearized as an AvrII/NsiI fragment

pBHRF PpAleurain-mcherry

The fragment C-terminal sequence PpAleurain as the 5'TS and an untranslated sequence as 3'TS were amplified by PCR by the following primer: (Cter-Ppaleufw/Cter-Ppaleu rv) for the 5'TS and (aleu-uts fw/ aleu-uts rv) for the 3'TS and cloned separately in pgreen vector. The mcherry sequence was amplified by PCR by the following primer: (mcherryfw/ mcherryfrv) and also cloned in pgreen vector. The mcherry fragment was cut by SmaI and cloned in Cter-Ppaleu–pgemt using the same restriction site. The 3'TS was cut and cloned by SpeI. Then Cter-Ppaleu–mcherry-pgemt was cut by NspV/XhoI and cloned in pBHRF using by

NspV/XhoI. Finally before the plant transformation the vector is linearized as a BstBI/AscI fragment.

4.4. Heterologous reporters

pBNRR 108 Hsp-P6-YFP
The fragment P6-YFP was provided (Peremyslov *et al.*, 2004)) in pgreen vector. The fragment P6-YFP was cut by BamHI/SalI and cloned in pBNRR-108-Hsp-ter35S using the same restriction sites. Finally before the plant transformation the vector is linearized as an AvrII/PacI fragment

pBNRR 108 -35S GONST1-RFP
The fragment AtGONST1-YFP was provided (Baldwin et al. 2001b) in pgreen vector. The fragment AtGONST1-YFP was cut by BamHI/SalI and cloned in pBNRR-108-Hsp-ter35S using the same restriction sites. Finally before the plant transformation the vector is linearized as an AvrII/PacI fragment

pBNRR 108 -35S Venus SYP61
The fragment Venus SYP61 was provided (Uemura et al. 2004) in pgreen vector. The fragment Venus SYP61 was cut by Xho/XbaI and cloned in pBNRR-108-Hsp-ter35S using the same restriction sites. Finally before the plant transformation the vector is linearized as an AvrII/PacI fragment

pBNRR 108 -35S ∂-TIP-YFP
The fragment 35S-∂-TIP-YFP was provided (Hunter et al., 2007) in pgreen vector. The fragment 35S-∂-TIP-YFP was cut by Xho/XbaI and cloned in pBNRR-108 using the same restriction sites. Finally before the plant transformation the vector is linearized as an AvrII/PacI fragment

pBNRR 108 -35S ɣ-TIP-YFP
The fragment 35S-ɣ-TIP-YFP was provided (Hunter et al., 2007) in pgreen vector. The fragment 35S-ɣ-TIP-YFP was cut by Xho/XbaI and cloned in pBNRR-108 using the same restriction sites. Finally before the plant transformation the vector is linearized as an AvrII/PacI fragment

5. Annex: RMR sequences

```
Physco3         MPSVSGESGLLDRIGSQREVVVSLGCLSLVLLTLLFGRGSADVLLLNTRNESRSFPDMEA 60
Physco4         MPSVAGESGLLERITSQREVMVSLGCLSLVLLTLFFGRGSADVLLLNTRNESRSFPDMEA 60
Physco5         MPSVVGESGFLSRITNQKEVMVSLACLSLVILTLLFGHGSAAVLLFNTKNESRSFPDMEA 60
Physco1         MPSVVAEAGFASRIMSYREIMISLAGLCLVLLTLLIGRVNSAVILLAGTNETWSFPDVES 60
Physco2         MPSLVVETGLVSRIMNHRELMISLAGLSLVLLTLLLGRVNSAVILLTESNESWSFPDTEA 60
AthaRMR1        ------------------MRLVVSSCLLVAAPFLSSLLRVSLATVVLNSISASFADLPA 41
                                      *:      .        .   . : ** *  :

Physco3         AFARPIPDEGVSGILHVANPLDACTPLKNDIP--KGER-LPPFVVISRGTCNFDKKVRNA 117
Physco4         AFARPVPDEGVTGILHVANPLDACAPLKNHIP--EGEP-LVPFVVISRGTCNFDKKVKNA 117
Physco5         AFTPSIPSGGVAGILHEANPLDACSPLKNLIP--KGEP-LPPFVLVSRGSCNFDKKVKNA 117
Physco1         RFAPRVPTAGVGGVLYASNPLDACSPLLNVST--PGKGSAPAFLLVQRGVCNFEIKVRLA 118
Physco2         SFSPRIPTTGIVGVLHASNPLDACSPLTNVSR--QGQTLFSDFLLVERGVCNFEVKVWNA 118
AthaRMR1        KFDGSVTKNGICGALYVADPLDGCSPLLHAAASNWTQHRTTKFALIIRGECSFEDKLLNA 101
                 *   :   *  * :: ::***.*  * :       .     * :: ** *.*: *:  *

Physco3         QKAGFQAAIVYNTIDFIDELVTMSGSDEDIDIYAVFVSWITGQALLGAVGENN-TCTLLP 176
Physco4         QVAGFQAAIVYNTMDFTDEMITMSGSAEDIDIYAVFVSWNTGQALLGAVGDNNVTCTLQA 177
Physco5         QDAGFQAAIVYNSMDFVGDLVIMSGSPEGIDIYAVFVSWLTGQALLGAVGDNN-TCTLVP 176
Physco1         QEAGFAAVIVYNDQDDR-ELVTMSGNPVNIHAYAVFVSKYSGEFLLKYAGDVGATCHIMP 177
Physco2         QEAGFEAVIIYNNQNDH-ELVTMSGSSNDIHAYSVFVSKVTGEFLLKYADDKGATCYIMP 177
AthaRMR1        QNSGFQAVIVYDNIDNE-DLIVMKVNPQDITVDAVFVSNVAGEILRKYARGRDGECCLNP 160
                * :** *.*:*:  :    :: *  .  .*   :***:  :*: *   .   .    : .

Physco3         AVKDNAWSITVFSSITFLAVSAVLSTFFFVRRDRLRGLGSR-LLSRELSRMDARDVDALP 235
Physco4         AAEDTAWSIMAVSSISLLAVSAVLSTFFFVRRHRLRHLGSR-FLSREPSGMNARDVQALP 236
Physco5         YIEDTAWSIMVVSSISLLAISAVLSTFFFVRRHSLRHRGSR-LLSREPSGMNARDVHALP 235
Physco1         AFENTAWSVMAVSFISLLAVSSVLATFFFVRQHRLRHLSAR-YLLREPAGMSVKEVNALP 236
Physco2         AFENTAWSVMAVSFISLLAVSSVLVTFFFVRQHRIQHLSAR-FLPKEPAGMSVKEVNTLP 236
AthaRMR1        PDRGSAWTVLAISFFSLLLIVTFLLIAFFAPRHWTQWRGRH----TRTIRLDAKLVHTLP 216
                  ...**:: ..* :::* : :.*   **. :.  :    :     .   :. : *.::*

Physco3         TFVFKGAGSDEAGTGETCAICLEDYESGEKLRHLPCHHDFHVGCIDQWLLTRKPFCPICK 295
Physco4         TFIFEDAGGDGAATGETCAICLEDYESGQKLRHLPCDHDFHVGCIDQWLLTRRPFCPICK 296
Physco5         TLIFKAVGG--AATGEMCAICLEDYESGEKLRLLPCQHDFHVGCIDQWLLTRRRFCPICK 293
Physco1         SLIFKCVED-GKCTSETCVVCLEDYIPGERLRLLPCQHEFHLDCIDQWLTLRKPFCPVCK 295
Physco2         SFVFKHIED-GKGTSETCAICLEDYVAGEKLRLLPCQHEFHLDCIDQWLTTRKPFCPVCK 295
AthaRMR1        CFTFTDSAH--HKAGETCAICLEDYRFGESLRLLPCQHAFHLNCIDSWLTKWGTSCPVCK 274
                 : *         :.  *.:*****  *: ** *** * **  *:*.**      **:**

Physco3         QDANVTPAYPAATETTPLLVSPV------------------VSIPVT---SSAATQTSPV 334
Physco4         QDANAAPRHQAATETTPLLVPPAGRA---------------VPVPSM---SSAATQTSPV 338
Physco5         QDASSAPVHPSATETTPLLVAPS-HI---------------FSVPAT---ASAATQTSPV 334
Physco1         RDAQSQVHEPVATETTPLMAAVGRALGGGSIR---------VGTSILSARSSPLFTTSVI 346
Physco2         RDAQSKVDKPVATETTPLLAAVGRALGVGESR---------VGTPMN---SSPLFAP-TG 342
AthaRMR1        HDIRTETMSSEVHKRESPRTDTS----------------------------TSRFAFAQS 306
                :*         . :  .                                    :

Physco3         ASPAD------HTPE---SSYANVSGEDLC------------------------------ 355
Physco4         GSPGV------HTTQ---SLPANVAGEDLC------------------------------ 359
Physco5         GSPTI------QTIQ---SSPSDVSGENLC------------------------------ 355
Physco1         NSPND------TPDTRIFSLSYPDGGEDLC------------------------------ 370
Physco2         ASPDE------TTDTRIFSLSSPDGSEDLC------------------------------ 366
AthaRMR1        SQSR---------------------------------------------------------- 310
                 ..
```

Alignment: Sequences alignment of RMR from Arabidopsis and *P.patens*.

Alignment of Full length aminoacid sequence of PpRMR1, PpRMR2, PpRMR3, PpRMR4, PpRMR5, and AtRMR1using ClustalW http://www.ebi.ac.uk/Tools/msa/clustalw2/.

```
              1         11        21        31        41        51
                 |         |         |         |         |         |
Barley           MAHARVLLLA LAVLATAAVA VASSSSFADS NPIRPVTDRA ASTLESAVLG ALGRTRHALR
Petunia          .S--.LS..L VL.AGLF... F.RTAN...E ....Q.VSDS FHE...GI.H VV.Q.....S
Arabidopsis      .S-.KTI.SS VVLVVLV.AS A.ANIG.DE. ....M.S.GL REVE..-.SQ I..QS..V.S
'Phypa 209158'   .E-S.G...V GI.VLGF.-G F.--A.LPTG DT..E...D. L.NGSVEQFA HALIGAEKR-
'Phypa 198150'   ..GRG...-- -T..VVFV-L AGLVA.LPLR DV.QQ...GV RVDGSVEQFA HALLGAEKQ-
'Phypa 224573'   .GAVENMA-- --LVVCLV.. LLLCGVV.NG DV..MP..VG KDQ.LA---- --------GQ
'Phypa 224348'   .GWG.RA.GL SL..LVI--. IGQQADAGRA .A.VDYEGNQ LHSDDAIL-- --------DV
'Phypa 63513'    ..SSTQGGVG AV.VSV.VLL L.GIACCYEE DGTSESFLHM TTD..HEN.L L-------EQ
'Phypa 204314'   .EAVL...V. AVA.CG.GCH G.E.TPG--- ----SLL.M TTD.GNER.L S-------EQ
'Phypa 208810'   .GCGGRMAMV .GLFLVLVL. MGWEQGNVGR ADAIMDYEAH ELHSDDGM.- --------DV
'Phypa 143194'   .VTDLEA.AS TSAGLFTEIL GH.RDVL--- ---------- ---------- ---------H
'Phypa 212380'   .KPISL..-- ------LCSV ILAAQAARVE PDLLESKRLI HQQ.LVDKVN .--------HP
'Phypa 104506'   ..YE.MGK.D .SL.LMLCAL FFAVQAGRLE PELLGNNRLI HQQALVDKVN .--------HP
'Phypa 209899'   ..RWGM.K-- .GSVLVLCGL ILA.QAARPE PDLLENNRLI HQQSLVDKIN .--------HP

              61        71        81        91        101       111
                 |         |         |         |         |         |
Barley           FARFAVRYGK SYESAAEVRR RFRIFSESLE EVRSTNRKGL PYRLGINRFS DMSWEEFQAT
Petunia          .....R.... R.D.VE.IKQ ..D..LDN.. MIN.H.D... S.K..V.E.. .LT.D..RRD
Arabidopsis      ....TH.... K.QNVE.MKL ..S..K.N.D LI....K... S.K..V.Q.A .LT.Q...R.
'Phypa 209158'   .ES.MKDF.. V.H.VE.YEH ..GV.KSN.L KALKHQALDP TASH.VTM.. .LTE...TSK
'Phypa 198150'   .ES.IKEF.. V.HTVE.YEH ..KV.KSN.L RALKHQALDP TASH.VTM.. .LTE...ATQ
'Phypa 224573'   ..AW.HKH.. V.SA.E.RAH ..LVWKDN.. YIQRHSE.N. S.W..LTK.A .LTN...RRQ
'Phypa 224348'   .HQWLETHSR V.R.LS.KHH ..Q..K.NFL YIHAH.KQQK S.W..L.K.. .LTHQ..R.Q
'Phypa 63513'    ..AW.HKH.. A.HD.EQCLH ..AVWKDN.A YI-RHSETNR T.S..LTK.A .LTN...RRM
'Phypa 204314'   .GAW.HKH.. V.S.LE.HAH .YMVWKDN.. YIQRHSE.NR S.W..LTK.A .ITND..RRQ
'Phypa 208810'   .HQWLE.HSR V.H.LS.KQ. ..Q..KDN.H YIHNH.KQEK S.W..L.K.. .LTHD..R.L
'Phypa 143194'   ..G..AK.K. E.KTVE.LKH ..VT.L..VK L.ETH.KGQH S.S.AV.E.A ..TF...RDS
'Phypa 212380'   R.TWKAGFND RF.GHTIEHL KKICGAKMTP ANELEPSIER VTHKHKK--- ----------
'Phypa 104506'   G.TWTAGFNE RFAKHTIEHL KKMCGAILTP ANKLEPSIET ISHKHKK--- ----------
'Phypa 209899'   G.TWKAGLND RFAKHTVEHL KKMCGAKMTP ANEVEPSIER VTHKHK.--- ----------

              121       131       141       151       161       171
                 |         |         |         |         |         |
Barley           RLGAA--QTC SATLAGNHLM RDAAALPE-- -TKDWREDGI VSPVKNQAHC GSCWTFSTTG
Petunia          ........N. ...TK.-N.K LRD.V..... .......A.. .......GK. ..........
Arabidopsis      K.......N. ....K.-SHK VTE....... .......... .....D.GG. ..........
'Phypa 209158'   Y..LK..RPS VLSS.PQAPP LPTED..P.. .NF....K.A .G...D.GG. ....A.....
```

Alignment 2 : Sequences alignment of aleurain from barley, petunia, Arabidopsis and *P.patens.*

The vacuolar targeting determinant of aleurain (Holwerda *et al*. 1992) identified by Roger's team SSSSFADSNPIR is positioned at the N terminus of the aleurain propeptide (highlight in green). An additional determinant, VTDRAAST, adjacent to the SSSSFADSNPIR determinant is also necessary for efficient vacuolar targeting (highlight in green). The isoleucine is conserved or is replaced by a leucine in *P.patens* aleurain sequences.

The chosen PpAleurain was Phypa 209899.

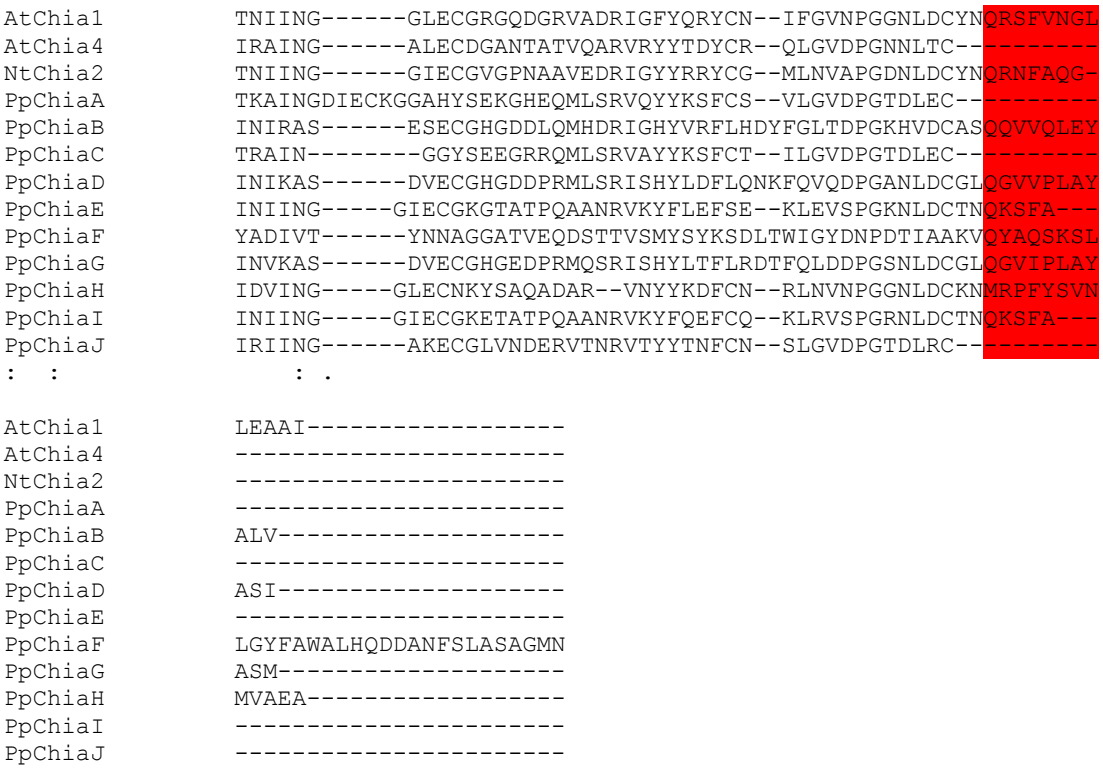

Alignment 3: Sequence alignments of Cter amino-acids of chitinase from *A. thaliana*, *N.tabacum* and *P.patens*.

The 7 C-terminal amino-acids of tobacco chitinase A are necessary and sufficient for the vacuolar localization of chitinases (Neuhaus *et al*. 1991). C-terminal vacuolar sorting determinant ctVSD could have variable length, and often contain hydrophobic residues usually present at the C-terminus (Frigerio *et al*. 2001). This consensus sequence at C-terminus part is highlighted in the alignment of the chitinase sequences (red colour). The consensus is not very conserved except the glutamine which is conserved in the different species. However it seems that this C-terminus is essentially composed of hydrophobic amino acids.

The chosen chitinase was PpchiaD

Bibliography

Adams JM, Cory S (1998) The Bcl-2 protein family - arbiters of cell survival. Science 281: 1322-1326

Ahmed SU, Rojo E, Kovaleva V, Venkataraman S, Dombrowski JE, Matsuoka K, Raikhel NV (2000) The plant vacuolar sorting receptor AtELP is involved in transport of NH(2)-terminal propeptide-containing vacuolar proteins in Arabidopsis thaliana. J. Cell Biol. 149: 1335-1344

Anandasabapathy N, Ford GS, Bloom D, Holness C, Paragas V, Seroogy C, Skrenta H, Hollenhorst M, Fathman CG, Soares L (2003) GRAIL: An E3 Ubiquitin Ligase that Inhibits Cytokine Gene Transcription Is Expressed in Anergic CD4+ T Cells. Immunity 18: 535-547

Anderberg HI, Kjellbom P, Johanson U (2012) Annotation of Selaginella moellendorffii Major Intrinsic Proteins and the Evolution of the Protein Family in Terrestrial Plants. Front Plant Sci 3: 33

Andreeva AV, Kutuzov MA, Evans DE, Hawes CR (1998) The structure and function of the Golgi apparatus - a hundred years of questions. J. Exp. Bot. 49: 1281-1291

Apse MP, Aharon GS, Snedden WA, Blumwald E (1999) Salt tolerance conferred by overexpression of a vacuolar Na+/H+ antiport in Arabidopsis. Science 285: 1256-1258

Aridor M, Fish KN, Bannykh S, Weissman J, Roberts TH, Lippincott-Schwartz J, Balch WE (2001) The Sar1 GTPase coordinates biosynthetic cargo selection with endoplasmic reticulum export site assembly. J. Cell Biol. 152: 213-229.

Baldwin TC, Handford MG, Yuseff M-I, Orellana A, Dupree P (2001a) Identification and Characterization of GONST1, a Golgi-Localized GDP-Mannose Transporter in Arabidopsis. Plant Cell 13: 2283-2295

Baldwin TC, Handford MG, Yuseff MI, Orellana A, Dupree P (2001b) Identification and characterization of GONST1, a golgi-localized GDP-mannose transporter in Arabidopsis. Plant Cell 13: 2283-2295

Barlowe C, Orci L, Yeung T, Hosobuchi M, Hamamoto S, Salama N, Rexach MF, Ravazzola M, Amherdt M, Schekman R (1994) COPII: a membrane coat formed by sec proteins that drive vesicle budding from the endoplasmic reticulum. Cell 77: 895-907

Barrieu F, Thomas D, Marty-Mazars D, Charbonnier M, Marty F (1998) Tonoplast intrinsic proteins from cauliflower (Brassica oleracea l. var. botrytis) - immunological analysis, cDNA cloning and evidence for expression in meristematic tissues. Planta 204: 335-344

Bassereau P (2010) Division of labour in ESCRT complexes. Nat Cell Biol 12: 422-423

Bassham D, Brandizzi F, Otegui MS, Sanderfoot A (2008) The Secretory System of Arabidopsis. The Arabidopsis Book

Bassham DC, Blatt MR (2008) SNAREs: Cogs and Coordinators in Signaling and Development. Plant Physiol. 147: 1504-1515

Becker B, Melkonian M (1996) The secretory pathway of protists - spatial and functional organization and evolution. Microbiol. Rev. 60: 697 ff.

Bednarek SY, Raikhel NV (1992) Intracellular Trafficking of Secretory Proteins - Mini Review. Plant Mol. Biol. 20: 133-150

Bednarek SY, Wilkins TA, Dombrowski JE, Raikhel NV (1990) A Carboxyl-Terminal Propeptide Is Necessary for Proper Sorting of Barley Lectin to Vacuoles of Tobacco. Plant Cell 2: 1145-1155

Bocock JP, Carmicle S, Madamba E, Erickson AH (2010) Nuclear targeting of an endosomal E3 ubiquitin ligase. Traffic 11: 756-766

Boehm M, Aguilar RC, Bonifacino JS (2001) Functional and physical interactions of the adaptor protein complex AP- 4 with ADP-ribosylation factors (ARFs). EMBO J. 20: 6265-6276.

Bolte S, Talbot C, Boutte Y, Catrice O, Read ND, Satiat-Jeunemaitre B (2004) FM-dyes as experimental probes for dissecting vesicle trafficking in living plant cells. J Microsc 214: 159-173

Bolwell GP (1988) Synthesis of Cell-Wall Components - Aspects of Control. Phytochemistry 27: 1235-1253

Borner GHH, Sherrier DJ, Weimar T, Michaelson LV, Hawkins ND, MacAskill A, Napier JA, Beale MH, Lilley KS, Dupree P (2005) Analysis of Detergent-Resistant Membranes in Arabidopsis. Evidence for Plasma Membrane Lipid Rafts. Plant Physiol. 137: 104-116

Boursiac Y, Chen S, Luu DT, Sorieul M, van den Dries N, Maurel C (2005) Early effects of salinity on water transport in Arabidopsis roots. Molecular and cellular features of aquaporin expression. Plant Physiol. 139: 790-805

Brandizzi F, Frangne N, Marc-Martin S, Hawes C, Neuhaus JM, Paris N (2002) The destination for single-pass membrane proteins is influenced markedly by the length of the hydrophobic domain. Plant Cell 14: 1077-1092

Brown JC, Jolliffe NA, Frigerio L, Roberts LM (2003) Sequence-specific, Golgi-dependent vacuolar targeting of castor bean 2S albumin. Plant J. 36: 711-719

Cao X, Rogers SW, Butler J, Beevers L, Rogers JC (2000) Structural requirements for ligand binding by a probable plant vacuolar sorting receptor. Plant Cell 12: 493-506

Chen CY, Ingram MF, Rosal PH, Graham TR (1999) Role for Drs2p, a P-type ATPase and potential aminophospholipid translocase, in yeast late Golgi function. J. Cell Biol. 147: 1223-1236

Cheng M-C, Hsieh E-J, Chen J-H, Chen H-Y, Lin T-P (2012) Arabidopsis RGLG2, Functioning as a RING E3 Ligase, Interacts with AtERF53 and Negatively Regulates the Plant Drought Stress Response. Plant Physiol. 158: 363-375

Connerly PL, Esaki M, Montegna EA, Strongin DE, Levi S, Soderholm J, Glick BS (2005) Sec16 is a determinant of transitional ER organization. Curr Biol 15: 1439-1447

Contento AL, Bassham DC (2012) Structure and function of endosomes in plant cells. J. Cell Sci. 125: 3511-3518

Cove DJ, Knight CD, Lamparter T (1997) Mosses as model systems. Trends Plant Sci 2: 99-105

Craddock CP, Hunter PR, Szakacs E, Hinz G, Robinson DG, Frigerio L (2008) Lack of a Vacuolar Sorting Receptor Leads to Non-Specific Missorting of Soluble Vacuolar Proteins in Arabidopsis Seeds. Traffic 9: 408-416

Culianez-Macia FA, Martin C (1993) DIP: a member of the MIP family of membrane proteins that is expressed in mature seeds and Dark-Grown seedlings of Antirrhinum majus. Plant J. 4: 717-725

Da Silva Conceiçao A, Marty-Mazars D, Bassham DC, Sanderfoot AA, Marty F, Raikhel NV (1997) The syntaxin homolog atPEP12p resides on a late post-Golgi compartment in plants. Plant Cell 9: 571-582

Dacks JB, Doolittle WF (2001) Reconstructing/Deconstructing the earliest eukaryotes. How comparative genomics can help. Cell 107: 419-425.

Dacks JB, Poon PP, Field MC (2008) Phylogeny of endocytic components yields insight into the process of nonendosymbiotic organelle evolution. Proc.Natl.Acad.Sci.USA 105: 588-593

Danielson J, Johanson U (2008) Unexpected complexity of the Aquaporin gene family in the moss Physcomitrella patens. BMC Plant Biology 8: 45

Denecke J, Aniento F, Frigerio L, Hawes C, Hwang I, Mathur J, Neuhaus JM, Robinson DG (2012) Secretory pathway research: the more experimental systems the better. Plant Cell 24: 1316-1326

Denecke J, Botterman J, Deblaere R (1990a) Protein secretion in plant cells can occur via a default pathway. Plant Cell 2: 51-59

Denecke J, Botterman J, Deblaere R (1990b) Protein Secretion in Plant Cells Occur via a Default Pathway. Plant Cell 2: 51-59

Dettmer J, Hong-Hermesdorf A, Stierhof YD, Schumacher K (2006) Vacuolar H+-ATPase activity is required for endocytic and secretory trafficking in Arabidopsis. Plant Cell 18: 715-730

Di Sansebastiano GP, Paris N, Marc-Martin S, Neuhaus J-M (1998) Specific accumulation of GFP in a non-acidic vacuolar compartment via a C-terminal propeptide-mediated sorting pathway. Plant J. 15: 449-457

Di Sansebastiano GP, Paris N, Marc-Martin S, Neuhaus J-M (2001) Regeneration of a lytic central vacuole and of neutral peripheral vacuoles can be visualized by green fluorescent proteins targeted to either type of vacuoles. Plant Physiol. 126: 78-86.

Di Sansebastiano GP, Renna L, Gigante M, De Caroli M, Piro G, Dalessandro G (2007) Green fluorescent protein reveals variability in vacuoles of three plant species. Biologia Plantarum 51: 49-55

Dombrowski JE, Schroeder MR, Bednarek SY, Raikhel NV (1993) Determination of the functional elements within the vacuolar targeting signal of barley lectin. Plant Cell 5: 587-596

Donaldson JG, Williams DB (2009) Intracellular Assembly and Trafficking of MHC Class I Molecules. Traffic 10: 1745-1752

Donohoe BS, Kang B-H, Staehelin LA (2007) Identification and characterization of COPIa- and COPIb-type vesicle classes associated with plant and algal Golgi. Proc.Natl.Acad.Sci.USA 104: 163-168

Ebine K, Okatani Y, Uemura T, Goh T, Shoda K, Niihama M, Morita MT, Spitzer C, Otegui MS, Nakano A, Ueda T (2008) A SNARE Complex Unique to Seed Plants Is Required for Protein Storage Vacuole Biogenesis and Seed Development of Arabidopsis thaliana. Plant Cell 20: 3006-3021

Epimashko S, Meckel T, Fischer-Schliebs E, Luttge U, Thiel G (2004) Two functionally different vacuoles for static and dynamic purposes in one plant mesophyll leaf cell. Plant J. 37: 294-300

Escobar NM, Haupt S, Thow G, Boevink P, Chapman S, Oparka K (2003) High-throughput viral expression of cDNA-green fluorescent protein fusions reveals novel subcellular addresses and identifies unique proteins that interact with plasmodesmata. Plant Cell 15: 1507-1523

Flückiger R (1999) Transformation of A. thaliana with GFP fusion proteins targeted to different compartments of the secretory pathway; characterisation of the fluorescent patterns. Biochem. Neuchâtel, Neuchâtel

Flückiger R, De Caroli M, Piro G, Dalessandro G, Neuhaus JM, Di Sansebastiano GP (2003) Vacuolar system distribution in Arabidopsis tissues, visualized using GFP fusion proteins. J. Exp. Bot. 54: 1577-1584

Foresti O, De Marchis F, de Virgilio M, Klein EM, Arcioni S, Bellucci M, Vitale A (2008) Protein Domains Involved in Assembly in the Endoplasmic Reticulum Promote Vacuolar Delivery when Fused to Secretory GFP, Indicating a Protein Quality Control Pathway for Degradation in the Plant Vacuole. Mol Plant 1: 1067-1076

Foresti O, Denecke J (2008) Intermediate organelles of the plant secretory pathway: identity and function. Traffic 9: 1599-1612

Foresti O, Gershlick DC, Bottanelli F, Hummel E, Hawes C, Denecke J (2010) A Recycling-Defective Vacuolar Sorting Receptor Reveals an Intermediate Compartment Situated between Prevacuoles and Vacuoles in Tobacco. Plant Cell 22: 3992-4008

Fotin A, Cheng Y, Sliz P, Grigorieff N, Harrison SC, Kirchhausen T, Walz T (2004) Molecular model for a complete clathrin lattice from electron cryomicroscopy. Nature 432: 573-579

Frigerio L (2008) Response to Rogers Letter. Plant Physiol. 146: 1026-a-1027

Frigerio L, Hinz G, Robinson DG (2008) Multiple vacuoles in plant cells: rule or exception? Traffic

Frigerio L, Jolliffe NA, Di Cola A, Hernández Felipe D, Paris N, Neuhaus J-M, Lord JM, Ceriotti A, Roberts LM (2001) The internal propeptide of the ricin precursor carries a sequence-specific determinant for vacuolar sorting. Plant Physiol. 126: 167-173

Frigerio L, Vitale A, Lord JM, Ceriotti A, Roberts LM (1998) Free ricin A chain, proricin, and native toxin have different cellular fates when expressed in tobacco protoplasts. J. Biol. Chem. 273: 14194-14199

Fuji K, Shimada T, Takahashi H, Tamura K, Koumoto Y, Utsumi S, Nishizawa K, Maruyama N, Hara-Nishimura I (2007) Arabidopsis Vacuolar Sorting Mutants (green fluorescent seed) Can Be Identified Efficiently by Secretion of Vacuole-Targeted Green Fluorescent Protein in Their Seeds. Plant Cell

Fukuda R, McNew JA, Weber T, Parlati F, Engel T, Nickel W, Rothman JE, Söllner TH (2000) Functional architecture of an intracellular membrane t-SNARE. Nature 407: 198-202

Furt F, Lemoi K, Tuzel E, Vidali L (2012) Quantitative analysis of organelle distribution and dynamics in Physcomitrella patens protonemal cells. BMC Plant Biol 12: 70

Gietl C, Schmid M (2001) Ricinosomes: an organelle for developmentally regulated programmed cell death in senescing plant tissues. Naturwissenschaften 88: 49-58.

Glick BS (2000) Organization of the Golgi apparatus. Curr Opin Cell Biol 12: 450-456

Glick BS, Malhotra V (1998) The curious status of the Golgi apparatus. Cell 95: 883-889

Gommel DU, Memon AR, Heiss A, Lottspeich F, Pfannstiel J, Lechner J, Reinhard C, Helms JB, Nickel W, Wieland FT (2001) Recruitment to Golgi membranes of ADP-ribosylation factor 1 is mediated by the cytoplasmic domain of p23. EMBO J. 20: 6751-6760.

Gong FC, Giddings TH, Meehl JB, Staehelin LA, Galbraith DW (1996) Z-membranes - artificial organelles for overexpressing recombinant integral membrane proteins. P Natl Acad Sci USA 93: 2219-2223

Goodbody KC, Venverloo CJ, Lloyd CW (1991) Laser Microsurgery Demonstrates That Cytoplasmic Strands Anchoring the Nucleus across the Vacuole of Premitotic Plant-Cells Are under Tension - Implications for Division Plane Alignment. Development 113: 931-939

Greenwood JS, Helm M, Gietl C (2005) Ricinosomes and endosperm transfer cell structure in programmed cell death of the nucellus during Ricinus seed development. Proc.Natl.Acad.Sci.USA 102: 2238-2243

Gu Y, Wang Z, Yang Z (2004) ROP/RAC GTPase: an old new master regulator for plant signaling. Curr. Opin. Plant Biol. 7: 527-536

Hamman BD, Hendershot LM, Johnson AE (1998) BiP maintains the permeability barrier of the ER membrane by sealing the lumenal end of the translocon pore before and early in translocation. Cell 92: 747-758

Hanson MA, Stevens RC (2000) Cocrystal structure of synaptobrevin-II bound to botulinum neurotoxin type B at 2.0 angstrom resolution. Nat. Struct. Biol. 7: 687-692
Hanton SL, Bortolotti LE, Renna L, Stefano G, Brandizzi F (2005) Crossing the divide--transport between the endoplasmic reticulum and Golgi apparatus in plants. Traffic 6: 267-277
Hanton SL, Matheson LA, Brandizzi F (2007) Studying protein export from the endoplasmic reticulum in plants. Methods Mol Biol 390: 297-308
Happel N, Höning S, Neuhaus J-M, Paris N, Robinson DG, Holstein SE (2004) Arabidopsis mu A-adaptin interacts with the tyrosine motif of the vacuolar sorting receptor VSR-PS1. Plant J. 37: 678-693
Hara-Nishimura I, Hatsugai N (2011) The role of vacuole in plant cell death. Cell Death Differ 18: 1298-1304
Hara-Nishimura I, Hatsugai N, Nakaune S, Kuroyanagi M, Nishimura M (2005) Vacuolar processing enzyme: an executor of plant cell death. Curr Opin Plant Biol 8: 404-408
Hara-Nishimura I, Kinoshita T, Hiraiwa N, Nishimura M (1998) Vacuolar processing enzymes in protein-storage vacuoles and lytic vacuoles. J. Plant Physiol. 152: 668-674
Harrison CJ, Roeder AH, Meyerowitz EM, Langdale JA (2009) Local cues and asymmetric cell divisions underpin body plan transitions in the moss Physcomitrella patens. Curr Biol 19: 461-471
Hartl FU (1996) Molecular chaperones in cellular protein folding. Nature 381: 571-580
Hawes C, Osterrieder A, Hummel E, Sparkes I (2008) The plant ER-Golgi interface. Traffic
Hay JC, Chao DS, Kuo CS, Scheller RH (1997) Protein interactions regulating vesicle transport between the endoplasmic reticulum and Golgi apparatus in mammalian cells. Cell 89: 149-158
Helenius A, Trombetta ES, Hebert DN, Simons Jf (1997) Calnexin, calreticulin and the folding of glycoproteins. Trends Cell Biol. 7: 193-200
Helms JB, Rothman JE (1992) Inhibition by brefeldin A of a Golgi membrane enzyme that catalyses exchange of guanine nucleotide bound to ARF. Nature 360: 352-354
Hepler PK, Vidali L, Cheung AY (2001) Polarized cell growth in higher plants. Annu Rev Cell Dev Biol 17: 159-187
Herman EM, Larkins BA (1999) Protein storage bodies and vacuoles. Plant Cell 11: 601-613
Hicks GR, Rojo E, Hong S, Carter DG, Raikhel NV (2004) Geminating pollen has tubular vacuoles, displays highly dynamic vacuole biogenesis, and requires VACUOLESS1 for proper function. Plant Physiol. 134: 1227-1239
Hiller MM, Finger A, Schweiger M, Wolf DH (1996) ER degradation of a misfolded luminal protein by the cytosolic ubiquitin-proteasome pathway. Science 273: 1725-1728
Hinz G, Colanesi S, Hillmer S, Rogers JC, Robinson DG (2007) Localization of vacuolar transport receptors and cargo proteins in the Golgi apparatus of developing Arabidopsis embryos. Traffic 8: 1452-1464
Hinz G, Hillmer S, Bäumer M, Hohl I (1999) Vacuolar storage proteins and the putative vacuolar sorting receptor BP-80 exit the Golgi apparatus of developing pea cotyledons in different transport vesicles. Plant Cell 11: 1509-1524
Hoffmann A, Nebenfuhr A (2004) Dynamic rearrangements of transvacuolar strands in BY-2 cells imply a role of myosin in remodeling the plant actin cytoskeleton. Protopl. 224: 201-210
Höfte H, Chrispeels MJ (1992) Protein sorting to the vacuolar membrane. Plant Cell 4: 995-1004
Hoh B, Hinz G, Jeong BK, Robinson DG (1995) Protein storage vacuoles form *de novo* during pea cotyledon development. J. Cell Sci. 108: 299-310

Hohe A, Egener T, Lucht JM, Holtorf H, Reinhard C, Schween G, Reski R (2004) An improved and highly standardised transformation procedure allows efficient production of single and multiple targeted gene-knockouts in a moss, Physcomitrella patens. Curr Genet 44: 339-347

Holwerda BC, Padgett HS, Rogers JC (1992) Proaleurain vacuolar targeting is mediated by short contiguous peptide interactions. Plant Cell 4: 307-318

Holwerda BC, Rogers JC (1992) Purification and Characterization of Aleurain - A Plant Thiol Protease Functionally Homologous to Mammalian Cathepsin-H. Plant Physiol. 99: 848-855

Holwerda BC, Rogers JC (1993) Structure, functional properties and vacuolar targeting of the barley thiol protease, aleurain. J. Exp. Bot. 44: 321-329

Hunter PR, Craddock CP, Di Benedetto S, Roberts LM, Frigerio L (2007) Fluorescent Reporter Proteins for the Tonoplast and the Vacuolar Lumen Identify a Single Vacuolar Compartment in Arabidopsis Cells. Plant Physiol.: pp.107.103945

Huotari J, Helenius A (2011) Endosome maturation. EMBO J. 30: 3481-3500

Hurtley SM, Helenius A (1989) Protein oligomerization in the endoplasmic reticulum. Annu Rev Cell Biol 5: 277-307

Inoue Y, Moriyasu Y (2006) Autophagy Is Not a Main Contributor to the Degradation of Phospholipids in Tobacco Cells Cultured under Sucrose Starvation Conditions. Plant Cell Physiol

Iversen TG, Skretting G, Llorente A, Nicoziani P, van Deurs B, Sandvig K (2001) Endosome to Golgi transport of ricin is independent of clathrin and of the Rab9- and Rab11-GTPases. Mol Biol Cell 12: 2099-2107

Jauh GY, Fischer AM, Grimes HD, Ryan CA, Rogers JC (1998) δ-tonoplast intrinsic protein defines unique plant vacuole functions. P Natl Acad Sci USA 95: 12995-12999

Jauh GY, Phillips TE, Rogers JC (1999) Tonoplast intrinsic protein isoforms as markers for vacuolar functions. Plant Cell 11: 1867-1882

Jiang CJ, Imamoto N, Matsuki R, Yoneda Y, Yamamoto N (1998) Functional characterization of a plant importin alpha homologue - nuclear localization signal (nls)-selective binding and mediation of nuclear import of nls proteins *in vitro*. J. Biol. Chem. 273: 24083-24087

Jiang L, Phillips TE, Hamm CA, Drozdowicz YM, Rea PA, Maeshima M, Rogers SW, Rogers JC (2001) The protein storage vacuole: a unique compound organelle. J. Cell Biol. 155: 991-1002.

Jiang L, Phillips TE, Rogers SW, Rogers JC (2000) Biogenesis of the protein storage vacuole crystalloid. J. Cell Biol. 150: 755-770

Jiang LW, Rogers JC (1998) Integral membrane protein sorting to vacuoles in plant cells: Evidence for two pathways. J. Cell Biol. 143: 1183-1199

Joazeiro CAP, Weissman AM (2000) RING Finger Proteins: Mediators of Ubiquitin Ligase Activity. Cell 102: 549-552

Johanson U, Karlsson M, Johansson I, Gustavsson S, Sjövall S, Fraysse L, A. W, Kjelbom P (2001) The Complete Set of Genes Encoding Major Intrinsic Proteins in Arabidopsis Provides a Fremework for a New Nomenclature for Major Intrinsic Proteins in Plants. Plant Physiol. 126: 1358-1369

Jolliffe NA, Brown JC, Neumann U, Vicre M, Bachi A, Hawes C, Ceriotti A, Roberts LM, Frigerio L (2004) Transport of ricin and 2S albumin precursors to the storage vacuoles of Ricinus communis endosperm involves the Golgi and VSR-like receptors. Plant J. 39: 821-833

Jolliffe NA, Craddock CP, Frigerio L (2005) Pathways for protein transport to seed storage vacuoles. Biochem Soc Trans 33: 1016-1018

Jürgens G (2004) Membrane trafficking in plants. Annu Rev Cell Dev Biol 20: 481-504
Kammerer W, Cove DJ (1996) Genetic analysis of the effects of re-transformation of transgenic lines of the moss physcomitrella patens. Molecular & General Genetics 250: 380-382
Karol KG, McCourt RM, Cimino MT, Delwiche CF (2001) The closest living relatives of land plants. Science 294: 2351-2353
Kervinen J, Tobin GJ, Costa J, Waugh DS, Wlodawer A, Zdanov A (1999) Crystal structure of plant aspartic proteinase prophytepsin: inactivation and vacuolar targeting. EMBO J. 18: 3947-3955
Khandelwal A, Cho SH, Marella H, Sakata Y, Perroud P-F, Pan A, Quatrano RS (2010) Role of ABA and ABI3 in Desiccation Tolerance. Science 327: 546-
Kirsch T, Paris N, Butler JM, Beevers L, Rogers JC (1994) Purification and initial characterization of a potential plant vacuolar targeting receptor. Proc.Natl.Acad.Sci.USA 91: 3403-3407
Kirsch T, Saalbach G, Raikhel NV, Beevers L (1996) Interaction of a potential vacuolar targeting receptor with amino- and carboxyl-terminal targeting determinants. Plant Physiol. 111: 469-474
Kogan MJ, Lopez O, Cocera M, Lopez-Iglesias C, De La Maza A, Giralt E (2004) Exploring the interaction of the surfactant N-terminal domain of gamma-Zein with soybean phosphatidylcholine liposomes. Biopolymers 73: 258-268
Koide Y, Matsuoka K, Ohto M, Nakamura K (1999) The N-terminal propeptide and the C terminus of the precursor to 20-kilo-dalton potato tuber protein can function as different types of vacuolar sorting signals. Plant Cell Physiol. 40: 1152-1159
Kutsuna N, Hasezawa S (2002) Dynamic organization of vacuolar and microtubule structures during cell cycle progression in synchronized tobacco BY-2 cells. Plant Cell Physiol 43: 965-973
Kutsuna N, Hasezawa S (2005) Morphometrical study of plant vacuolar dynamics in single cells using three-dimensional reconstruction from optical sections. Microsc Res Techniq 68: 296-306
Kutsuna N, Kumagai F, Sato MH, Hasezawa S (2003) Three-dimensional reconstruction of tubular structure of vacuolar membrane throughout mitosis in living tobacco cells. Plant Cell Physiol 44: 1045-1054
Lam SK, Tse YC, Robinson DG, Jiang L (2007) Tracking down the elusive early endosome. Trends Plant Sci 12: 497-505
Lang D, Eisinger J, Reski R, Rensing SA (2005) Representation and high-quality annotation of the Physcomitrella patens transcriptome demonstrates a high proportion of proteins involved in metabolism in mosses. Plant Biol (Stuttg) 7: 238-250
Langhans M, Hawes C, Hillmer S, Hummel E, Robinson DG (2007) Golgi Regeneration after BFA-Treatment in BY-2 Cells Entails Stack Enlargement and Cisternal Growth Followed by Division. Plant Physiol.: pp.107.104919
Laval V, Masclaux F, Serin A, Carriere M, Roldan C, Devic M, Pont-Lezica RF, Galaud JP (2003) Seed germination is blocked in Arabidopsis putative vacuolar sorting receptor (atbp80) antisense transformants. J Exp Bot 54: 213-221
Lee HK, Cho SK, Son O, Xu Z, Hwang I, Kim WT (2009) Drought Stress-Induced Rma1H1, a RING Membrane-Anchor E3 Ubiquitin Ligase Homolog, Regulates Aquaporin Levels via Ubiquitination in Transgenic Arabidopsis Plants. Plant Cell
Lewis MJ, Pelham HRB (1992) Ligand-induced redistribution of a human KDEL receptor from the Golgi-complex to the endoplasmic reticulum. Cell 68: 353-364
Li HW, Li WX, Ding SW (2002) Induction and suppression of RNA silencing by an animal virus. Science 296: 1319-1321

Ligrone R, Ducket JG, Renzaglia KS (2000) Conducting tissues and phyletic relationships of bryophytes. Philos Trans R Soc Lond B Biol Sci 355: 795-813
Liu YC, Vidali L (2011) Efficient polyethylene glycol (PEG) mediated transformation of the moss Physcomitrella patens. J Vis Exp
Losev E, Reinke CA, Jellen J, Strongin DE, Bevis BJ, Glick BS (2006) Golgi maturation visualized in living yeast. Nature 441: 1002-1006
Mahon P, Bateman A (2000) The PA domain: a protease-associated domain. Protein Sci 9: 1930-1934
Malhotra V, Rothman JE (1988) Role of an N-Ethylmaleimide-Sensitive Transport Component in Promoting Fusion ofTransport Vesicles with Cisternae of the Golgi Stack. Cell 54: 221-227
Marty-Mazars D, Clémencet M-C, Cozolme P, Marty F (1995) Antibodies to the tonoplast from the storage parenchyma cells of beetroot recognize a major intrinsic protein related to TIPs. Eur. J. Cell Biol. 66: 106-118
Marty F (1978) Cytochemical studies on GERL, provacuoles, and vacuoles in root meristematic cells of Euphorbia. Proc Natl Acad Sci U S A 75: 852-856
Marty F (1999) Plant vacuoles. Plant Cell 11: 587-599
Maruyama N, Mun LC, Tatsuhara M, Sawada M, Ishimoto M, Utsumi S (2006) Multiple vacuolar sorting determinants exist in soybean 11S globulin. Plant Cell 18: 1253-1273
Matheson LA, Hanton SL, Brandizzi F (2006) Traffic between the plant endoplasmic reticulum and Golgi apparatus: to the Golgi and beyond. Curr Opin Plant Biol 9: 601-609
Matsuoka K, Bassham DC, Raikhel NV, Nakamura K (1995) Different sensitivity to wortmannin of two vacuolar sorting signals indicates the presence of distinct sorting machineries in tobacco cells. J. Cell Biol. 130: 1307-1318
Matsuoka K, Nakamura K (1991) Propeptide of a precursor to a plant vacuolar protein required for vacuolar targeting. P Natl Acad Sci USA 88: 834-838
Matsuoka K, Nakamura K (1999) Large alkyl side-chains of isoleucine and leucine in the NPIRL region constitute the core of the vacuolar sorting determinant of sporamin precursor. Plant Mol. Biol. 41: 825-835
Matsuoka K, Neuhaus J-M (1999) Cis-elements of protein transport to the plant vacuoles. J. Exp. Bot. 50: 165-174
Matsuura-Tokita K, Takeuchi M, Ichihara A, Mikuriya K, Nakano A (2006) Live imaging of yeast Golgi cisternal maturation. Nature 441: 1007-1010
Mellman I, Simons K (1992) The Golgi complex - In vitro veritas? Cell 68: 829-840
Miao Y, Yan PK, Kim H, Hwang I, Jiang L (2006) Localization of Green Fluorescent Protein Fusions with the Seven Arabidopsis Vacuolar Sorting Receptors to Prevacuolar Compartments in Tobacco BY-2 Cells. Plant Physiol. 142: 945-962
Mo B, Tse YC, Jiang L (2006) Plant prevacuolar/endosomal compartments. Int Rev Cytol 253: 95-129
Morre DJ, Clegg ED, Lunstra DD, Mollenhauer HH (1974) An electron-dense stain for isolated fragments of plasma and acrosome membranes from porcine sperm. Proc Soc Exp Biol Med 145: 1-6
Movafeghi A, Happel N, Pimpl P, Tai GH, Robinson DG (1999) Arabidopsis Sec21p and Sec23p homologs. Probable coat proteins of plant COP-coated vesicles. Plant Physiol. 119: 1437-1446
Mukhopadhyay D, Riezman H (2007) Proteasome-independent functions of ubiquitin in endocytosis and signaling. Science 315: 201-205
Muntz K (1998) Deposition of storage proteins. Plant Mol. Biol. 38: 77-99

Murphy KA, Kuhle RA, Fischer AM, Anterola AM, Grimes HD (2005) The functional status of paraveinal mesophyll vacuoles changes in response to altered metabolic conditions in soybean leaves. Functional Plant Biology, p 10

Nebenführ A, Gallagher LA, Dunahay TG, Frohlick JA, Mazurkiewicz AM, Meehl JB, Staehelin LA (1999) Stop-and-go movements of plant Golgi stacks are mediated by the acto-myosin system. Plant Physiol. 121: 1127-1141

Neuhaus J-M (1999) Plant chitinases (PR-3, PR-4, PR-8, PR-11). In: Datta SK, Muthukrishnan S (eds) Pathogenesis-related proteins in plants. CRC Press, Cambridge, pp 77-105

Neuhaus J-M, Ahl-Goy P, Hinz U, Flores S, Meins F, Jr. (1991a) High-level expression of a tobacco chitinase gene in Nicotiana sylvestris - Susceptibility of transgenic plants to Cercospora Nicotianae infection. Plant Mol. Biol. 16: 141-151

Neuhaus J-M, Martinoia E (1999) Plant cell vacuoles. Encyclopedia of Life Sciences. Macmillan Publishers, Basingstoke

Neuhaus J-M, Paris N (2005) Plant vacuoles. from biogenesis to function. In: Samaj J, Baluska F, Menzel D (eds) Plant Endocytosis, pp 63-82

Neuhaus J-M, Pietrzak M, Boller T (1994) Mutation analysis of the C-terminal vacuolar targeting peptide of tobacco chitinase: low specificity of the sorting system, and gradual transition between intracellular retention and secretion into the extracellular space. Plant Journal 5: 45-54

Neuhaus J-M, Sticher L, Meins F, Jr., Boller T (1991b) A short C-terminal sequence is necessary and sufficient for the targeting of chitinases to the plant vacuole. Proc.Natl.Acad.Sci.USA 88: 10362-10366

Neuhaus JM, Rogers JC (1998) Sorting of proteins to vacuoles in plant cells. Plant Mol. Biol. 38: 127-144.

Nielsen KJ, Hill JM, Anderson MA, Craik DJ (1996) Synthesis and structure determination by nmr of a putative vacuolar targeting peptide and model of a proteinase inhibitor from Nicotiana alata. Biochem. 35: 369-378

Nishiyama T, Hiwatashi Y, Sakakibara I, Kato M, Hasebe M (2000) Tagged mutagenesis and gene-trap in the moss, Physcomitrella patens by shuttle mutagenesis. DNA research : an international journal for rapid publication of reports on genes and genomes 7: 9-17

Oda Y, Higaki T, Hasezawa S, Kutsuna N (2009a) Chapter 3. New insights into plant vacuolar structure and dynamics. International review of cell and molecular biology 277: 103-135

Oda Y, Hirata A, Sano T, Fujita T, Hiwatashi Y, Sato Y, Kadota A, Hasebe M, Hasezawa S (2009b) Microtubules regulate dynamic organization of vacuoles in Physcomitrella patens. Plant Cell Physiol 50: 855-868

Okita TW, Rogers JC (1996) Compartmentation of proteins in the endomembrane system of plant cells. Annual Review of Plant Physiology & Plant Molecular Biology

Okubo-Kurihara E, Sano T, Higaki T, Kutsuna N, Hasezawa S (2009) Acceleration of vacuolar regeneration and cell growth by overexpression of an aquaporin NtTIP1;1 in tobacco BY-2 cells. Plant Cell Physiol 50: 151-160

Olbrich A, Hillmer S, Hinz G, Oliviusson P, Robinson DG (2007a) Newly formed vacuoles in root meristems of barley and pea seedlings have characteristics of both protein storage and lytic vacuoles. Plant Physiol. 145: 1383-1394

Olbrich A, Hillmer S, Hinz G, Oliviusson P, Robinson DG (2007b) Newly Formed Vacuoles in Root Meristems of Barley and Pea Seedlings Have Characteristics of both Protein Storage and Lytic Vacuoles. Plant Physiol.: pp.107.108985

Otegui MS, Herder R, Schulze J, Jung R, Staehelin LA (2006) The Proteolytic Processing of Seed Storage Proteins in Arabidopsis Embryo Cells Starts in the Multivesicular Bodies. Plant Cell 18: 2567-2581

Otegui MS, Noh YS, Martinez DE, Vila Petroff MG, Staehelin LA, Amasino RM, Guiamet JJ (2005) Senescence-associated vacuoles with intense proteolytic activity develop in leaves of Arabidopsis and soybean. Plant J. 41: 831-844

Ovecka M, Lang I, Baluska F, Ismail A, Illes P, Lichtscheidl IK (2005) Endocytosis and vesicle trafficking during tip growth of root hairs. Protopl. 226: 39-54

Panteris E, Apostolakos P, Quader H, Galatis B (2004) A cortical cytoplasmic ring predicts the division plane in vacuolated cells of Coleus: the role of actomyosin and microtubules in the establishment and function of the division site. New Phytologist 163: 271-286

Paris N, Rogers JC (1996) The role of receptors in targeting soluble proteins from the secretory pathway to the vacuole. Plant Physiol. and Biochem. 34: 223-227

Paris N, Rogers SW, Jiang L, Kirsch T, Beevers L, Phillips TE, Rogers JC (1997) Molecular cloning and further characterization of a probable plant vacuolar sorting receptor. Plant Physiol. 115: 29-39

Paris N, Stanley CM, Jones RL, Rogers JC (1996) Plant cells contain two functionally distinct vacuolar compartments. Cell 85: 563-572

Park JH, Oufattole M, Rogers JC (2007) Golgi-mediated vacuolar sorting in plant cells: RMR proteins are sorting receptors for the protein aggregation/membrane internalization pathway. Plant Sci. 172: 728-745

Park M, Kim SJ, Vitale A, Hwang I (2004) Identification of the protein storage vacuole and protein targeting to the vacuole in leaf cells of three plant species. Plant Physiol. 134: 625-639

Park M, Lee D, Lee G-J, Hwang I (2005) AtRMR1 functions as a cargo receptor for protein trafficking to the protein storage vacuole. J. Cell Biol. 170: 757-767

Patterson GH, Hirschberg K, Polishchuk RS, Gerlich D, Phair RD, Lippincott-Schwartz J (2008) Transport through the Golgi apparatus by rapid partitioning within a two-phase membrane system. Cell 133: 1055-1067

Pelham HRB (1998) Getting through the Golgi complex. Trends Cell Biol. 8: 45-49

Pelham HRB, Rothman JE (2000) The debate about transport in the Golgi - Two sides of the same coin? Cell 102: 713-719

Peremyslov VV, Pan YW, Dolja VV (2004) Movement protein of a closterovirus is a type III integral transmembrane protein localized to the endoplasmic reticulum. J Virol 78: 3704-3709

Pressel S, Ligrone R, Duckett JG (2008) Cellular differentiation in moss protonemata: a morphological and experimental study. Ann Bot 102: 227-245

Raposo G, Marks MS, Cutler DF (2007) Lysosome-related organelles: driving post-Golgi compartments into specialisation. Curr Opin Cell Biol

Reisen D, Marty F, Leborgne-Castel N (2005) New insights into the tonoplast architecture of plant vacuoles and vacuolar dynamics during osmotic stress. BMC Plant Biol 5: 13

Rensing SA, Ick J, Fawcett JA, Lang D, Zimmer A, Van de Peer Y, Reski R (2007) An ancient genome duplication contributed to the abundance of metabolic genes in the moss Physcomitrella patens. BMC Evol Biol 7: 130

Rensing SA, Lang D, Zimmer AD, Terry A, Salamov A, Shapiro H, Nishiyama T, Perroud PF, Lindquist EA, Kamisugi Y, Tanahashi T, Sakakibara K, Fujita T, Oishi K, Shin IT, Kuroki Y, Toyoda A, Suzuki Y, Hashimoto S, Yamaguchi K, Sugano S, Kohara Y, Fujiyama A, Anterola A, Aoki S, Ashton N, Barbazuk WB, Barker E, Bennetzen JL, Blankenship R, Cho SH, Dutcher SK, Estelle M, Fawcett JA, Gundlach H,

Hanada K, Heyl A, Hicks KA, Hughes J, Lohr M, Mayer K, Melkozernov A, Murata T, Nelson DR, Pils B, Prigge M, Reiss B, Renner T, Rombauts S, Rushton PJ, Sanderfoot A, Schween G, Shiu SH, Stueber K, Theodoulou FL, Tu H, Van de Peer Y, Verrier PJ, Waters E, Wood A, Yang L, Cove D, Cuming AC, Hasebe M, Lucas S, Mishler BD, Reski R, Grigoriev IV, Quatrano RS, Boore JL (2008) The Physcomitrella genome reveals evolutionary insights into the conquest of land by plants. Science 319: 64-69

Renzaglia KS, Schuette S, Duff RJ, Ligrone R, Shaw AJ, Mishler BD, Duckett JG (2007) Bryophyte phylogeny: Advancing the molecular and morphological frontiers. Bryologist 110: 179-213

Reski R (1998) Development, genetics and molecular biology of mosses. Botanica Acta 111: 1-15

Ritzenthaler C, Nebenfuhr A, Movafeghi A, Stussi-Garaud C, Behnia L, Pimpl P, Staehelin LA, Robinson DG (2002) Reevaluation of the effects of brefeldin A on plant cells using tobacco Bright Yellow 2 cells expressing Golgi-targeted green fluorescent protein and COPI antisera. Plant Cell 14: 237-261

Rivera-Serrano EE, Rodriguez-Welsh MF, Hicks GR, Rojas-Pierce M (2012) A small molecule inhibitor partitions two distinct pathways for trafficking of tonoplast intrinsic proteins in Arabidopsis. PLoS One 7: e44735

Robinson DG, Hinz G, Holstein SEH (1998) The molecular characterization of transport vesicles. Plant Mol. Biol. 38: 49-76

Robinson DG, Hoh B, Hinz G, Jeong BK (1995) One vacuole or two vacuoles: Do protein storage vacuoles arise de novo during pea cotyledon development? J. Plant Physiol. 145: 654-664

Robinson DG, Langhans M, Saint-Jore-Dupas C, Hawes C (2008) BFA effects are tissue and not just plant specific. Trends Plant Sci 13: 405-408

Rojo E, Gillmor CS, Kovaleva V, Somerville CR, Raikhel NV (2001) VACUOLELESS1 is an essential gene required for vacuole formation and morphogenesis in Arabidopsis. Developmental Cell 1: 303-310

Rojo E, Sharma VK, Kovaleva V, Raikhel NV, Fletcher JC (2002) CLV3 is localized to the extracellular space, where it activates the Arabidopsis CLAVATA stem cell signaling pathway. Plant Cell 14: 969-977

Roldan JA, Rojas HJ, Goldraij A (2012) Disorganization of F-actin cytoskeleton precedes vacuolar disruption in pollen tubes during the in vivo self-incompatibility response in Nicotiana alata. Ann Bot 110: 787-795

Rolland-Lagan AG (2008) Vein patterning in growing leaves: axes and polarities. Curr Opin Genet Dev 18: 348-353

Rothman JE (1994) Mechanism of intracellular protein transport. Nature 372: 55-63

Rothman JE, Orci L (1996) Budding vesicles in living cells. Sci. Am. 274: 50-55

Rothman JE, Söllner TH (1997) Throttles and Dampers: Controlling the Engine of Membrane Fusion. Science 276: 1212-1213

Russinova E, Borst JW, Kwaaitaal M, Cano-Delgado A, Yin Y, Chory J, de Vries SC (2004) Heterodimerization and endocytosis of Arabidopsis brassinosteroid receptors BRI1 and AtSERK3 (BAK1). Plant Cell 16: 3216-3229

Saidi Y, Finka A, Chakhporanian M, Zryd JP, Schaefer DG, Goloubinoff P (2005) Controlled expression of recombinant proteins in Physcomitrella patens by a conditional heat-shock promoter: a tool for plant research and biotechnology. Plant Mol. Biol. 59: 697-711

Saint-Jean B, Seveno-Carpentier E, Alcon C, Neuhaus JM, Paris N (2010) The cytosolic tail dipeptide Ile-Met of the pea receptor BP80 is required for recycling from the prevacuole and for endocytosis. Plant Cell 22: 2825-2837

Saito C, Morita MT, Kato T, Tasaka M (2005) Amyloplasts and vacuolar membrane dynamics in the living graviperceptive cell of the Arabidopsis inflorescence stem. Plant Cell 17: 548-558

Saito C, Ueda T, Abe H, Wada Y, Kuroiwa T, Hisada A, Furuya M, Nakano A (2002) A complex and mobile structure forms a distinct subregion within the continuous vacuolar membrane in young cotyledons of Arabidopsis. Plant J. 29: 245-255.

Samaj J, Baluska F, Voigt B, Schlicht M, Volkmann D, Menzel D (2004) Endocytosis, actin cytoskeleton, and signaling. Plant Physiol. 135: 1150-1161

Samaj J, Read ND, Volkmann D, Menzel D, Baluska F (2005) The endocytic network in plants. Trends Cell Biol. 15: 425-433

Sanderfoot A (2007) Increases in the Number of SNARE Genes Parallels the Rise of Multicellularity among the Green Plants. Plant Physiol.: pp.106.092973

Sanderfoot AA, Ahmed SU, Marty-Mazars D, Rapoport I, Kirchhausen T, Marty F, Raikhel NV (1998) A putative vacuolar cargo receptor partially colocalizes with atPEP12p on a prevacuolar compartment in *Arabidopsis* roots. P Natl Acad Sci USA 95: 9920-9925

Sanderfoot AA, Kovaleva V, Zheng H, Raikhel NV (1999) The t-SNARE AtVAM3p resides on the prevacuolar compartment in Arabidopsis root cells. Plant Physiol. 121: 929-938

Sanmartin M, Ordonez A, Sohn EJ, Robert S, Sanchez-Serrano JJ, Surpin MA, Raikhel NV, Rojo E (2007) Divergent functions of VTI12 and VTI11 in trafficking to storage and lytic vacuoles in Arabidopsis. Proc.Natl.Acad.Sci.USA 104: 3645-3650

Sato MH, Nakamura N, Ohsumi Y, Kouchi H, Kondo M, Hara-Nishimura I, Nishimura M, Wada Y (1997) The atVAM3 encodes a syntaxin-related molecule implicated in the vacuolar assembly in *Arabidopsis thaliana*. J. Biol. Chem. 272: 24530-24535

Schaefer D, Grimsley N, Zrÿd J-P (1993) Transformation of the moss Physcomitrella patens. ?

Schaefer D, Zryd J (1997) Efficient gene targeting in the moss *Physcomitrella* patens. Plant J. 11: 1195-1206

Schaefer D, Zryd JP, Knight CD, Cove DJ (1991) Stable transformation of the moss Physcomitrella patens. Mol. Gen. Genet. 226: 418-424

Schaefer DG (2001) Gene targeting in Physcomitrella patens. Curr Opin Plant Biol 4: 143-150

Schroeder MR, Borkhsenious ON, Matsuoka K, Nakamura K, Raikhel NV (1993) Colocalization of barley lectin and sporamin in vacuoles of transgenic tobacco plants. Plant Physiol. 101: 451-458

Segui-Simarro JM, Staehelin LA (2006) Cell cycle-dependent changes in Golgi stacks, vacuoles, clathrin-coated vesicles and multivesicular bodies in meristematic cells of Arabidopsis thaliana: a quantitative and spatial analysis. Planta 223: 223-236

Sheahan MB, Rose RJ, McCurdy DW (2007) Actin-filament-dependent remodeling of the vacuole in cultured mesophyll protoplasts. Protopl. 230: 141-152

Shen Y, Wang J, Ding Y, Gouzerh G, Neuhaus J-M, Jiang L (2011) The Rice RMR1 Defines a Novel Organelle as a Prevacuolar Compartment for the Protein Storage Vacuole Pathway. Molecular Plant

Shimada T, Fuji K, Tamura K, Kondo M, Nishimura M, Hara-Nishimura I (2003a) Vacuolar sorting receptor for seed storage proteins in Arabidopsis thaliana. Proc.Natl.Acad.Sci.USA 100: 16095-16100

Shimada T, Hiraiwa N, Nishimura M, Hara-Nishimura I (1994) Vacuolar processing enzyme of soybean that converts proproteins to the corresponding mature forms. Plant Cell Physiol 35: 713-718

Shimada T, Kuroyanagi M, Nishimura M, Hara-Nishimura I (1997) A pumpkin 72-kDa membrane protein of precursor-accumulating vesicles has characteristics of a vacuolar sorting receptor. Plant Cell Physiol. 38: 1414-1420

Shimada T, Yamada K, Kataoka M, Nakaune S, Koumoto Y, Kuroyanagi M, Tabata S, Kato T, Shinozaki K, Seki M, Kobayashi M, Kondo M, Nishimura M, Hara-Nishimura I (2003b) Vacuolar processing enzymes are essential for proper processing of seed storage proteins in Arabidopsis thaliana. J. Biol. Chem. 278: 32292-32299

Struhl K (1983) The new yeast genetics. Nature 305: 391-397

Su LL, Iwai H, Lin JT, Fathman CG (2009) The Transmembrane E3 Ligase GRAIL Ubiquitinates and Degrades CD83 on CD4 T Cells. The Journal of Immunology 183: 438-444

Suga S, Komatsu S, Maeshima M (2002) Aquaporin Isoforms Responsive to Salt and Water Stresses and Phytohormones in Radish Seedlings. Plant Cell Physiol. 43: 1229-1237

Surpin M, Raikhel N (2004) Traffic jams affect plant development and signal transduction. Nat Rev Mol Cell Biol 5: 100-109

Swanson SJ, Bethke PC, Jones RL (1998) Barley aleurone cells contain two types of vacuoles. Characterization Of lytic organelles by use of fluorescent probes. Plant Cell 10: 685-698

Swiezewska E, Thelin A, Dallner G, Andersson B, Ernster L (1993) Occurrence of prenylated proteins in plant cells. Biochem Biophys Res Commun 192: 161-166

Tague BW, Dickinson CD, Chrispeels MJ (1990) A short domain of the plant vacuolar protein phytohemagglutinin targets invertase to the yeast vacuole. Plant Cell 2: 533-546

Taiz L (1992) The Plant Vacuole. J Exp Biol 172: 113-122

Theissen G, Saedler H (2001) Plant biology. Floral quartets. Nature 409: 469-471.

Tormakangas K, Hadlington JL, Pimpl P, Hillmer S, Brandizzi F, Teeri TH, Denecke J (2001) A vacuolar sorting domain may also influence the way in which proteins leave the endoplasmic reticulum. Plant Cell 13: 2021-2032

Tranque P, Crossin KL, Cirelli C, Edelman GM, Mauro VP (1996) Identification and characterization of a RING zinc finger gene (C-RZF) expressed in chicken embryo cells. Proc Natl Acad Sci U S A 93: 3105-3109.

Traub LM, Kornfeld S (1997) The trans-Golgi network: a late secretory sorting station. Curr Opin Cell Biol 9: 527-533

Tse YC, Mo B, Hillmer S, Zhao M, Lo SW, Robinson DG, Jiang L (2004) Identification of multivesicular bodies as prevacuolar compartments in Nicotiana tabacum BY-2 cells. Plant Cell 16: 672-693

Ueda T, Uemura T, Sato MH, Nakano A (2004) Functional differentiation of endosomes in Arabidopsis cells. Plant J. 40: 783-789

Uemura T, Ueda T, Ohniwa RL, Nakano A, Takeyasu K, Sato MH (2004) Systematic analysis of SNARE molecules in Arabidopsis: dissection of the post-Golgi network in plant cells. Cell Struct Funct 29: 49-65

Uemura T, Yoshimura SH, Takeyasu K, Sato MH (2002) Vacuolar membrane dynamics revealed by GFP-AtVam3 fusion protein. Genes Cells 7: 743-753

Van Gestel K, Slegers H, Von Witsch M, Samaj J, Baluska F, Verbelen JP (2003) Immunological evidence for the presence of plant homologues of the actin- related protein Arp3 in tobacco and maize: subcellular localization to actin-enriched pit fields and emerging root hairs. Protopl. 222: 45-52

Vermeer JEM, van Leeuwen W, Tobena-Santamaria R, Laxalt AM, Jones DR, Divecha N, Gadella TWJ, Munnik T (2006) Visualization of PtdIns3P dynamics in living plant cells. Plant J. 47: 687-700

Vertel BM, Walters LM, Mills D (1992) Subcompartments of the endoplasmic reticulum. Semin Cell Biol 3: 325-341

Vitale A, Boston RS (2008) Endoplasmic reticulum quality control and the unfolded protein response: insights from plants. Traffic

Vitale A, Ceriotti A (2004) Protein quality control mechanisms and protein storage in the endoplasmic reticulum. A conflict of interests? Plant Physiol. 136: 3420-3426

Vitale A, Chrispeels MJ (1992) Sorting of Proteins to the Vacuoles of Plant Cells. BioEss 14: 151-160

Vitale A, Denecke J (1999) The endoplasmic reticulum - Gateway of the secretory pathway. Plant Cell 11: 615-628

Vitale A, Hinz G (2005) Sorting of proteins to storage vacuoles: how many mechanisms? Trends Plant Sci 10: 316-323

Vitale A, Raikhel NV (1999) What do proteins need to reach different vacuoles? Trends Plant Sci 4: 149-155

Voglmayr H (2000) Nuclear DNA amounts in mosses (musci). Annals of Botany 85: 531-546

Wang H, Rogers JC, Jiang L (2011) Plant RMR proteins: unique vacuolar sorting receptors that couple ligand sorting with membrane internalization. FEBS J. 278: 59-68

Wang Y, Cipriano DJ, Forgac M (2007) Arrangement of Subunits in the Proteolipid Ring of the V-ATPase. J. Biol. Chem. 282: 34058-34065

Waters MG, Griff IC, Rothman JE (1991) Proteins involved in vesicular transport and membrane fusion. Curr Opin Cell Biol 3: 615-620

Yano K, Hattori M, Moriyasu Y (2007) A Novel type of Autophagy Occurs together with Vacuole Genesis in Miniprotoplasts Prepared from Tobacco Culture Cells. Autophagy 3: 215-221

Yoneda A, Kutsuna N, Higaki T, Oda Y, Sano T, Hasezawa S (2007) Recent progress in living cell imaging of plant cytoskeleton and vacuole using fluorescent-protein transgenic lines and three-dimensional imaging. Protopl. 230: 129-139

Zhang JX, Flint HJ (1992) A Bifunctional Xylanase Encoded by the xynA Gene of the Rumen Cellulolytic Bacterium Ruminococcus-Flavefaciens-17 Comprises Two Dissimilar Domains Linked by an Asparagine/Glutamine-Rich Sequence. Mol Microbiol 6: 1013-1023

Zouhar J, Muñoz A, Rojo E (2010) Functional specialization within the vacuolar sorting receptor family: VSR1, VSR3 and VSR4 sort vacuolar storage cargo in seeds and vegetative tissues. Plant J. 64: 577-588

Zouhar J, Rojo E (2009) Plant vacuoles: where did they come from and where are they heading? Curr Opin Plant Biol